Exploration Into the Effects of Hypoxia in an *In Vitro* Canine Glioblastoma Model

by

Jennifer Wiggins Koehler

A dissertation submitted to the Graduate Faculty of
Auburn University
in partial fulfillment of the
requirements for the Degree of
Doctor of Philosophy

Auburn, AL
May 7, 2013

Keywords: canine, dog, cancer,
glioblastoma, brain, hypoxia

Approved by

Nancy Cox, Chair, Professor, Department of Pathobiology and Interim Director, Scott-Ritchey Research Center
Calvin Johnson, Co-chair, Dean, College of Veterinary Medicine
Tatiana Samoylova, Associate Research Professor, Scott-Ritchey Research Center

Abstract

Glioblastomas are aggressive, lethal primary brain tumors that affect human and canine patients. A subpopulation representing a variably large percentage of the bulk of tumor cells has been identified to have stem cell-like properties based on expression of certain molecular markers and growth properties in specialized culture conditions. This cancer stem-like cell (CSLC) population has been demonstrated to have increased resistance to radiation and chemotherapy, and is postulated to drive the bulk of tumor growth, invasion, regrowth, and treatment failure. Expression of several of these markers in human tumors, including CD133, nestin, and HIF2α, are associated with increasing tumor grade and/or a negative prognostic outcome, and because of their known roles in developmental biology have been utilized as markers for identifying CSLC. The role of the microenvironment in acquisition and maintenance of the stem-like state has not been fully elucidated; however, there is mounting evidence to indicate that hypoxia plays a crucial role. Although rodent and *in vitro* models exist to study the biology of glioblastoma and potential therapeutics, canine patients with naturally-occurring tumors offer a unique opportunity to serve as a bridge between these models and human clinical trials. Their usefulness in this regard necessitates a detailed and systematic investigation of the comparative biology of the disease beyond the histomorphologic level. In this body of work, we utilize an *in vitro* canine glioblastoma model system to demonstrate that hypoxia produces transcriptional upregulation of multiple putative CSLC and angiogenesis markers, and that siRNA-mediated gene silencing of HIF2α abrogates some of these effects and increases susceptibility to the chemotherapeutic agent doxorubicin.

Acknowledgements

I would like to express my gratitude to my committee chair, Dr. Nancy Cox, my co-chair, residency coordinator, and department head, Dr. Calvin Johnson, and my committee member, Dr. Tatiana Samoylova, for their support during this project. They fostered my independence and allowed me to learn from my mistakes, and in the process taught me a great deal about the logistics of managing a research project and of balancing the rewards and responsibilities associated with a life in academia. Special thanks are extended to Ms. Nancy Morrison, Ms. Regina Williams, Dr. Maninder Sandey, Ms. Allison Church-Bird and Ms. Atoska Gentry for expertise in technical matters in the lab, as well as their kindness, generosity, and moral support. I would also like to thank Dr. Bruce Smith for sharing lab space, materials, and for many lively discussions over the years about this project and others. I would like to thank Drs. Curt Bird, Emily Graff, Anne-Marie O'Neill, and Heather Gray-Edwards for their humor, support, and critical analysis of aspects of the project. Additionally, I would like to thank Dr. Sharon Roberts for being my outside reader. And last here but always first in my life, I would like to express my deep love and gratitude to my husband Pop for being phenomenally supportive, my two sons Hans and Hudson for being incredible people who amaze me in new ways every day, and my own parents Fred and Sydney Wiggins for fostering in me a love of learning and a desire to make a difference in the world. Thank you all so much.

Table of Contents

Tables

Figures

Abbreviations

ALDH: aldehyde dehydrogenase

CNS: central nervous system

$CoCl_2$: cobalt chloride

CSLC: cancer stem-like cell

DMEM: Dulbecco's modified Eagle's medium

EGF: epidermal growth factor

EGFR: epidermal growth factor receptor

bFGF: basic fibroblast growth factor

FIH: factor inhibiting HIF

GBM: glioblastoma (multiforme)

GFAP: glial fibrillary acidic protein

HAS: HIF ancillary sequence

HIF: hypoxia-inducible factor

HLH: helix-loop-helix

HRE: hypoxia-responsive element

IPC: intermediate progenitor cell

PHD: prolyl hydroxylase

ROS: reactive oxygen species

RTK: receptor tyrosine kinase

SP: side population

VEGF: vascular endothelial growth factor

VEGF-R: vascular endothelial growth factor receptor

VHL: vonHippel-Lindau

WHO: World Health Organization

CHAPTER I.

INTRODUCTION AND LITERATURE REVIEW

Central nervous system tumors: incidence, epidemiology, risk factors, and classification

The central nervous system (CNS) is immensely important to the survival and well-being of higher order animals. Like all body systems, it can develop primary neoplasms derived from its various constituent cell populations. The reliance of the CNS on precise anatomical and functional organization, as well as its bony confinement and limited capacity for renewal after insult, mean that perturbations deemed benign or insignificant in other organ systems can often cause profound dysfunction or even death. This situation is well illustrated by the fact that although tumors of the brain and spinal cord constitute a mere 2% of adult human primary neoplasms in terms of numbers, they inflict a disproportionate amount of morbidity and mortality within this group, with a 5-year survival rate in the lowest 1/3 of all cancers [1, 2]. Furthermore, in children primary brain neoplasms are the leading cause of death from solid tumor cancer, collectively making up 21% of all childhood cancers [1]. Approximately 64,000 new cases of benign and malignant primary brain tumors are diagnosed annually in the United States [1].

With the exception of rare inherited neoplastic syndromes such as Li-Fraumeni and Turcot syndromes [3], as well as history of exposure to therapeutic ionizing radiation, there are currently no unambiguously identified risk factors for development of brain tumors [4]. People of Caucasian descent are over-represented in both incidence and mortality, and there is a slightly

higher incidence in males [1]. Environmental risk factors that have been proposed but not definitively proven in humans include exposure to herbicides, fungicides and various other chemicals, electromagnetic fields, previous head trauma, and dietary N-nitroso compounds (such as those found in preserved meats) [3]. Cell phone usage as a potential risk factor has been investigated but neither experimental nor, perhaps more importantly, epidemiological data supports a link between cell phone usage and risk of intracranial neoplasia (reviewed in [3]).

Classification of brain tumors into subtypes is complicated by the fact that the histogenesis, or cell of origin, of many CNS tumors remains a mystery, one made even more challenging by the bewildering variety of microscopic appearances these tumors often present to the pathologists tasked with providing an accurate diagnosis. In an effort to provide meaningful diagnostic and prognostic information to clinicians, various classification schemes have been attempted and revised. In the past, these relied on features that could be appreciated with simple light microscopy such as growth patterns, cellular morphology, and resemblance to more differentiated cells. As modern investigative methods have been introduced, tools such as immunohistochemistry, chromosomal copy-number analysis, genetic and epigenetic analysis, and gene expression profiles have allowed further refinement of these classifications.

At this writing, the system most widely used by pathologists for classification of CNS tumors is the 2007 World Health Organization (WHO) Classification of Tumours of the Central Nervous System, Fourth Edition [5]. Within this system, distinct tumor entities are still defined primarily by their morphological appearances and patterns of growth, with attempts at incorporation of currently available immunohistochemical and molecular or genetic information when they are known and of proven prognostic value. Louis et al., in Greenfield's Neuropathology [3], acknowledges one of the limitations of morphology-based classification by

saying that “it must be recognized that histological appearances may not reflect cells of origin, i.e. that a tumour having cells resembling astrocytes does not necessarily result from transformation of astrocytes.” In the WHO classification system, in addition to a morphological diagnosis, CNS tumors are also given a grade in an attempt to assign a numerical value to the expected biological behavior: grade 1 (benign) to IV (highly malignant). One significant pitfall to this grading system is that small surgical biopsies, the size of which are often dictated by the critical importance of preserving adjacent non-neoplastic nervous tissue, may fail to adequately represent the overall nature of these often remarkably heterogeneous tumors. Likewise, basing prognosis on histopathological appearance alone fails to consider clinical parameters such as patient age, duration of disease, ability to perform radical excision, and others that have been shown to have a profound impact on eventual outcome [6]. For all of these reasons, it is vitally important that we continue to explore the molecular biology of CNS tumors via basic research methods and correlate that information with patient data to develop sophisticated and specific classification systems that will assist in the development of more accurate diagnoses and prognoses and more effective patient-specific therapies.

Gliomas: incidence and classification

Tumors that have been classified based on morphology and ancillary information as arising from the non-neuronal glial support cells of the CNS (astrocytes and oligodendroglia) or their progenitors are broadly referred to as “gliomas”. Gliomas account for 31% of all primary CNS tumors and 80% of malignant ones [1]. Technically, the term “glioma” can apply to a wide range of tumors of varying grades with morphologic differentiation toward astrocytic, oligodendrocytic, mixed astrocytic-oligodendrocytic or ependymal lines. In practicality,

however, the most clinically important entities in terms of morbidity, mortality, and overall treatment failure are the malignant, high-grade, astrocytic tumors (grade III anaplastic astrocytoma and grade IV glioblastoma), and it is on this category of glioma that the current project and much of the reviewed literature will focus. Despite decades of intense investigation into the biology of malignant glial tumors, survival for people with high-grade glial tumors remains dismal, with generally less than a two-year survival rate for those with grade IV tumors [1, 3]. In the past, the most aggressive, grade IV tumors were termed "glioblastoma multiforme" (GBM), an aptly descriptive older term that is reflective of their highly heterogeneous microscopic appearance. It is a term still favored by some neuropathologists and widely present in the literature despite the fact that the "multiforme" was officially removed in the third edition of the WHO classification of CNS tumors. A further division of the glioblastoma category into multiple subtypes (proneural, proliferative [which in turn encompasses 'neural' and 'classical' subtypes], and mesenchymal) has been made recently by Phillips et al. based on gene expression profiling [7]. In their study, they showed that these subclasses have prognostic value and resemble the various stages of neurogenesis. Tumors displaying the so-called "proneural" signature, which express markers associated with the differentiated neuronal lineage, were associated with longer survival times compared to the subclasses expressing markers associated with neural stem cells. Poor prognosis was also linked to expression of genes more commonly associated with mesenchymal tissues or proliferation and angiogenesis.

Terminology regarding "gliomas" in the literature can be confusing, primarily due to an inconsistent level of clarity regarding tumor grade, common conflation of the broad term "glioma" with high-grade malignant tumors, and changes in classification schemes subsequent to

original publication. Here the attempt will be made to use the most specific terminology possible when the discriminating information is available and where such differentiation is relevant to the topic or data at hand. If a distinction between grade III anaplastic astrocytomas and grade IV glioblastomas is possible and relevant to the cited information, these specific terms will be used; otherwise the terms “high-grade” or “malignant” gliomas will be used. If the reader encounters the general term “glioma”, she or he should consider that the information pertains to all grades of tumor.

High-grade gliomas: form follows function

In contrast to grade I tumors, which have a compact growth pattern and are generally amenable to surgical resection unless anatomically unapproachable, grade II, III, and IV tumors are characterized by a diffuse and extensive infiltration of the surrounding and distant brain structures and a tendency to progress over time (or post-treatment) to a more malignant phenotype via the acquisition of additional genetic alterations [3]. Features that suggest malignancy include cytological atypia, increased mitotic activity, high cellularity, microvascular proliferation, and necrosis. The distinction between glioblastoma and anaplastic astrocytoma is primarily based on the presence of areas of necrosis, at the periphery of which there is often pseudopalisading of neoplastic cells, along with the presence of highly anaplastic cells (though this may be multifocal), high mitotic activity and peripheral tortuous to glomeruloid microvascular proliferation [3] (Figure 1). Exceptions to these criteria, such as the so-called “small cell” glioblastoma, can complicate diagnosis and necessitate additional investigative measures.

Many, if not all, of the classic microscopic features of high-grade gliomas can be considered visible manifestations of the intrinsic tumor properties that successfully conspire to thwart current treatment modalities. In particular, the propensity for marked, widespread infiltration and migration of individual neoplastic cells preferentially along white matter tracts, sub-pial regions, and blood vessels precludes initial local control via surgical resection. Also, in the case of glioblastoma, areas of necrosis and robust (but ineffective) tortuous neovascularization produce microenvironmental conditions such as hypoxia and acidity that may contribute to acquisition of a radioresistant and chemoresistant stem-like phenotype, a feature of great importance to the relevance of this project.

Understanding the cell of origin: the intersection of gliogenesis and neoplasia

Any effort to understand the biology of glial neoplasms must incorporate current knowledge about normal gliogenesis in the embryo. Rudolph Virchow, the founder of modern pathology, first suggested the presence of supportive cells in the central nervous system in 1846, but hypothesized that they were of mesenchymal origin. Forty years later, Wilhelm His demonstrated a CNS origin of these cells, but proposed that neurons and glial cells came from two distinct progenitor pools [8]. More recent studies have shown that cells previously considered part of the dedicated "glial" lineage due to expression of surface glial-associated markers and certain intermediate filaments (radial glial cells) are in fact a neural stem cell compartment capable of generating both neurons and glial cells. Likewise, while it was once thought that glial cells were merely passive players in the nervous system milieu, they have in more recent times become appreciated for their roles in both active shaping of the

microenvironment and direct interaction and modification of neuronal growth and communication.

Not surprisingly for such a critical developmental process, early neural development occurs in a tightly temporally and spatially regulated fashion. The earliest origin of both neurons and glia is the pseudostratified neuroepithelial ectoderm lining the ventricles of the developing brain. Early in development, these neuroepithelial cells divide symmetrically to produce more neuroepithelial cells, and possibly early neurons. As the developing brain epithelium thickens, the neuroepithelial cells elongate and become radial glia (RG) that divide asymmetrically to produce 1) neurons, 2) intermediate progenitor cells (IPCs) that will in turn produce the "macroglial" (in contrast to *micro*glial cells, which are mesenchymal bone marrow-derived cells of the monocyte-macrophage system) supporting cells of the CNS, 3) ependymal cells that line the ventricles and produce cerebrospinal fluid, and 4) type "B" cells, the resident neural stem cells that persist in the adult subventricular zone and are capable of generating neurons and oligodendrocytes in a limited fashion throughout life via production of intermediate precursor cells. After the conversion of neuroepithelial cells to RG cells, the newly-formed RG extend long, diametrically opposed cell processes to contact both basal (meningeal, and eventually basal lamina and blood vessels) and apical (ventricular) surfaces, while retaining their cell bodies in the area immediately adjacent to the ventricles known as the ventricular zone (VZ) [9]. An important temporally concurrent step is the conversion of the neuroepithelial tight junctional complexes into adherens junctions [10], which is followed shortly thereafter by the formation of astrocyte-like contacts with endothelial cells of the forming vasculature [11]. After asymmetric division of RG cells to produce neurons, newly formed neurons use these radial glial processes as a scaffolding upon which to migrate toward the surface. Later, neurons produced from

intermediate precursor cells also use this scaffolding. At the end of embryonic development, RG detach from the apical surface and begin to express astrocytic surface markers [12-14], as well as the intermediate filament proteins nestin, vimentin, RC1/RC2 [15], and glial fibrillary acidic protein (GFAP) [16]. In addition to temporal regulation of progenitor heterogeneity, there is also spatial regulation, with early morphogen gradients leading to the establishment of different domains of neural progenitor cells in different areas of the brain producing distinct subtypes of neurons and macroglial cells [17-19]. Mechanistically, in addition to active promotion of neurogenesis, there also exists with some genes an antagonistic inhibitory balance between neurogenesis and gliogenesis, particularly early astrocytogenesis. Extracellular signaling cues can also affect gliogenesis and differentiation.

In summary, the process of gliogenesis involves a complex orchestration of genetic, epigenetic and extracellular signaling mechanisms. Early in embryogenesis, regulators of proliferation and stemness such as Notch and Wnt ensure adequate self-renewal of the stem cell population. Later, there is a shift to neurogenesis and neuronal migration, followed by a switch to gliogenesis often mediated by negative regulation by HLH proteins of bHLH transcription factors. As gliogenesis progresses, input from both epigenetic mechanisms and a variety of extracellular signals and microenvironmental cues influence differentiation. The fact that neurons and glia share a common progenitor ensures that their fates are inextricably linked, and because of this the study of gliogenesis has and will continue to provide important clues for unraveling the mysteries of many neurodegenerative and neoplastic CNS disorders, including gliomas.

Development gone awry: cancer as organ system and the cancer stem cell hypothesis

As previously discussed, high-grade gliomas and in particular glioblastomas are histopathologically heterogeneous tumors comprising complex arrangements of highly pleomorphic and infiltrative tumor cells, proliferating tortuous blood vessels, infiltrating inflammatory cells, and areas of necrosis. Pathologists and researchers have for nearly a hundred years attempted to better describe and define the underlying mechanism of this heterogeneity and lack of linear progression to malignancy, from Virchow's early postulating about the possible stem cell origin of cancers to Bailey and Cushing's classifications in the 1920's [20] to Rosenblum et al.'s proposals in 1981 of inherent variations in the chemosensitivity of clonogenic cells [21]. More recently, the concept of a "cancer stem cell" was proposed in the context of acute myeloid leukemia [22, 23], and was later extended to many solid organ neoplasms (reviewed in [24]), including gliomas. In this theoretical model, the bulk of the tumor is produced not by simple exponential clonal expansion of the entire population of neoplastic cells but rather is propagated by a (variably) small subset of cells that: 1) express markers classically used to identify embryonic or mesenchymal stem cells, 2) are capable of both self-renewal (symmetric division) and production of more differentiated daughter cells (asymmetric division) over prolonged passage *in vitro,* and 3) are capable of recapitulating the original tumor phenotype in xenograft assays when injected in relatively low numbers as compared to the "non-stem" population. The initial flurry of excitement over this theory centered primarily on the search for cell-associated markers and unique genomic and signaling pathways that might be exploited for targeted therapeutics; in glioblastoma this subpopulation of cells has been demonstrated to have increased chemoresistance [25] and radioresistance [26]. More recent investigations, however, have muddied the waters somewhat by exploring the complex confounding issues of potential microenvironmental influence on the acquisition of a stem-like

phenotype and gene expression profile (reviewed in [27]). Most recently, there have been investigations into stochastic state transitions that arise spontaneously within cells and give rise to a phenotypic equilibrium between "stem-like" and "non-stem-like" cells in some cell lines [28]. Terminology in the literature with regard to this cell population has been and remains confusing. Some authors refer to the stem-like population as "tumor initiating cells", a somewhat misleading term that refers not to the initial cell of origin of the tumor but to the subpopulation of cells capable of recapitulating the tumor in xenograft assays. Others use the terms "cancer stem cells" or "(tumor) stem cells". For the sake of clarity and consistency, throughout this work this population of cells will be referred to as cancer stem-like cells (CSLCs). Various methods to separate this subpopulation from the bulk of cells and propagate it *in vitro* for study have been proposed, each with its own set of supporting evidence and pitfalls. These methods rely on features such as: behavior in culture conditions (the neurosphere assay), expression of enzymes (side population, ABC transporters, and aldehyde dehydrogenase), or expression of molecular markers (CD133, nestin, SSEA-1, and HIF2α). What follows is a brief summary of evidence in support of each of these methods in glioblastomas, along with information about their known limitations.

Markers of cancer stem-like cells

In vitro growth assays

In 1992, Reynolds and Weiss described a method for isolating and culturing neural stem cells from adult mouse brain in which a small percentage of isolated cells, when grown in a defined serum-free media containing epidermal and basic fibroblast growth factors, formed free-floating spherical aggregates of cells [29]. Ignatova et al., in the Steindler lab [30] first

demonstrated that human glioblastoma cells, when cultured according to these methods, formed similar free-floating spheroidal aggregates of cells that variably expressed lineage markers of neural (βIII-tubulin) or glial (GFAP) cells, or had co-expression of both, and had upregulation of mRNA transcripts specific for genes associated with neural cell fate determination via the Notch-signaling pathway (Delta and Jagged) and cell survival at G2 or mitotic phases (Survivin). Although the formation of spheres in culture has come to be accepted as a *de facto* measure of self-renewal capacity and clonality (and thus stem-like behavior), there are increasing numbers of investigators who challenge this paradigm based on the growing body of experimental evidence that is shedding light on the limitations of the method. Firstly, spheres are difficult to grow, propagate, and dissociate for passaging, requiring specialized media, conditions, and (personal observation) luck. The spherical shape of the cellular aggregates makes estimation of cell numbers difficult and standardization of certain assays and molecular analyses extremely challenging. The three-dimensional nature of spheres creates a gradient in which cells at the center of the sphere are further removed from nutrients and oxygen than are those at the periphery, in effect creating differing microenvironments that may affect cell differentiation and death. Secondly, spheres represent a heterogeneous population, with a small number of cells exhibiting a true stem-like phenotype, and the much greater majority of cells consisting of differentiated and dying progeny [31]. While only bona fide stem cells can produce spheres over extended passaging (>6), more differentiated progenitor cells can give rise to secondary and tertiary spheres in the short term [32]. Since the rate of secondary sphere formation from dissociated glioblastoma spheres varies from 3-20% [33, 34], and only an estimated 6% of sphere-forming cells are true stem cells [32], this translates to a prevalence rate of less than 1-2%. Thirdly, real-time imaging of single-cell derived spheres labeled with different fluorescent

proteins demonstrated that migration and fusion of spheres with each other in routine sphere-culturing conditions is common, calling into question the concept of spheres as a *de facto* measure of clonality [35]. An alternative method for establishing CSLC-rich cultures from patient-derived glioblastoma specimens was proposed nearly simultaneously by two groups in England [36, 37] and is referred to as the "Cambridge protocol". In this protocol cells are grown on laminin-coated cultureware in serum-free media supplemented with N2 and/or B27 (defined mixtures of amino and fatty acids, hormones, and proteins), epidermal growth factor (EGF), and basic fibroblast growth factor (bFGF-2), as originally described for neural stem cells [38]. Both groups demonstrated that cell lines maintained in this way for >20 passages displayed various stem cell properties, maintained expression of stem cell markers, and were capable of initiating high-grade gliomas in xenotransplantation models when implanted in small numbers.

Molecular markers

CD133

The five-transmembrane-domain glycosylated protein CD133 was first identified by its extracellular epitope on human CD34+ hematopoietic stem and progenitor cells [39], and was given the name AC133 antigen. Soon thereafter, a mouse homolog that was localized to the apical microvilli of neuroepithelial stem cells was found and named prominin-1 [40]. A second glycosylated epitope, spatially distinct from AC133, was later identified, and was named AC141 [41]. Antibodies to these two separate epitopes (AC133 and AC141) are used to identify CD133-1/prominin-1 and CD133-2/prominin-2, respectively. The function of this protein has yet to be fully elucidated, but it is suspected to play a role as an organizer of plasma membrane topology, specifically with regard to lipid composition [42, 43]. Since its discovery in hematopoietic stem

cells, it has been used to identify a variety of stem and progenitor populations in many different solid tumors (reviewed in [44]). Singh and colleagues later used this marker to separate out a subpopulation of cells from brain tumors that were capable of self-renewal and multi-lineage differentiation; they identified these as "brain tumor stem cells" [45, 46]. Although analysis via flow cytometry of CD133-labeled cells indicates a low to nearly undetectable prevalence in primary human glioblastoma cultures, cultures generated from sphere-forming cells, and most established cell lines [46-50], a few studies have shown very high percentages (20-60%) of CD133+ cells in some glioblastoma cell lines (so-called glioma stem cell-enriched (GSC) lines) [46, 48, 51]. There is convincing evidence to support the presence of CD133+ stem cells within gliomas, namely that several published studies show that when freshly dissociated human gliomas are separated into CD133+ and CD133- cells, the CD133+ fraction displays increased *in vitro* stem cell properties such as proliferation, self-renewal, sphere formation, and ability to divergently differentiate, as well as demonstrating *in vivo* the ability of very small numbers of implanted cells to initiate tumors that recreate the original histopathology in mouse xenograft models [33, 46]. Additionally, in a study of 95 patients with gliomas, the proportion of CD133+ cells, as well as their organization into clusters, was a statistically significant prognostic indicator for both decreased progression-free survival and overall survival regardless of tumor grade, patient age, and degree of initial resection, as well as an independent risk factor for tumor regrowth and time to malignant progression in grade II and III astrocytomas [52]. Despite this evidence in support of the existence of CD133+ GSLCs, there is a growing parallel body of evidence that CD133- GSLCs exist as well, including the lack of detectable CD133 in some fresh glioblastoma samples, and the ability of some CD133- cells to produce tumors *in vivo* [50, 51]. Interestingly, CD133- cells subsequently derived from CD133+ cell lines are unable to form

tumors *in vivo* [53], suggesting that perhaps these cells differ from *de novo* CD133- cells, but cells that are initially CD133-, when co-cultured with CD133+ cells, *are* capable of forming tumors, and at a rate that is dose-dependent on the percentage of CD133+ cells in culture [26].

Another cause for concern when considering the validity and utility of CD133 as a biomarker of cancer stem-like cells is the fact that lowering the environmental oxygen tension results in a marked increase in expression of both the AC133 and AC141 epitopes, as well as upregulation of CD133 mRNA levels [54, 55]. Indeed, this mirrors the immunohistochemical distribution of CD133+ cells in areas surrounding necrosis or ineffective neovascularization seen in histopathology. In fact, the very ability to detect CD133 with available antibodies has been called into question for several reasons. Firstly, both AC133 and AC141 mAbs recognize glycosylated epitopes and may underestimate CD133 if glycosylation is not present, and at least one study has shown that glioblastoma cells negative via immunostaining for AC133 express a truncated form of the protein that can be recognized by antibodies (unfortunately no longer commercially available) directed against a separate, nonglycosylated, epitope [56]. AC133 and AC141 epitopes can be down-regulated independently of CD133 protein or mRNA [57, 58], and the tissue distribution of CD133 mRNA is much more widespread than AC133 expression [41]. As of this writing, 28 splice variants of human CD133 have been discovered [59] and, in addition to being expressed in a tissue-dependent fashion, are also regulated epigenetically via methylation [60]. Taken together these facts suggest that, until the function and full range of expression of CD133 is understood and a more thorough repertoire of methods exists to recognize a variety of epitopes and isoforms, caution should be exercised with regard to the reliability of this marker for either prospective or retrospective identification of cancer stem cells in glioblastoma.

Nestin

Nestin is a class IV intermediate filament that is present in stem and progenitor cells in the mammalian CNS during development [61]. During neurogenesis, it is expressed in stem cells, radial glial cells, and glial-restricted progenitor cells, and is progressively replaced by vimentin and then glial fibrillary acidic protein (GFAP) in astrocyte precursors [62-64]. In adults, nestin is expressed in neural stem cells of the subventricular zone and occasionally in endothelial cells [65]. In glioblastomas, the degree of nestin expression has been correlated with tumor grade and prognosis [65-68]. Intriguingly, nestin is upregulated in *in vitro* models by activation of the Notch pathway, a key pathway involved in maintenance of pluripotency, angiogenesis, and tumorigenesis via its regulation of cell-cell signaling and cell fate switching [69]. Notch signaling also is required for the conversion of a hypoxic stimulus into increased motility, invasiveness, and epithelial-mesenchymal transition in glioblastoma *in vitro* models, and hypoxia causes marked upregulation of Notch downstream pathways [70]. Thus, in the setting of glioblastoma, nestin may serve dual roles as a known marker of stem and progenitor cells as well as somewhat of a measure of Notch activation, and would be expected to be increased in hypoxic conditions because of this upregulation.

SSEA-1/CD15

Stage-specific embryonic antigen-1 (SSEA-1), also known as CD15 and LeX, is a fucose-containing trisaccharide that is highly expressed on stem cells in the developing brain as well as in the adult subventricular zone neural stem cell population [71, 72]. Son et al., in the laboratory of Howard Fine, used SSEA-1 to identify a population of CD133- cells within both freshly dissociated patient specimens and established glioblastoma CSLC-enriched cell lines [51]. This

population fulfilled all criteria for stem cell identification set forth by the authors, namely that they were clonogenic *in vitro*, expressed stem cell markers, were capable of neuronal and/or glial differentiation, were tumorigenic *in vivo* in serial transplantation assays, and were able to generate xenograft tumors that recapitulated the biological and genomic features of the parental tumor. The use of this marker may therefore be of utility in identifying a subset of tumor stem cells that do not express CD133 as recognized by currently available antibodies.

Functional assays

Side population method

This functional separation method is based on the use of Hoescht 33342, a fluorescent dye that binds to AT-rich areas within the minor groove of DNA [73]. All live cells are capable of uptake of the dye, but efflux can only be accomplished by a small percentage of cells, sortable by flow cytometry [74]. These cells are termed the "side" population (SP) because they fall to the side of the bulk of analyzed cells on FACS plots. Since its discovery, it has been used to separate stem and progenitor cells from a wide variety of normal and neoplastic tissues (reviewed in [75]), and experimental data has shown that the SP cell fraction has an increased ability for self-renewal and greater tumorigenic capacity in NOD-SCID mouse serial transplantation models than non-SP fraction, with as few as 50 SP cells initiating rapid tumor growth versus 500 non-SP cells that are required for production of tumors with similar frequency [76-83]. The ability of SP cells to efflux Hoescht 33342 dye is mediated by the ATP-binding cassette (ABC) transporter protein family, a superfamily of membrane pumps that mediate ATP-dependent transport of endogenous and xenobiotic compounds across lipid bilayer membranes and out of the cell (reviewed in [84]). They are present in large numbers in both normal stem

cells and CSLCs, but are inactive on most mature/differentiated cells [85]. In addition to having important effects on maintenance of the blood-brain and blood-cerebrospinal fluid barrier, these proteins also contribute to tumor chemoresistance via active transport of drugs out of the cells. The three main ABC transporter proteins responsible for this drug resistance are ABCB1/MDR1 (multidrug resistance protein 1), ABCC1/MRP1 (multidrug resistance-associated protein 1), and ABCG2/BCRP (breast cancer resistance protein); all have been identified in CSLCs of various tumor types (reviewed in [86]), and in human and rodent glioblastoma models specifically [76]. Of these, knock-out mouse models identify ABCG2 as the most responsible for the SP phenotype, with near-total loss of the bone marrow phenotype in $ABCG^{-/-}$ mice [87]. Although q-PCR identifies higher levels of ABCG2 mRNA in the glioma SP than non-SP fractions [76, 88], knockdown of this gene does not eliminate the ability of SP cells from human glioma cell lines to form tumors in mice [80]. This fact, coupled with the fact that not all normal tissue or cancer stem-like subpopulations have SP cells [89], suggests that either the SP assay lacks sensitivity or that it merely identifies one of several populations of stem-like cells. One additional note of caution for use of this assay is the documented toxicity of the Hoescht 33342 dye for non-SP cells [90-93], which may lead to experimental bias when determining viability and proliferation capacity of the SP vs. non-SP subpopulations.

Aldehyde dehydrogenase

As a member of the aldehyde dehydrogenase superfamily, which are NAD(P)-dependent enzymes, aldehyde dehydrogenase has two important functions with regard to stem cells. Firstly, it catalyzes oxidation of aldehydes to carboxylic acids and is important in cell detoxification for this reason, as aldehydes have the potential to be both cytotoxic and carcinogenic. Secondly, it

catalyzes the reaction of retinol to retinoic acid, an important modulator of cell differentiation and proliferation [94]. ALDH activity is measured most commonly by a commercially available assay, the Aldefluor™ assay (Stemcell Technologies), which relies on the ability of ALDH to convert the proprietary fluorescent substrate BIODIPY®-aminoacetaldehyde (BAAA) into the fluorescent product BIODIPY®-aminoacetate (BAA), which is detectable by flow cytometry. This assay has the added benefit of excluding dead cells from analysis, as only cells with intact plasma membranes and functional ALDH are able to convert the substrate and retain the product. Active efflux of BAA is prevented by ABC transporter blockers in the assay buffer, and the use of diethylaminobenzaldehyde (DEAB), an ALDH inhibitor, is used in a parallel sample to provide a negative control (technical bulletin, Stemcell Technologies). This assay has been used to identify stem cell populations in normal and neoplastic tissue [95], including glioblastoma [96].

Influence of the microenvironment: hypoxia and cancer stem-like cells

In addition to the inherent pitfalls in each of the currently available methods for *ex vivo* isolation of putative cancer stem cells for analysis and experimental manipulation, there exist additional pitfalls that are associated with propagation of any cell *in vitro.* Discussion of the myriad factors known to affect stem cell maintenance, differentiation, and proliferation in culture are well beyond the scope of this review. Though variables such as media composition, pH, and substrate stiffness have all been shown to impact the phenotype, growth pattern, and gene expression profiles of many types of normal and cancer stem cells, arguably no parameter of the artificial environment is as important and capable of profound effects as oxygen level. This is not surprising considering the critical role of oxygen in energy production, the most fundamental

of cell functions, as well as maintenance of pluripotency. In glioblastoma, there are three distinct anatomic hypoxic niches: 1) adjacent to areas of necrosis, 2) in perivascular areas, and 3) at the invasive edge of the tumor [27]. The first is fairly straightforward, but the second may seem counterintuitive until one considers that neovascularization often occurs in areas of the tumor that have had hypoxia-mediated upregulation of pro-angiogenic factors such as VEGF [97], and that these hypoxic conditions may persist despite the recruitment of new vessels. Glioma vasculature is often leaky, tortuous, and irregularly anastomosing, with arterio-venous shunts that might lead to lowered regional oxygen levels. In areas of rapid growth, the leading edge of the tumor can extend beyond the reach of existing vasculature, causing vascular damage and necrosis in the invaded tissue. Cells expressing stem cell markers have been identified in neural tumors in at least the first two of these niches [98], and have been postulated in the third [27]. The recognition of the biological importance of these hypoxic niches [99], as well as the fact that embryonic and mesenchymal stem cells reside in hypoxic niches, calls into question the use of the standard cell culture condition of 20% oxygen in cancer stem cell research. Explorations into the influence of reduced oxygen tension on the expression profile and phenotype of a variety of cancer cell lines, and correlation of this data with data from patient-derived biopsy samples prior to *in vitro* manipulation have demonstrated a strong role for hypoxia-induced transcription factors in both poor prognosis and the acquisition of a stem-like phenotype, even among cells not identified as CSLCs upon initial separation (reviewed in [100]).

When cells are exposed to hypoxic stress, they temporarily arrest in the cell cycle, decrease their energy consumption, secrete survival factors, and increase expression of proangiogenic genes [100]. Both transcriptional and post-translational mechanisms contribute to these responses, and the primary modulators of gene regulation in response to hypoxia are the

hypoxia-inducible factors (HIFs). The HIFs are members of the basic helix-loop-helix/Per-Arnt-Sim (bHLH/PAS) family of transcription factors that function as heterodimers composed of an oxygen-labile α subunit and a constitutively expressed, oxygen-stable β subunit. Mammalian species possess three α isoforms: HIF1α, HIF2α (EPAS1), and HIF3α, and three β subforms: Arnt1-3. HIF1α and HIF2α are the best characterized and most structurally similar, while HIF3α's function is less clear as it exists as multiple splice variants, some of which exert inhibitory transcriptional control over the other isoforms [101]. In normoxic conditions, HIF proteins have a short half-life of less than 5 minutes [102, 103], being targeted for ubiquitination and proteasomal degradation by the von Hippel-Lindau (VHL) tumor suppressor protein [104, 105] after hydroxylation of specific proline residues within an oxygen dependent domain by HIFα-specific prolyl hydroxylases (PHDs) [106]. Under hypoxic conditions, oxygen is unavailable to the PHDs as a co-substrate, and HIFα subunits are stabilized and subsequently translocate to the nucleus where they form a heterodimer complex with the β subunits. Once formed, the heterodimer binds to hypoxia-responsive elements (HREs) that contain a core RCGTG sequence, and HIF ancillary sequences (HASs) composed of imperfect inverted tandem repeats that recruit transcription factor complexes other than HIF as well [107]. More than 70 genes have been identified as bona fide direct HIF targets containing the HRE. More than 200 genes have been identified via microarray as being affected by hypoxia, and are therefore possible direct or indirect targets of HIFs [108]. Once the HIFs are bound to HREs, they must recruit additional transcriptional coactivators to form a fully functional initiation complex [109]. Though interactions with cofactors steroid receptor coactivator-1 (SRC-1) and transcription intermediary factor 2 (TIF-2) have been demonstrated indirectly, direct interaction has been proven only for p300/Creb-binding protein (CBP) [110-113]. Additional regulation of HIFα is

via hydroxylation of an asparagine residue in the C-terminal transactivation domain by factor inhibiting HIF (FIH), which inhibits interactions between HIFα and transcriptional coactivators [113] .

Beyond this "canonical" HIF pathway, a picture is emerging of additional "noncanonical" mechanisms of HIF regulation. In addition to protein regulation by hydroxylases, there is also evidence of negative regulation of HIFα at the mRNA level by miRNAs [114, 115] and mRNA destabilizing proteins [116], as well as post-translational modifications such as acetylation [117-119] and small ubiquitin-like modifier (SUMO) conjugation [120, 121]. Additionally, there is indirect regulation of HIFs via positive modulation of PHDs by factors such as iron, ascorbate, and 2-oxoglutarate levels, and by negative modulation by reactive oxygen species (ROS), nitric oxide, and TCA cycle intermediates succinate and fumarate (reviewed in [122]). The story of ROS regulation of HIF is made more convoluted by the fact that, although it has been demonstrated that peroxide-derived ROS directly inhibit PHD activity (likely via oxidation of PHD-bound Fe^{2+}) [123], there is also ROS inhibition of FIH, which has been shown to have even more sensitivity to oxidative stress than PHDs [124]. Although experimental evidence suggests that mitochondria produce significantly lower ROS under steady-state hypoxic versus normoxic conditions [125], far less is known about the effects of the spatially and temporally irregular and intermittent hypoxia that is likely to occur in the tumor environment. Sirtuin-3 (SIRT-3) is a mitochondrial deacetylase previously described as a tumor suppressor based on the presence of lowered mitochondrial integrity, abnormal metabolic function, and an increase in tumorigenic phenotype in SIRT3-/- cells [126]. It recently was shown to exert this effect via its destabilization of HIF1α through inhibition of ROS production [127] and subsequent removal of ROS inhibitory influence on PHDs and FIH. When considering the role of oxygen with regard

to stem cell biology, it is important to note that in contrast to more differentiated cells, these cells have decreased mitochondrial respiration. This is related to the shift toward the glycolytic metabolic pathway, a pathway known to be necessary for maintaining pluripotency in embryonic stem cells [128, 129]. The shift to glycolysis even in the presence of adequate oxygen (the so-called Warburg effect), though less desirable from an energy standpoint (2 ATP per glucose molecule vs. 36), does three things that are beneficial for both embryos and cancer cells: 1) it helps promote proliferation via an increased production of the metabolic intermediates necessary for amino acid and production and membrane synthesis; 2) it decreases production of ROS (a known DNA mutagen); and 3) it leads to decreased extracellular pH via the increase in lactic acid production, which aids in invasion and implantation of the blastocyst, and invasion of the surrounding parenchyma by cancer cells [122].

As mentioned before, HIF1α and HIF2α have both redundant and unique, or even opposing, functions, and the understanding of the complex relationship between these two factors is still in its early stages. At this writing, far more investigation has been done with regard to HIF1α, and many studies investigating hypoxia in cancer have not examined concurrently the role of HIF2α. During development, HIF2α is most abundant in vascular endothelial cells. Various knockout mouse models demonstrate that while HIF1α$^{-/-}$ mice die by embryonic day 11 with severe disorganization of the vascular system and gross neural tube defects, HIF2α$^{-/-}$ mice exhibit embryonic death by hemorrhage only rarely. Instead, HIF2α$^{-/-}$ mice have varying degrees of vascular disorganization (despite apparently normal vessel formation) or die neonatally of respiratory distress syndrome due to decreased VEGF levels, impaired fetal lung maturation, and surfactant insufficiency [130-133]. In the adult organism, while HIF1α is expressed ubiquitously in many cells of the body, expression of HIF2α is more

limited, with selective expression in vascular endothelial cells, type II pneumocytes, hepatocytes, renal interstitial cells, and myeloid lineage cells [134]. HIFs also are regulated differentially with regard to oxygen levels, with HIF2α being stabilized at more moderate oxygen concentrations of 2-5% and in chronic hypoxic conditions, while HIF1α accumulates only at lower concentrations of 0-2% and only in more acute hypoxia [135-137]. *In vivo*, while alveolar oxygen concentration is in the 14% range [138], close to atmospheric oxygen, normal brain oxygen levels range from 5-10%, and within glioblastomas can range from 10% to as low as 0.1%, with the majority of cells existing at 6-7% [139-141]. In several *in vitro* tumor models, exposure of cells to chronic moderate-to-severe hypoxia results in sustained elevated levels of HIF2α, while levels of HIF1α increase in response to acute hypoxia, but decline within several hours [136, 142]. This differential regulation is due at least in part to the presence of hypoxia-associated factor (HAF), an E3 ubiquitin ligase that binds to binds to both HIFs, but at different sites; when bound to HIF1α, it causes VHL-dependent proteasomal degradation, while binding to HIF2α leads to increased transactivation without degradation [143]. HAF is overexpressed in a variety of tumors [144-146], including glioblastoma, and experimental overexpression of HAF leads to a shift in hypoxia-dependent transcription from HIF1α to HIF2α [143].

Many cancers express or overexpress one or both HIF1α and HIF2α, and with few exceptions increased expression is correlated to poorer prognosis (reviewed in [147]). However, as mentioned previously, many of these studies failed to examine both HIF1α and HIF2α concurrently, and so it is difficult to draw conclusions with regard to differential importance. Analysis of human patient glioblastoma specimens at the mRNA level showed a correlation between increased expression of HIF2α , but not HIF1α, with poor survival [137]. With regard to the role of HIFs in the acquisition of the CSLC phenotype in glioblastoma, two separate

research groups have demonstrated a particularly compelling role for HIF2α, but not HIF1α. Work from the laboratory of Jeremy Rich [148] used a model in which cell cultures were enriched or depleted of putative CSLCs based on initial separation by CD133 staining, and then analyzed for stem-like behavior (via neurosphere assay, tumorigenic capability in mouse xenografts, and expression of stem cell genes) after transduction of a non-degradable form of HIF2α in which two proline residues are mutate to alanine (referred to as HIF2α -PA) to prevent hydroxylation by PHDs [149]. In their model, they demonstrate that expression of HIF2α-PA alone is sufficient to reprogram the differentiated, non-stem-like population of cells toward an undifferentiated state. Transduction with HIF2α-PA increased the percentage of CD133+ cells, induced morphological changes including sphere formation, and increased transcript levels of target stem cell genes OCT4, NANOG, and c-MYC. Furthermore, while expression of HIF1α was present in both glioblastoma CSLCs and normal neural stem cells, expression of HIF2α was restricted to CSLCs; therefore, the authors suggest that HIF2α represents a tempting CSLC-specific, NSC-sparing therapeutic target. Work in the laboratory of Frisén and Acker [150] using multiple established human glioblastoma cell lines demonstrated that hypoxia of 1% leads to overexpression of CD133 and side population signature genes, and that siRNA-mediated knockdown of HIF2α, but not HIF1α, abrogated these effects.

To elucidate the common and disparate DNA targets of HIF1α versus HIF2α, chromatin immunoprecipitation in conjunction with a human promoter microarray (ChIP-CHIP analysis) was performed on MCF7 breast cancer cells cultured in 1% oxygen or dimethyloxalylglycine (DMOG)-induced chemical hypoxia for 16 hours [151]. This work showed several differences between the genome-wide association patterns of HIF1α versus HIF2α and highlighted the fact that both HIFα isoforms bind to an identical core DNA sequence (RCGTG), and many loci

bound both isoforms with similar affinity; however, siRNA-mediated knockdown of HIF1α produced down-regulation of 15.6% of its gene targets versus only 1.5% for HIF2α. The authors suggest that these results indicate that HIF2α's effects under these experimental conditions may be more indirect.

In summary, while much remains to be elucidated about the complex influence of the microenvironment in general, and oxygen tension specifically, on the development and maintenance of the cancer stem cell phenotype, recent work offers compelling justification for further examination into the role of HIF2α in glioblastoma biology and the potential role of HIF2α-targeted therapy.

Animal models and the utility of the canine patient

Various animal models have been used to study the biology of high-grade astrocytic tumors and evaluate the safety and efficacy of potential therapeutics, including xenografts in immunocompromised mice, transgenic mice, allogeneic transplants in *in utero*-tolerized dogs, and chemical-induced rodent models. Each of these models has its advantages, but each in some way fails to fully reflect the true biology of naturally-occurring *de novo* disease. One particular concern of rodent models is the failure to reproduce the practical challenges associated with treating much physically larger and more complex human and non-human animal brains. Domestic canine patients with spontaneous high-grade gliomas provide us with a unique opportunity to study naturally-occurring disease in higher-order mammals whose brain and body often differ only moderately in size and complexity from human patients. Thanks to the benefit of modern sophisticated veterinary medicine and preventive care, pet dogs frequently have extended life spans as compared to their feral or lupine counterparts, with a similar proportion of

juvenile, adult, and geriatric stages as their human caretakers. Because these dogs live in close physical proximity to their owners, they often encounter many of the same indoor and outdoor environmental exposures as well. Over the past several hundreds of years, extensive inbreeding of dogs has occurred due to human selection for specific physical or temperamental traits. This fact allows for the study of polymorphic loci responsible for breed-associated predispositions (such as those of the brachycephalic breeds for developing gliomas, and of dolichocephalic breeds for meningiomas), which in turn may lead to discovery or deeper understanding of the loci responsible for analogous diseases in humans [152]. Many people in our society view their companion animals increasingly as members of the family and are willing to pursue sophisticated and thorough diagnostic and therapeutic options. With informed consent, many of these owners have been willing to enroll their dogs in preliminary clinical trials that not only benefit directly the pets themselves, but also serve as a valuable large-animal model stepping stone for promising future therapies for the corresponding human disease.

In comparison to the body of work surrounding human high-grade gliomas, there is a relative paucity of published data on canine gliomas, and the majority of that is primarily concerned with diagnostics, therapeutics, and clinical outcomes rather than fundamental basic research. As of this writing, there has been no published peer-reviewed data on the effects of defined microenvironmental conditions on the expression patterns of canine high-grade gliomas in an *in vitro* model. What we do know is that dogs, in general, and certain breeds disproportionately, suffer from gliomas very similar in gross and histopathological appearance to their human counterparts. Unfortunately, the veterinary WHO classification system for nervous system tumors has not been updated since 1999 and uses a three-tier classification system for astrocytic tumors (low-, medium-, and high-grade), in contrast to the aforementioned four-tier

system recommended in the human WHO guidelines. Nevertheless, classic features such as diffuse and invasive growth, highly pleomorphic cell populations, high mitotic rates, areas of necrosis flanked by pseudopalisading cells, and peripheral tortuous to glomeruloid neovascularization are well documented in high-grade canine tumors, and some veterinary pathologists grade them according to human diagnostic criteria. Determining the true incidence of brain tumors in the canine population is problematic, as there is currently a wide discrepancy in the degree to which owners are willing and able to pursue advanced diagnostics such as MRI and brain biopsy that are necessary for definitive diagnosis. Nevertheless, there are several published studies available that report the incidence of primary brain tumors ranging from 20 per 100,000 (0.02%) [153] in a population of dogs in the United Kingdom in a single year, to 1.9% of a population of 6,175 dogs necropsied in a multi-year single-center study in the United States, with 70% of those being gliomas [154]. Survival and progression data in cases of canine high-grade gliomas is skewed as well, due to the fact that when clinical signs become severe and cease to be medically manageable, many owners choose to humanely euthanize these animals rather than allowing the disease to progress to its natural endpoint. This leads to underestimation of progression and survival times both with and without therapeutic intervention and makes comparison among cases less meaningful. Certain breeds such as Boxers, Boston terriers, and French Bulldogs are highly predisposed to gliomas [155], with a relative risk of 23.3 for Boston terriers and 5.2 for boxers of developing any glial tumor compared with reference breeds. Much of the work that has been published regarding canine gliomas has focused on biomarkers that have been proven to be useful in human patients as diagnostic tools and prognostic indicators, rather than basic molecular and genetic research. A brief review of the current state of knowledge regarding canine gliomas follows.

Activating mutations and overexpression of the epidermal growth factor receptor (EGFR) are common in human malignant gliomas, and are important in the progression to a more malignant phenotype. EGFR is a member of the receptor tyrosine kinase (RTK) family, and increased EGFR activity enhances mitogenesis and angiogenesis via PI3K and Ras signaling pathways while reducing apoptosis [156]. Additionally, EGFR upregulation can enhance invasion and migration via upregulation of matrix metalloproteinases and collagens [157]. A recent study correlated immunohistochemical reactivity for EGFR with tumor invasiveness in canine astrocytic tumors [158], but EGFR status as a prognostic or predictive marker was not examined. Another canine study, using tissue microarray and immunohistochemistry, showed increased EGFR expression in 57% of examined glioblastomas, 40% of grade III astrocytomas, and 28% of grade II astrocytomas, closely paralleling the expression profile distribution of human astrocytic tumors [159]. Similar results were found by these authors with regard to platelet-derived growth factor receptor alpha and insulin-like growth factor binding protein 2, both of which are members of the RTK family that are known to be important in human glioma biology and represent possible therapeutic targets.

Signaling through its two RTK receptors, VEGFR-1 (Flt-1) and VEGFR-2 (KDR), vascular endothelial growth factor (VEGF) is a key regulator of both normal and pathological angiogenesis [160]. Upregulation of VEGF by factors such as decreased oxygen tension results in tumor neovascularization and increased vascular permeability that can lead to peritumoral edema [161, 162]. VEGF receptors are expressed by vascular endothelial cells within the tumor and at its periphery, but are largely absent in normal human brain endothelial cells (reviewed in [162]). In dogs, increased intratumoral expression of VEGF mRNA correlates with increasing glioma tumor grade; however, mRNA levels of its receptors VEGFR-1 and -2 did not

significantly differ among tumor grades [163-165]. Three isoforms of VEGF are recognized in the dog: $VEGF_{120}$, $VEGF_{164}$, and $VEGF_{188}$; $VEGF_{164}$ is the most highly expressed of the three [163].

The *p53* tumor suppressor gene functions as the "guardian of the genome" by inducing cell cycle arrest at G1 or apoptosis in cases of DNA damage. In humans, loss of this gene appears to be an early event in gliomagenesis, and has been identified in both low and high-grade gliomas (reviewed in [166]). A recent publication identified a single point mutation of *p53* in one out of twelve analyzed DNA samples derived from formalin-fixed paraffin-embedded canine glioma tissue [158]. A more recent, larger study [167] examined genomic DNA from a series of 37 glial and 51 non-glial canine brain tumors for the presence of mutations involving exons 3-9 , which cover the DNA-binding domain in which 90% of human mutations are found. In this study, the rate of exonic mutations was 3.4% overall, and 5.5% in astrocytic tumors, which is a markedly lower rate than the 26% found in human brain tumors [168]. These authors also tested the canine glioblastoma cell line J3T (used in our work) and found no mutations. Whether this decreased rate of *p53* mutation as compared to human gliomas is a function of disparate biology or simply unfortunate distribution of smaller sample populations is unclear and will only be clarified with large-scale multi-institutional studies.

Justification of the project

In conclusion, justification for this project lies with several key facts: 1) high-grade gliomas continue to inflict significant morbidity and mortality in both humans and dogs despite decades of intensive research; 2) dogs may serve as valuable large-animal models of naturally-occurring disease, and clinical trials in dogs may serve as an intermediate step between rodent

models and human clinical trials; and 3) the usefulness of canine patients to serve in this capacity and the ability to develop novel therapeutic modalities for dogs requires a more detailed understanding of the comparative biology of the canine disease in both *in vitro* and *in vivo* models. This molecular study details *in vitro* evaluation of hypoxia on a canine glioblastoma cell line as an initial first step to understanding how hypoxia affects canine glioblastoma biology.

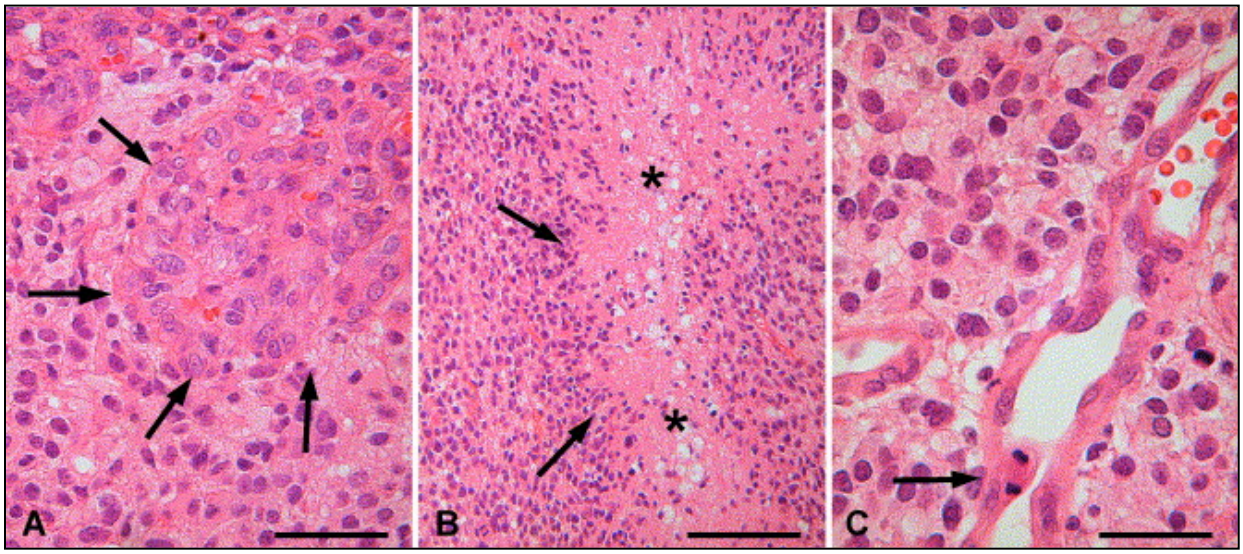

Figure 1. Histopathological features of glioblastoma. (A) Typical tuft-like peripheral "glomeruloid" vascular proliferation (arrows). Scale bar: 70 μm. (B) Necrotic area in tumor (asterisk) surrounded by pseudopalisading tumor cells (arrows). Scale bar: 150 μm. (C) High power magnification of microvascular proliferation. Note thickened vessel wall with mitotic figure (arrow). Scale bar: 50 μm. Reproduced with permission by Elsevier from: Jansen, M., et al., *Current perspectives on antiangiogenesis strategies in the treatment of malignant gliomas*. Brain Research Reviews, 2004. 45(3): p. 143-163.

CHAPTER II.

INITIAL EVALUATION OF AN *IN VITRO* CANINE GLIOBLASTOMA MODEL TO EXPLORE THE EFFECTS OF HYPOXIA ON EXPRESSION OF SELECTED PUTATIVE CANCER STEM-LIKE CELL MARKERS

Introduction

In keeping with the overall justification of the project, namely the need for additional molecular-level investigation into the comparative biology of canine glioblastoma and its appropriateness as a potential comparative and translational model for the human disease, the purpose of this initial study was to serve as an exploratory assessment of the effect of hypoxic environmental conditions on the acquisition of a CSLC gene expression profile in a canine glioblastoma *in vitro* model. In order to maximize resources, a panel of three of the most promising and widely examined glioblastoma CSLC markers possessing non-redundant function was selected: CD133, nestin, and HIF2α (all discussed in Chapter I). Additionally, CD31 expression was examined. CD31, also known as platelet endothelial cell adhesion marker (PECAM), is an immunoglobulin superfamily member that is present on the surface of platelets, monocytes, neutrophils, and certain types of T cells, and comprises a large portion of endothelial cell intercellular junctions. Two separate groups have shown that, in addition to having areas of tortuous neovascularization, glioblastomas also contain areas in which cancer cells have undergone transdifferentiation to become endothelial-like cells that have the same chromosomal derangements as the parent cancer cell [169, 170]. Furthermore, exposure of glioblastoma cell

lines to either 2% oxygen or the chemical hypoxia mimetic desferoxamine increased CD31 expression even in the presence of anti-VEGF antibodies [170].

Materials and methods

Cell culture

The canine glioblastoma cell line J3T, a gift from Dr. Michael Berens (Translational Genomics Research Institute, Phoenix, AZ), was used for this study. When grown in serum-supplemented medium, these cells grow as an adherent monolayer. When grown on standard Corning polystyrene culture ware in defined serum-free medium (DMEM supplemented with B27, 20-ng/mL EGF, and 20-ng/mL bFGF), they form two populations: an adherent fraction ("adherent") and floating spheroidal aggregates of cells ("spheres"). Spheres were collected and manually dissociated, then placed on Corning polystyrene cultureware coated with laminin (Sigma) diluted 1:100, according to the Cambridge protocol [36, 37]. For the purpose of this preliminary study, four different cell culture conditions were compared: 1) DMEM supplemented with 10% fetal calf serum on uncoated culture ware in 20% oxygen 2) defined serum-free medium (adherent fraction) on uncoated culture ware in 20% oxygen, 3) defined serum-free medium (spheres) on laminin-coated culture ware in 20% oxygen, and 4) defined serum-free medium (spheres) on laminin-coated culture ware in 2% oxygen chambers. Cells were cultured for 6-7 days in each of their respective culture conditions prior to collection for RNA extraction and subsequent q-PCR analysis.

Hypoxic chambers

To produce low oxygen concentrations without the use of costly specialized incubators and hoods, lab-built hypoxic chambers were constructed according to a published Nature

protocol by Wright and Shay [171]. Briefly, one-liter Nalgene containers were inverted and ½ inch holes drilled through the bottom. Culture flasks were placed inside these containers and silicone vacuum grease (Dow Corning) was applied to the threads before screwing the lids on. A specialized gas mixture consisting of 2% oxygen, 5% carbon dioxide, and 93% nitrogen (Airgas, Theodore, AL) was pumped through a low-flow medical oxygen regulator (VWR catalog #55850-388) connected to silicone bubble tubing at a rate of 2L/minute for two minutes, and then the holes were sealed quickly with vacuum grease-coated silicone corks. Chambers were then placed within a standard CO_2 incubator delivering conditions of 37°C, 5% CO_2, and 100% humidity. When cultures required addition of growth factors or media change, these processes were performed in standard environmental oxygen, and then cells were returned to the chambers and re-gassed as before.

RNA extraction

Cells were dissociated using a proprietary enzyme product (Accutase, Thermo Scientific), centrifuged at 500 rcf for 3 minutes, and flash frozen in liquid nitrogen and stored at -80°C until RNA extraction with Tri-Reagent (Molecular Research Center) according to published protocols [172]. Extracted RNA was resuspended in DNAse, RNAse, sterile, endotoxin-free water with a pH of 7.0 and evaluated on a Nanodrop spectrophotometer (Thermo Scientific) for concentration and assessment of measurements at 230, 260, and 280 nm wavelengths with subsequent calculation of 260/280 and 260/230 ratios. RNA samples were subjected to electrophoresis on a non-denaturing agarose gel for confirmation of distinct 18S and 28S ribosomal bands indicative of a lack of degradation. Extracted RNA was frozen at -80°C until use and not subjected to repeated freeze-thaw cycles.

q-PCR

cDNA was produced using the Quanta Biosciences qScript cDNA kit, utilizing 1-µg of RNA per 20-µL reaction. This kit contains a mixture of an engineered Moloney murine leukemia virus reverse transcriptase and a ribonuclease inhibitor protein, and uses a mix of both oligo(dT) and random hexamer primers. Upon completion of the reaction, 3-ul of undiluted product was used in q-PCR reactions. Primer sequences for CD133 and nestin were from a published report [173], while primer sequences for HIF2α and CD31 were designed by us using the Primer3 program at NCBI (http://www.ncbi.nlm.nih.gov/tools/primer-blast) to produce a product approximately 200 base pairs long, with a G-C content less than 65%, and spanning at least one intron (Table 1). Sequences were amplified using SYBR green master mix (Bio-Rad) on a Bio-Rad C1000 thermal cycler and analyzed using CFX Manager 1.6 software. All primers were purchased from a single source (Eurofins MWG Operon), reconstituted in nuclease-free water, stored at -20°C until use, and not subjected to excessive freeze-thaw cycles. Each primer pair was optimized for cycling conditions and tested for comparable efficiency using a modified standard curve method over a wide range of template dilutions. Samples were run in technical triplicates and plates included negative controls consisting of reverse transcriptase-omitted products of the cDNA reaction (no-RT control) and samples in which nuclease-free water was substituted for cDNA template (no-template control). PCR products were subjected to electrophoresis on agarose gel containing 5% Gel Red (Biotium) and visualized on a Fotodyne convertible UV transilluminator to confirm a single band of the expected size. Products were purified and submitted to the Harvard University DNA sequencing core laboratory at Massachusetts General Hospital for confirmation of product identity.

Statistical analysis

Calculations of relative gene expression were made using the Bio-Rad CFX Manager 1.6 software according to the ΔΔCt method [174], using the cell cycle-independent ribosomal protein L37 for normalization. Significance was tested by one-way analysis of variance (ANOVA) using SAS 9.3 with macros published by Zhenyi Xue [175] for the analysis of relative expression data with standard deviations, with significance level set as $p \leq 0.05$.

Results

Because there has been much work published that examines the use of sphere formation in defined media as an indicator of stem-like behavior, in our model we attempted to culture J3T cells according to a modified version of the Reynolds and Weiss protocol [29] using a defined serum-free medium supplemented with B27 and human epidermal and basic fibroblast growth factors ("SFM"). The initial aliquot of cells received from Dr. Berens' lab was expanded in DMEM/10% fetal calf serum, then split into multiple aliquots of approximately 1-2 x 10^6 cells in freezing medium (fetal calf serum with 10% DMSO) and kept at -180° C until use. Production of spheres by different aliquots of J3T cells was erratic and unpredictable, limiting our ability to standardize experiments with regard to time in culture and number of passages. The best results were achieved by seeding cells at a low density (~1-5 x 10^5 per T-75 flask), replenishing growth factors every 48-72 hours, and collecting floating cells and either culturing separately in SFM or putting them back into flasks when changing media. In general, when spheres formed, they formed after approximately 5-8 days in culture and appeared as variably-sized roughly spherical aggregates of cells either floating completely freely in the culture medium or tethered to the flask bottom by a single thread-like process (Figure 2A). A much larger fraction of the cells, and in

some cases, all of the cells, grew as an adherent monolayer with a plump, rounded, spindle-shaped to stellate morphology (Figure 2B). Collected spheres were then either dissociated with gentle trituration or plated without dissociation onto laminin-coated culture ware (Cambridge protocol), to which they attached (Figure 3A) and spread out to form a tightly adherent monolayer of stellate to triangular cells (Figure 3B) with morphology similar to cells cultured in DMEM/10% fetal calf serum.

Sphere-forming cells from the J3T canine glioblastoma cell line, when cultured on laminin-coated flasks in defined serum-free medium according to the Cambridge protocol in 2% oxygen for seven days, showed statistically significant transcriptional upregulation of the putative glioma CSLC markers CD133, HIF2α, and nestin relative to cells grown in 20% oxygen in 1) serum-supplemented medium, 2) serum-free medium (adherent), and 3) serum-free medium (spheres) on laminin-coated culture ware (Figures 4, 5, 6), and statistically significant upregulation of angiogenesis marker CD31 relative to cells grown in 20% oxygen in 1) serum-supplemented media, and 2) serum-free medium (spheres) on laminin-coated culture ware (Figure 7). There was, however, minimal difference in gene expression among samples grown in normoxic conditions with the exception of CD133 expression, which was upregulated in the sphere-forming cells grown per the Cambridge protocol in 20% oxygen compared to the serum-supplemented cells and the adherent fraction in serum-free medium.

Discussion

The Cambridge protocol is an alternative method for establishing CSLC-rich cultures from primary patient-derived glioma samples that was proposed nearly simultaneously by two groups in England [36, 37]. This method involves growing primary sphere-forming cells as a

monolayer on laminin-coated culture ware in a similar defined serum-free media as the Reynolds and Weiss protocol [29]. This allows for expansion of cells as a monolayer, which avoids many of the disadvantages of the sphere assay such as heterogeneity of spheres, death of cells at the interior, uneven exposure to growth factors and oxygen, and difficulty in performing cell-based assays. Both research groups demonstrated that cell lines maintained in this way for >20 passages displayed stem cell properties and maintained expression of stem cell markers, including the ability of small numbers of cells to initiate high-grade tumors recapitulating the original histopathologic appearance in xenotransplantation models. Although these authors were developing cell lines from freshly dissociated patient specimens, we included this method in our experimental design based on its proven utility in providing an environment conducive to the growth and expansion of CSLCs.

The purpose of this exploratory study was multifaceted. Despite the growing interest in the use of companion dogs with naturally-occurring gliomas as promising large animal models for pre-clinical trials of novel therapeutics and the work of several groups investigators, there remains a relative paucity of basic research confirming the similarities between the canine and human disease at a molecular level. Many techniques used in human *in vitro* studies have either not been validated in canine models, or the results have not been published. In this preliminary study, we have demonstrated several important and previously unverified similarities between canine and human glioblastomas with regard to response to hypoxia. We confirmed that the Cambridge protocol can be used with this particular well-established canine glioblastoma cell line, and that these cells, when exposed to 2% oxygen for prolonged periods, show significant transcriptional upregulation of genes (CD133, HIF2α, and nestin) identified as putative CSLC markers when compared to cells grown in either serum-supplemented or defined serum-free

media in 20% oxygen. We further validated the use of a low-cost lab-built hypoxic chamber constructed according to previously published protocols [171]. Because the study of hypoxia often involves the use of expensive specialized incubators, this will likely be of particular interest to veterinary and comparative researchers who often work with very limited budgets and could not otherwise produce these experimental conditions.

Comparison among various human and rodent *in vitro* glioblastoma hypoxia studies in the literature is extremely difficult, owing to the lack of standardization in terms of 1) type of sample used (freshly dissociated, primary cultures, established cell lines, CSLC-enriched cultures separated initially based on different markers), 2) specific composition of culture medium used, 3) oxygen level used and whether it was incubator-generated, chamber-generated, or chemically-generated, 4) time in culture prior to experimental manipulation and time in hypoxia, and others. Nevertheless, our results confirm that this canine *in vitro* model adequately recapitulates some of the responses to hypoxia documented in multiple human glioblastoma studies [44, 52, 53, 55, 65-69, 100, 147, 148, 150, 176-179], and provides additional strong support for consideration of the effect of hypoxia on acquisition of the CSLC phenotype. An additional finding of interest was increased CD31 expression in the hypoxic cells when compared to the normoxic serum-supplemented and sphere-forming cells (and closely approaching statistical significance in the adherent fraction cells). Although the full biological significance of this cannot be elucidated without further work documenting additional gene expression and morphologic changes consistent with endothelial transdifferentiation, it is intriguing.

One limitation of this model system was the use of an established cell line. The significant time, expense, and technical difficulty involved in establishing a stable, single-cell-

derived cell line from primary patient specimen, as well as the unfortunate paucity of clinical specimens available for culture during this time period precluded inclusion of primary patient-derived cell lines in this part of the study. Currently, there are no commercially available canine glioblastoma cell lines. Dr. Michael Berens' J3T canine glioblastoma cell line was initially derived from a spontaneous canine glioblastoma in a Boxer breed dog, and has been well characterized [180-183]. It has been unfortunately also serially passaged in the presence of fetal calf serum, which has been shown in some human glioblastoma cell lines to result in variably significant phenotypic and expression profile changes that do not reflect the nature of the primary tumor from which the cells were originally derived [184]. This may be the reason that in our hands sphere formation was erratic and rare, and may have some significant implications for the overall utility of this particular model with regard to CSLC investigations. Because overall there was not a very significant difference between sphere-forming cells grown in normoxia and mixed cells grown in normoxia, and because sphere formation was problematic, subsequent investigations dispensed with attempts to produce spheres and instead utilized mixed J3T cells grown according to the Cambridge protocol. The decision to use this cell line was a compromise between the availability and dependability of a well-characterized line and the awareness of the potential for serum-induced alterations. At the time of our initial experiments, no data had been published on this cell line with regard to the identification of putative CSLCs or other distinct subpopulations within the line. Subsequently, one group of investigators reported that J3T cells, when passaged in nude mouse xenografts, were capable of diverging into two separate populations that the authors named J3T-1 and J3T-2 [182]. As measured by immunocytochemistry and q-PCR, these populations appeared to have different expression profiles and produce histopathologically distinct tumors in their mouse model. J3T-1 cells

clustered around newly developed vessels at tumor borders, whereas J3T-2 cells showed diffuse single-cell infiltration into surrounding normal brain tissue. It is not clear whether the divergent populations occurred as a result of selection pressure and acquisition of additional genetic mutations in the investigators' study or whether these differences exist in the earlier-passage cells as well.

Additional limitations of the model with regard to the hypoxia chambers were the inability to monitor the integrity of the chambers and the inability to perform necessary cell manipulations in lowered oxygen, thereby creating a situation of intermittent rather than consistent hypoxia. While intermittent hypoxia may indeed mimic the *in vivo* microenvironment in some areas of a tumor, for the purposes of standardizing conditions across experiments and generating data that investigates a single specific environmental condition it is more desirable to minimize variation. For this reason, we chose to limit the studies detailed in subsequent chapters to time frames within which no cell manipulation was required, and to evaluate the efficacy of chemical hypoxia mimetics. Despite its limitations, this study details for the first time several important similarities between canine and human glioblastoma with regard to the influence of hypoxia on expression of multiple putative CSLC markers at the transcriptional level *in vitro*.

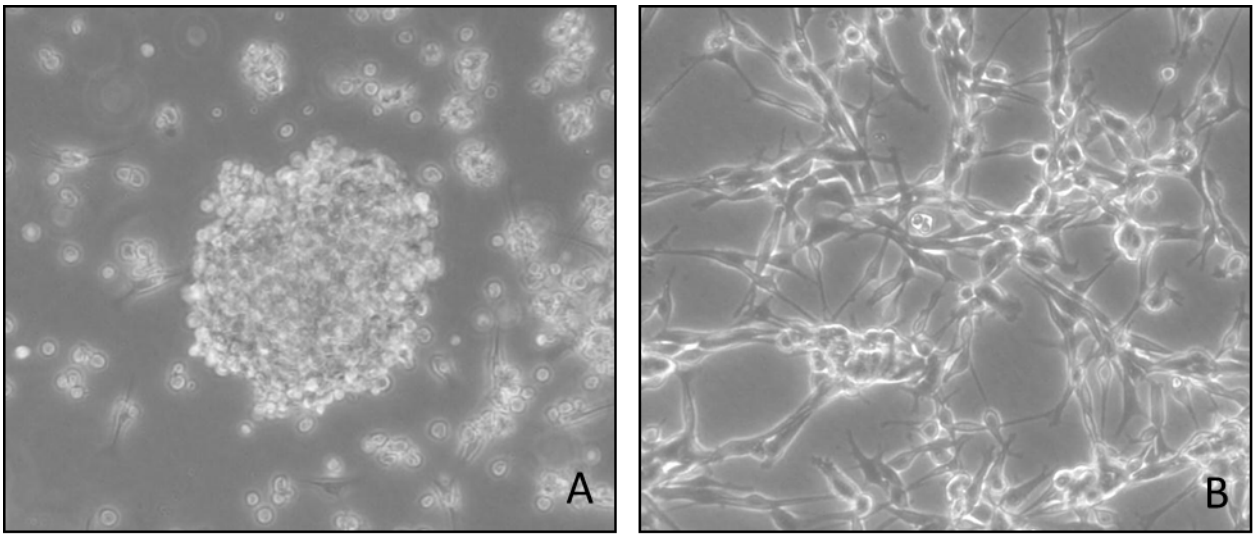

Figure 2. Phase-contrast photomicrographs of J3T canine glioblastoma cells grown in defined serum-free medium on non-coated culture ware, forming two populations of cells visualized as (A) floating, roughly spherical aggregates of tightly compacted, small, rounded cells (spheres), and (B) non-sphere-forming cells growing an adherent monolayer with a plump, rounded, bipolar spindle-shaped to stellate morphology (adherent).

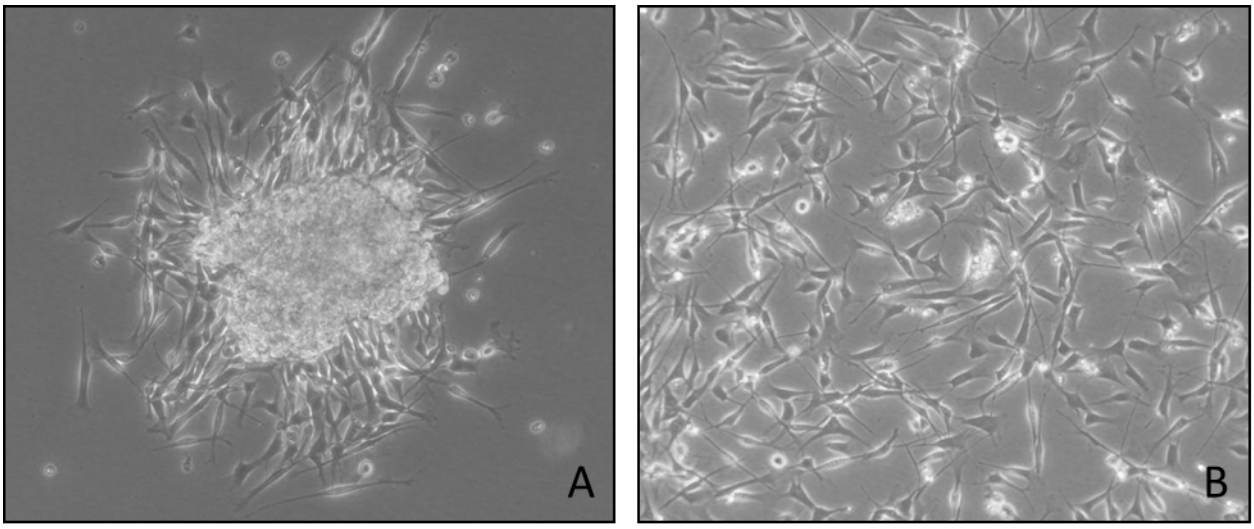

Figure 3. Phase-contrast photomicrograph of a J3T canine glioblastoma sphere grown in defined serum-free medium on laminin-coated culture ware as per the Cambridge protocol, (A) approximately 24 hours after plating, and (B) approximately one week after plating. Note that cells migrate outward to form a tightly adherent monolayer with morphology similar to that of cells cultured in serum-supplemented medium (not shown).

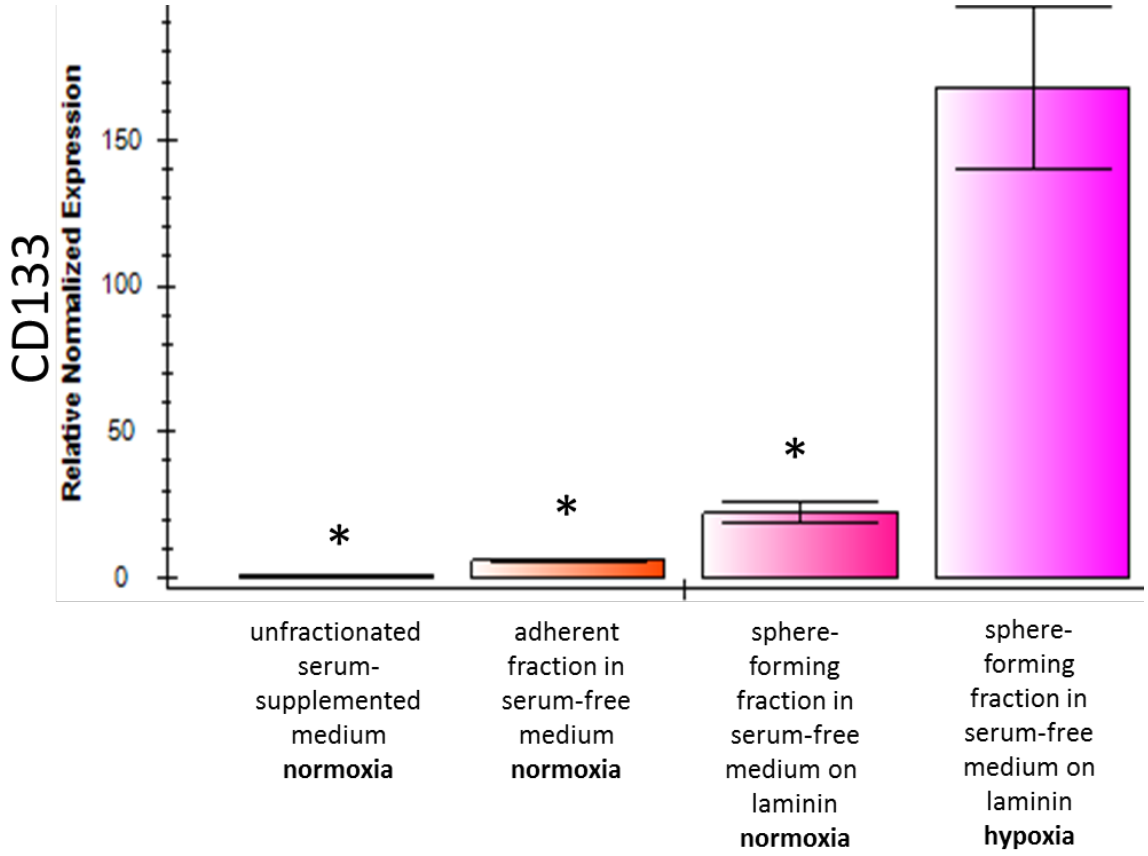

Figure 4. Relative normalized expression levels of CD133 as measured by q-PCR in canine J3T glioblastoma cells under various culture conditions. Expression is displayed in arbitrary units. Bars denote +/- one standard error of the mean. Asterisks indicate statistically significant difference ($p \leq 0.05$) from sphere-forming cells grown in serum-free medium on laminin-coated culture ware for seven days in 2% oxygen.

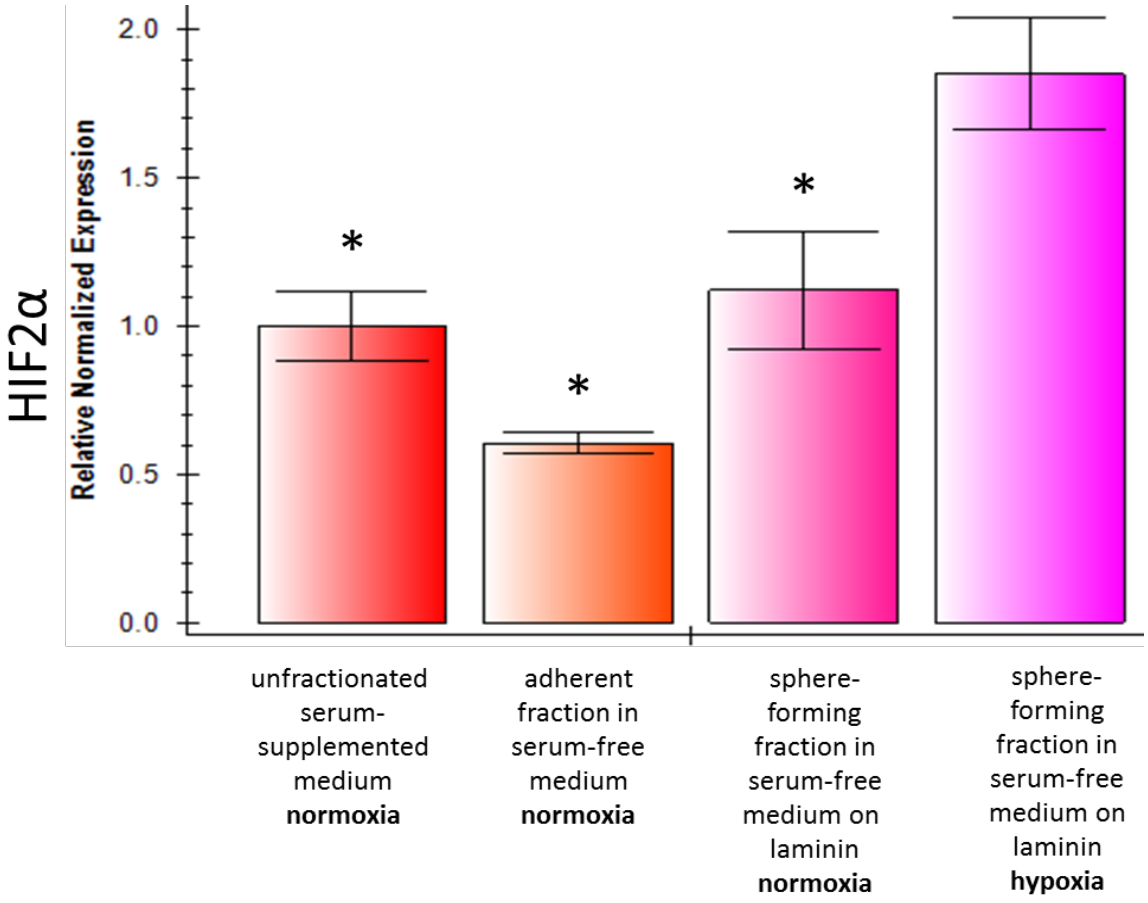

Figure 5. Relative normalized expression levels of HIF2α as measured by q-PCR in canine J3T glioblastoma cells under various culture conditions. Expression is displayed in arbitrary units. Bars denote +/- one standard error of the mean. Asterisks indicate statistically significant difference ($p \leq 0.05$) from sphere-forming cells grown in serum-free medium on laminin-coated culture ware for seven days in 2% oxygen.

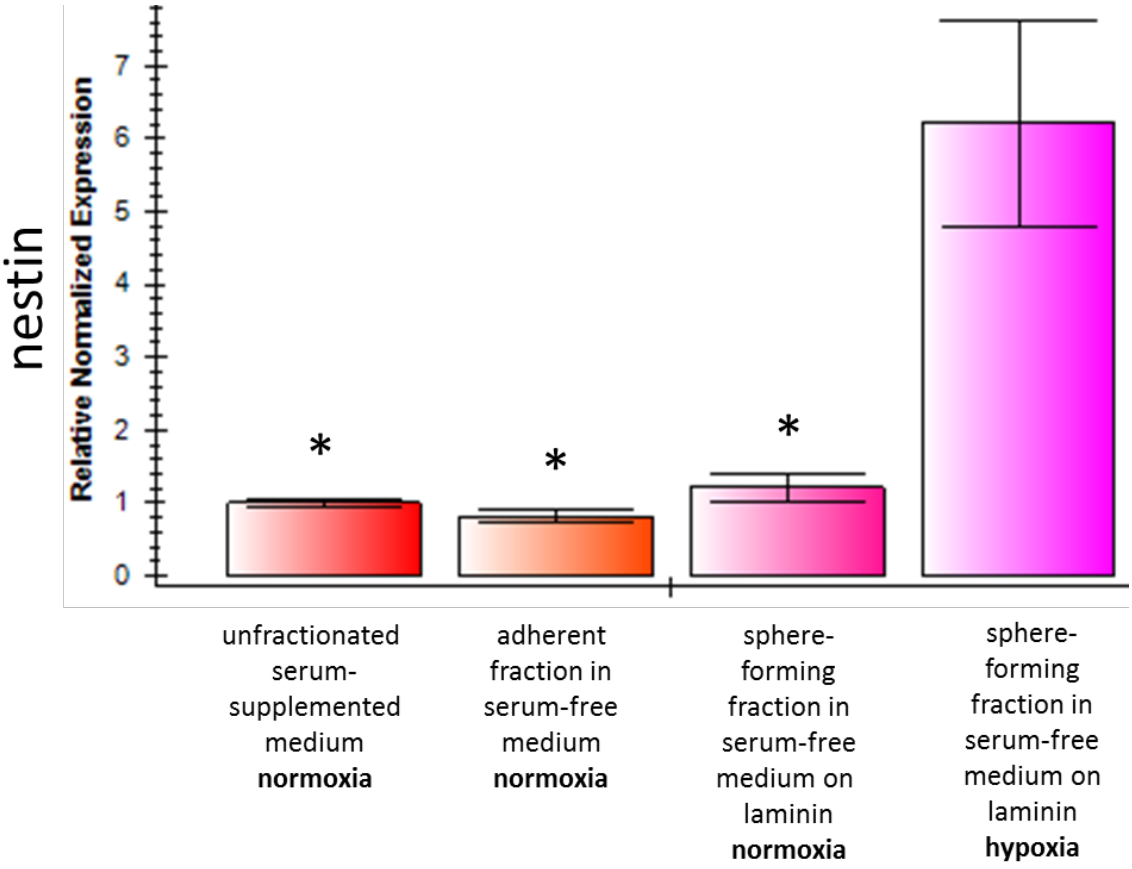

Figure 6. Relative normalized expression levels of nestin as measured by q-PCR in canine J3T glioblastoma cells under various culture conditions. Expression is displayed in arbitrary units. Bars denote +/- one standard error of the mean. Asterisks indicate statistically significant difference ($p \leq 0.05$) from sphere-forming cells grown in serum-free medium on laminin-coated culture ware for seven days in 2% oxygen.

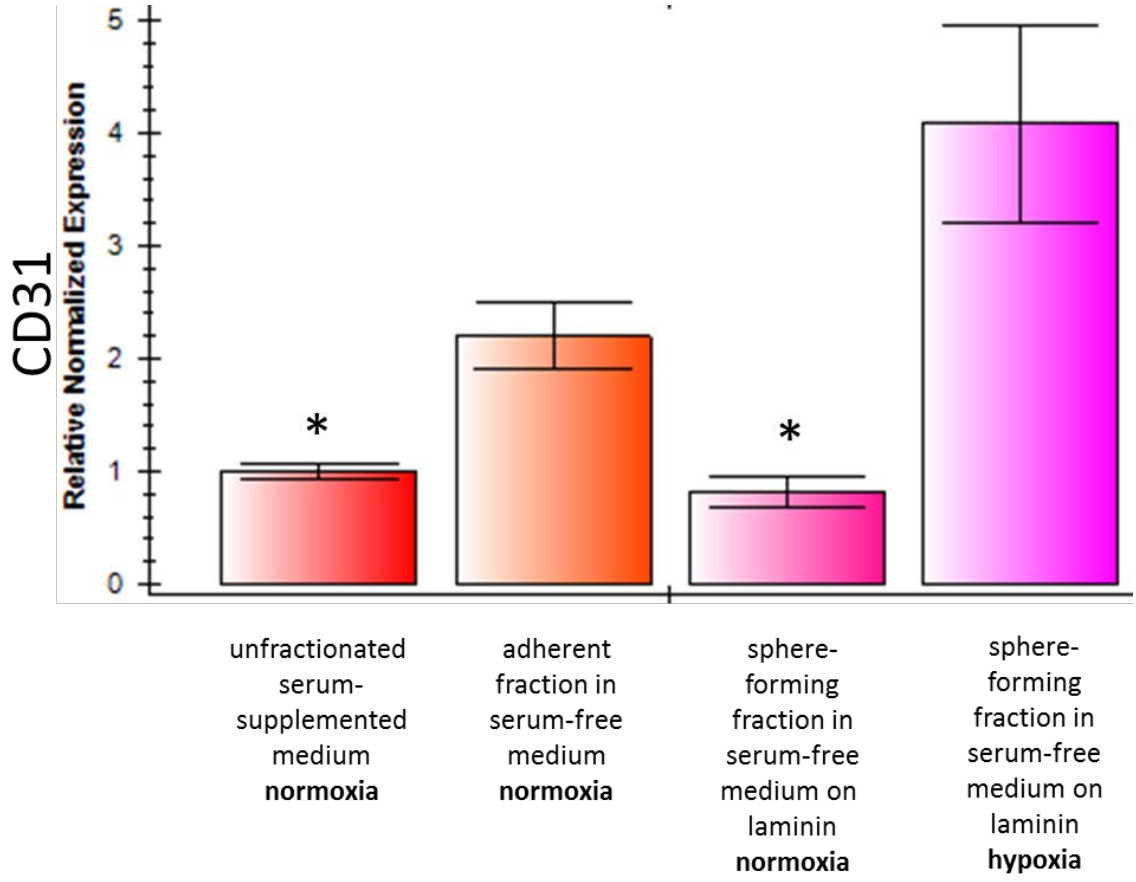

Figure 7. Relative normalized expression levels of CD31 as measured by q-PCR in canine J3T glioblastoma cells under various culture conditions. Expression is displayed in arbitrary units. Bars denote +/- one standard error of the mean. Asterisks indicate statistically significant difference ($p \leq 0.05$) from sphere-forming cells grown in serum-free medium on laminin-coated culture ware for seven days in 2% oxygen.

Target	Forward sequence (5’-3’)	Reverse sequence (5’-3’)
CD133	GGACACAAAAGCCAACAATC	ATCTTGACCCATTGCAGGTA
nestin	GAGAACCAGGAGCAAGTGAA	TTTCCAGAGGCTTCAGTGTC
HIF2α	CATGGGACTCACACAGGTGGAGC	TCCGGCCTCTGTTGGTGACTGT
CD31	CCAAGGCCAAGCAGACGCCA	CCACATCCAACGTCAGAGGCTCTTT

Table 1. Primer sequences for selected putative cancer stem-like cell markers.

CHAPTER III.

DEALING WITH UNEXPECTED CHALLENGES: A CASE STUDY IN INACCURATE CELL LINE IDENTIFICATION

Introduction

Because of the aforementioned challenges inherent in the J3T cell line with regard to erratic and unpredictable sphere formation, we reached out to another researcher who had published data concerning the derivation of a cancer stem-like cell line from a canine glioblastoma. This researcher generously agreed to share the cell line, and upon receiving the initial vial the cells were expanded in culture and this first passage was split into aliquots and frozen at -180° C for future experimental use.

Materials and methods

Cells were grown according to the Cambridge protocol with the use of hypoxic chambers, as described in Chapter II. The cells had a slightly different morphology from the J3T cells (Figure 8), but this was not considered unexpected as this line was purportedly enriched in stem-like cells. RNA extraction methods included 1) the Trireagent method as previously described, 2) Trireagent extraction with phenol/chloroform cleanup and ethanol precipitation, and 3) silica column-based kits (5 Prime). RNA integrity was assessed with electrophoresis on a non-denaturing agarose gel with visualization of bands as previously described. cDNA synthesis and q-PCR protocols were performed as described in Chapter II. Cell cultures were checked for mycoplasma contamination using a Takara PCR-based mycoplasma detection kit containing

primers that amplify eleven species of mycoplasma (*M. fermentans, M. hyorhinis, M. arginini, M. orale, M. salivarium, M. hominis, M. pulmonis, M. arthritidis, M. neurolyticum, M. hyopneumoniae, M. capricolum*) and one species of ureaplasma (*U. urealyticum*). A PCR designed to amplify the D-loop of *Mus musculus domesticus* mtDNA corresponding to position 15582-16290 (gift of Dr. Michael Irwin, Auburn University), as well as a multiplex PCR to identify mouse-specific and dog-specific targets was performed according to Cooper et al. [185] using sequences originally published by Parodi et al. [186] (Table 2).

Results

Multiple attempts to perform q-PCR yielded erratic, poor to absent amplification of products when using the same previously sensitive and specific primers that were used successfully with J3T cells (Chapter II). The assumption was first made that the RNA extraction process, which is so often the culprit in cases of PCR failure, was to blame. In the first phases of the project, RNA quantity and quality were assessed using only Nanodrop spectrophotometric readings and evaluating 260/280 and 260/230 ratios. Eventually, after multiple repeated failed attempts at PCR using various RNA extraction methods, RNA samples were assessed for degradation on a non-denaturing 2% agarose gel. It was determined that in addition to high quality Nanodrop readings, there were two distinct bands representative of 18S and 24S ribosomal RNA (Figure 9), indicating that all samples were non-degraded as well as being of good concentration and free of contaminants that could inhibit RT or PCR reactions. PCR primers were tested on normal dog tissues and again on J3T cells, with positive results that confirming that the primers and all other components of the PCR reaction were functioning appropriately. Both these new cells and the J3T cells were negative for mycoplasma

contamination via PCR. After these troubleshooting steps were performed and failed to demonstrate a flaw in any of the examined methods, the conclusion was reached that the only other possibility was that the cells that were given to us were likely inadvertently contaminated with cells from another species or were not of canine origin. A PCR reaction was performed on genomic DNA from the cell line, using primers for a verified mouse-specific mitochondrial target, using a comparable amount of normal mouse genomic DNA as a positive control. The reaction showed amplification of the target in these cells with a similar intensity as control mouse DNA. An additional multiplex PCR for mouse and dog performed as described by Cooper et al. [185] using primer sequences designed to amplify a segment of the COX-1 gene first published by Parodi et al. [186], comparing this cell line to the J3T cell line, normal dog, and normal mouse, confirmed that the identity of these cells was indeed 100% murine and not a murine/canine mix or canine (Figure 10). At this time, the use of this cell line was terminated, and the decision was made to return to the J3T canine glioblastoma cell line for future experiments.

Discussion

The problem of cell line misidentification has been known since the 1950's and despite awareness of its ubiquity remains an embarrassingly common phenomenon [187]. In fact, the initial development of the American Type Culture Collection (ATCC) in 1962 was a response to the large number of misidentified cell lines uncovered with karyotyping and immunologic methods [187]. As early as 1966, Gartler reported that 18 human cancer cell lines purported to be of independent origin were in reality HeLa cervical cancer cells, the first human cancer cell line to be established [188]. Between 1969 and 2004, the PubMed-listed publications using

cultured cells increased two- to two-and-a-half-fold, while during this same time period publications reporting results using misidentified cell lines increased ten-fold [189, 190]. In one study, a survey sent to laboratory personnel actively involved in cell culture research showed that of 483 respondents, 32% were using HeLa cells in their labs, 9% were unwittingly using HeLa-contaminated cell lines, 35% obtained their cells from other research labs rather than large repositories like ATCC, and only 33% tested their cells to confirm their identity [189]. One of the most egregious examples of misidentification is the MCF7/AdrR (renamed NCI/ADR-RES) purported multi-drug resistant breast cancer cell line that has been shown by DNA-fingerprinting analysis to be an ovarian carcinoma cell line OVCAR-8; over 300 papers using this misidentified line have been published [191]. A study examining the identity of human esophageal adenocarcinoma lines concluded that results of experiments conducted with misidentified cell lines had resulted in over 100 publications, recruitment of patients into clinical trials, at least eleven United States patents, and three NIH cancer research grants [192].

Although the attitude toward cell line misidentification has been historically largely one of denial and persecution of whistle-blowers, in recent years there has been a surge in both awareness and commitment to establishing standards to recognize and prevent the problem. In 2007, Dr. Roland Nardone and a panel of fellow scientists expressed their strong concern regarding the evidence of widespread cell line misidentification and its devastating effects including damaging public health, wasted resources, and loss of confidence in the scientific community [193]. They urged the NIH to adopt a “no identification, no money” policy that would require researchers using cell lines to provide proof of the identity of the cells used in their experimental work. In response in this letter, the NIH issued a short position statement (Notice Number: NOT-OD-08-017) in which they stated that it would be impractical for the

agency to require all applicants and grantee institutions to use specific methods to prove the identity of all cell lines used in funded research, and that instead the burden lay with reviewers, professional societies, and the researchers themselves to establish acceptable experimental methods.

As a supplemental attachment to an article detailing cell line misidentification, Drs. Amanda Capes-Davis, R. Ian Freshney, et al. provide an Excel spreadsheet detailing over 350 misidentified and contaminated cell lines [194]. Methods that can be used to identify cell lines include isoenzyme analysis, karyotyping, human leukocyte antigen (HLA)-typing, immunotyping, and DNA fingerprinting, as well as short tandem repeat (STR) profiling [187]. STRs are small DNA repeat sequences of 3-5 bases that have been used in forensic identification and paternity testing. The assay involves simultaneous amplification of multiple stretches of polymorphic DNA in a single tube, with subsequent labeling of amplified products with different fluorophores for easy identification [187]. One drawback of STR profiling is that it will not detect cross-species contamination, for which multiplex PCR remains the preferred method because it can detect single-species identity as well as mixed-species identity.

In our case, the cross-contamination or misidentification of cells by the researcher was almost certainly inadvertent due to mislabeling of stored cells or contamination from mouse xenograft assays. It is highly unlikely that the contamination occurred at our institution, due to several routine preventative protocols: 1) cells received from the investigator were expanded and frozen immediately after the first passage, 2) testing by multiplex PCR was performed on cells frozen at the intial split as well as later passage cells with similar results, 3) the primary investigator (JK) was not concurrently culturing any cells of murine origin, 4) each investigator working with cultured cells uses separate, labeled reagents and media, 5) cells were cultured in

canted-neck vented flasks that have a 0.2-μm mesh membrane that allows gas exchange but not cell contamination. Although the exhaustive trouble-shooting steps it prompted were expensive, time-consuming, and frustrating, it led to a Center-wide confirmation of the species of origin and mycoplasma status of all maintained cell lines and further validated that the standard protocols in place at our institution prevent cross-contamination of cell lines. It also reinforced the crucial importance of this aspect of quality control in cell culture-based research.

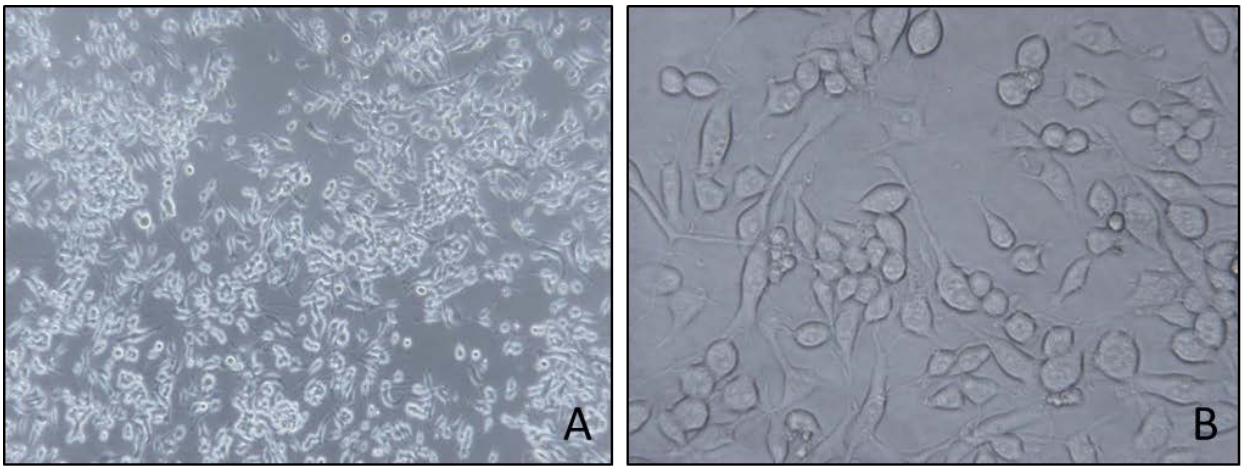

Figure 8. Cells of unknown origin grown in serum-free medium. Phase-contrast micrographs taken at 100x (A) and 400x (B) magnifications.

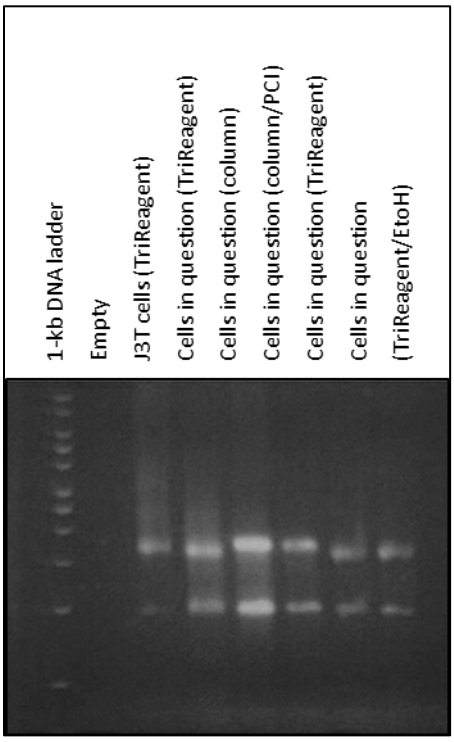

Figure 9. Gel electrophoresis of extracted RNA samples demonstrating distinct 18S and 28S bands consistent with a lack of degradation in all samples.

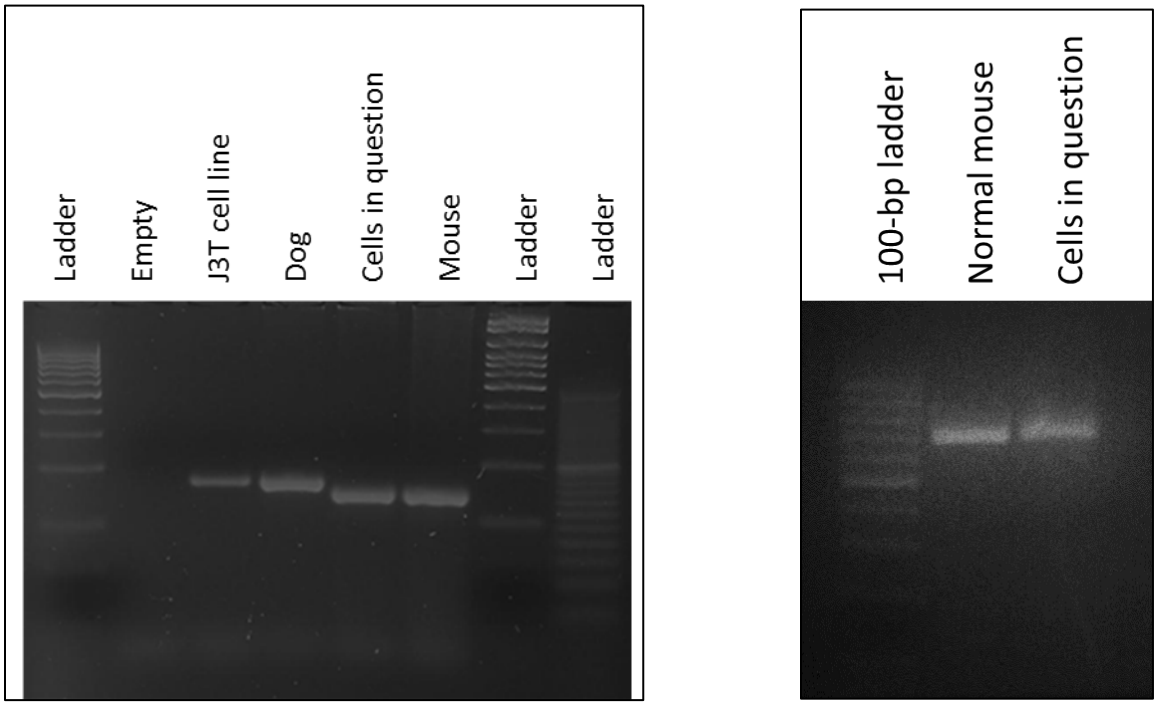

Figure 10. Gel electrophoresis of products of multiplex PCR reaction using primers designed to amplify murine and canine targets (left) and mouse mitochondrial DNA (right), demonstrating the murine identity of cells in question, and confirming the canine identity of J3T cells.

Target	Size	Forward sequence (5'-3')	Reverse sequence (5'-3')
COX-1 *(Canis familiaris)*	172 bp	GAACTAGGTCAGCCCGGTACTT	TTCGGGGGAATGCCATGTC
COX-1*(Mus musculus)*	150 bp	ATTACAGCCGTACGCTCCTAT	CCCAAAGAATCAGAACAGATGC
mtDNA *(Mus musculus)*	709 bp	CATTAAACTAATGTTATAAGG	TTATTGCGTAATAGAGTATGA

Table 2. Primer sequences for species-specific PCR reactions.

CHAPTER IV.

EVALUATION OF TRANSCRIPTIONAL EXPRESSION PROFILES OF SELECTED STEM AND ANGIOGENESIS MARKERS AT DIFFERENT TIME POINTS IN TWO MODELS OF HYPOXIA

Introduction

Our previous work demonstrated that prolonged exposure to 2% oxygen conditions caused significant up-regulation of multiple putative CSLC markers and one angiogenesis-related marker in the canine J3T glioblastoma cell line grown per the Cambridge protocol. In those experiments, low oxygen environmental conditions were produced with an inexpensive lab-built hypoxia chamber constructed according to published protocols [171]. This method has several drawbacks, including the inability to maintain cells at 2% oxygen for short periods during necessary manipulations such as addition of growth factors or media changes, and the inability to confirm oxygen levels within the chamber and at the cell interface during the experiment. For these reasons, we decided to examine transcriptional expression of HIF2α at multiple earlier time points, and to compare the results obtained with the hypoxic chamber with that of the chemical hypoxia mimetic cobalt II chloride hexahydrate ($CoCl_2$). This agent avoids the intermittent increases in oxygen level associated with the chambers, and mimics the effect of hypoxia by 1) interacting with HIFαs and preventing their degradation via prolyl hydroxylases, and 2) generating increased reactive oxygen species that inhibit prolyl hydroxylases and factor inhibiting HIF [195]. Another reason for the evaluation of early time points was that future

siRNA-mediated gene silencing experiments would be performed at shorter time points to avoid the dilution effect that occurs with transient transfections due to cell proliferation.

Because of the high degree of cross-talk between hypoxia and angiogenesis, we also chose to examine expression of the three most abundant isoforms of vascular endothelial growth factor A ($VEGF_{120,}$ $VEGF_{164,}$ and $VEGF_{188}$) over these same time points. VEGF is a member of the cysteine knot family of growth factors that plays a central role in both normal and tumor angiogenesis. The three main isoforms in humans are $VEGF_{121,}$ $VEGF_{165,}$ and $VEGF_{189}$, with $VEGF_{165}$ being the most abundant isoform in both normal and neoplastic cells [196, 197]. VEGF is overexpressed at both the mRNA and protein levels in human astrocytic tumors [198-206]. Additionally, recent work has demonstrated a direct role for VEGF in neurogenesis, neuronal migration, neuronal survival, and axon guidance, separate from its role in angiogenesis (reviewed in [207]). In mice and dogs, the isoforms differ in length by lacking one amino acid at the n-terminal, reflected in the isoform designations of $VEGF_{120,}$ $VEGF_{164,}$ and $VEGF_{188}$ [208, 209]. Increased levels of VEGF mRNA relative to normal brain have been documented in canine gliomas as well, with $VEGF_{164}$ being the most abundant isoform, and increased levels of VEGF corresponding to higher grade and more malignant tumors but not the degree of peritumoral edema [165].

Materials and methods

Cell culture

J3T canine glioblastoma cells were grown according to the Cambridge protocol as previously described in Chapter II. Cells were dissociated, counted, and seeded into individual petri dishes at densities that allowed adequate numbers of cells for early time point collections

but did not allow for confluency by the end of the experiment. Cells were allowed to rest overnight in defined serum-free medium on laminin-coated cultureware before beginning experimental manipulations. Cells were collected at the beginning of the experiment (time 0), and after 4, 8, 12, 24, and 48 hours. For each time point except time 0, cells were grown in parallel in 20% oxygen (normoxia), 2% oxygen chambers (2% hypoxia), or in 20% oxygen in media containing 100-µM $CoCl_2$ (chemical hypoxia).

q-PCR

RNA extraction, q-PCR conditions, and primer sequences were as previously described in Chapter II, with the addition of primers for vascular endothelial growth factor A (VEGFA) isoforms $VEGF_{120,}$ $VEGF_{164,}$ and $VEGF_{188}$ which were previously published [165](Table 3), and the exceptions that detection of products was with Bio-Rad SsoFast™ EvaGreen® and that expression levels of genes of interest were normalized to the housekeeping gene eukaryotic translation elongation factor 2 (eEF2). This housekeeping gene was chosen because in mouse studies it has been shown to be expressed uniformly across and within a wide variety of tissues, and is not affected by experimental conditions such as steroid hormones, adrenalectomy, and gonadectomy [210]. Additionally, unlike L37, it has multiple exons, which enables primers to be designed to span an intron and avoid the possibility of amplification of any contaminating genomic DNA.

Protein expression

Because much of the regulation of HIF2α occurs at the post-translational level, confirmation of a corresponding increase in protein was made by performing immunocytochemistry for HIF2α (rabbit polyclonal anti-HIF2α, Novus Biologicals) on J3T cells

grown for 24 hours under these three experimental conditions (20% O_2, 2% O_2, 100-µM $CoCl_2$). Binding was visualized using a fluorescent secondary antibody (goat anti-rabbit Alexa-fluor 594) with DAPI nuclear stain (Vectashield, Life Technologies) and imaged using high-resolution fluorescence microscopy in the lab of Dr. Vitaly Vodyanoy in the Department of Anatomy, Physiology, and Pharmacology at the Auburn University College of Veterinary Medicine per his previously published protocols [211]. Confirmation of the specificity of the antibody was via Western blot of whole-cell extracts using electrophoresis in a Bio-Rad 4-15% Tris-HCl Criterion gel, transfer to nitrocellulose membranes, staining with rabbit polyclonal anti-HIF2α (Novus biological) using actin staining as a loading control, and visualized using the Odyssey™ infrared imaging system (Li-Cor Biosciences).

Statistical analysis

Calculations of relative gene expression were made using the Bio-Rad CFX Manager 1.6 software according to the ΔΔCt method [174], using the housekeeping gene eEF2 for normalization. For each time point, the experimental samples were individually compared to the time-point control (20% oxygen) using a two-tailed two-sample t-test in SAS 9.3 with macros published by Zhenyi Xue [175] for the analysis of summary data, with significance level set as $p \leq 0.05$.

Results

HIF2α mRNA levels fluctuated to a small degree over the time course in the 20% oxygen (normoxic) samples, reinforcing the importance of having a normoxic control for comparison at each time point. When comparing HIF2α expression levels in cells grown in 2% oxygen (2% hypoxia), there was a statistically significant decrease compared to the normoxic control at 4

hours, then a significant increase compared to the control at 12 and 24 hours (Figure 11). Conversely, when comparing HIF2α expression levels in cells grown in the presence of the chemical hypoxia mimetic $CoCl_2$ (chemical hypoxia), there was not a statistically significant difference between treated and control samples at any of the examined time points.

$VEGF_{120}$ mRNA levels (Figure 12) were upregulated compared to the control sample at 4, 8, 12, 24, and 48 hours in the 2% hypoxia samples, and at 24 and 48 hours in the chemical hypoxia samples. $VEGF_{164}$ mRNA levels (Figure 13) were upregulated compared to the control sample at 12, 24, and 48 hours in both 2% hypoxia and chemical hypoxia samples. $VEGF_{188}$ mRNA levels (Figure 14) were upregulated compared to the control at 4, 12, 24, and 48 hours in 2% hypoxia, and at 12, 24, and 48 hours in the chemical hypoxia samples. Upregulation of VEGF isoforms ranged from moderate to marked (up to 30-fold difference), with the most elevated levels observed at the 12-hour time point in 2% hypoxia samples, and at the 48-hour time point in chemical hypoxia samples.

Immunocytochemical staining showed increased levels of HIF2α compared to the normoxic control in both the cytoplasm and nucleus of cells grown in either 2% hypoxia or chemical hypoxia for 24 hours (Figure 15). Western blot showed a single band at the expected size of ~120 kD, with a nonspecific band at approximately 90 kD. Communication with the antibody manufacturer suggests that this is a common finding in whole-cell extracts, and that the company believes this band to represent HIF breakdown products.

Discussion

The purpose of this study was to characterize the effects of two methods of *in vitro* hypoxia induction, a chamber-generated 2% oxygen environment and $CoCl_2$-induced chemical

hypoxia, on mRNA expression of HIF2α and the three main isoforms of $VEGF_{120}$, $VEGF_{164}$, and $VEGF_{188}$. The purpose of this was two-fold: firstly, to add to the overall body of knowledge about the behavior of canine glioblastoma at the gene expression level and secondly, to evaluate commonly used experimental time points for differences in the degree of transcriptional upregulation produced by two different methods of hypoxia induction. Production of hypoxic conditions for *in vitro* experiments has been with done with either a decrease in environmental oxygen (using hypoxic chambers/incubators or specialized microfluidic devices) and with chemical compounds such as desferrioxamine, cobalt, nickel and zinc that mimic the effects of hypoxia primarily via the direct or indirect inhibition of PHD enzymes responsible for HIF degradation. The first method likely more accurately recapitulates conditions present near areas of vascular-related hypoxia such as ischemia or ineffective vascularization, but requires expensive and specialized equipment to produce and consistently maintain and monitor precise oxygen levels. Chemical hypoxia, on the other hand, is inexpensive and easy to use, but still presents some issues, including the inability to calculate what level of hypoxia correlates to a given chemical concentration, and the effect that increasing cell numbers over time has on the chemical saturation and kinetics of affected enzymes. Although both methods have been used in some studies, most work does not directly and systematically compare the two within the same model system.

Our work demonstrates that there are significant differences between chamber-induced 2% hypoxia and $CoCl_2$ chemically-induced hypoxia with regard to the degree of transcriptional upregulation of all examined VEGF isoforms and the time points at which upregulation first and maximally occurs. This has implications at the experimental level in terms of choice of time points to examine the effects of experimental manipulation, and also provides some important

biological insight into the pattern of VEGF expression over time in response to sustained hypoxia. This pattern of expression in response to global hypoxia could be relevant within the clinical context of an intratumoral vascular incident that causes the patient to present for neurologic signs. It is important to note that although the timing of increases in VEGF expression in the two hypoxic conditions varied, the maximum fold-differences at peak time points were not markedly different. This confirmed that 1) regulation of VEGF in this model system is primarily under the control of HIFs and/or ROS, as these are the major pathways known to be affected by $CoCl_2$, and 2) the response of canine glioblastoma cells in this system to either 2% or chemical hypoxia results in marked increases in VEGF mRNA. The modest increases in HIF2α mRNA expression seen with 2% oxygen, as well as the lack of increase with exposure to $CoCl_2$, are consistent with the fact that the majority of regulation of this gene is at the post-translational level. Nevertheless, the fact that $CoCl_2$ failed to produce any upregulation at these time points suggests that either 1) the concentration of chemical was below the threshold needed to affect HIF2α transcription, 2) the mechanism of action of the chemical potentiated post-translational protein stabilization to such a degree that it precluded the need for transcriptional upregulation, or 3) that $CoCl_2$ levels were decreased on a per-cell basis at later time points due to cell replication and subsequent increased cell numbers. The finding of increased HIF2α protein in both the cytoplasm and nucleus with immunocytochemistry is functionally important because it demonstrates that there is stabilization of the protein and translocation to the nucleus, which is required for the HIFs activity as transcription factors.

Further work is necessary to more fully characterize the response of canine glioblastoma *in vitro* to various levels of oxygen and various types and concentrations of chemical hypoxia

mimetics. These results offer a valuable and previously unreported insight into the biological behavior of canine glioblastoma cells in response to hypoxia.

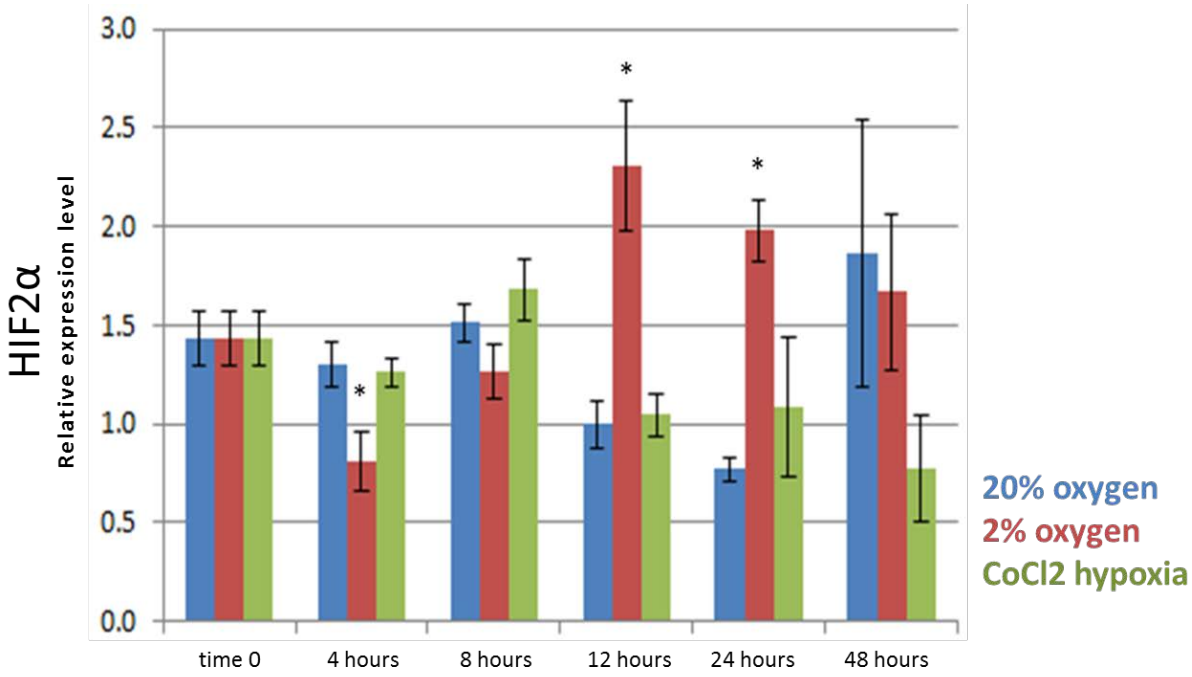

Figure 11. Relative normalized expression levels of HIF2α over time points as measured by q-PCR in canine J3T glioblastoma cells grown according to the Cambridge protocol. Expression is displayed in arbitrary units. Bars denote standard deviation. Asterisks indicate statistically significant difference ($p \leq 0.05$) between hypoxic and normoxic (20% oxygen) samples at each time point.

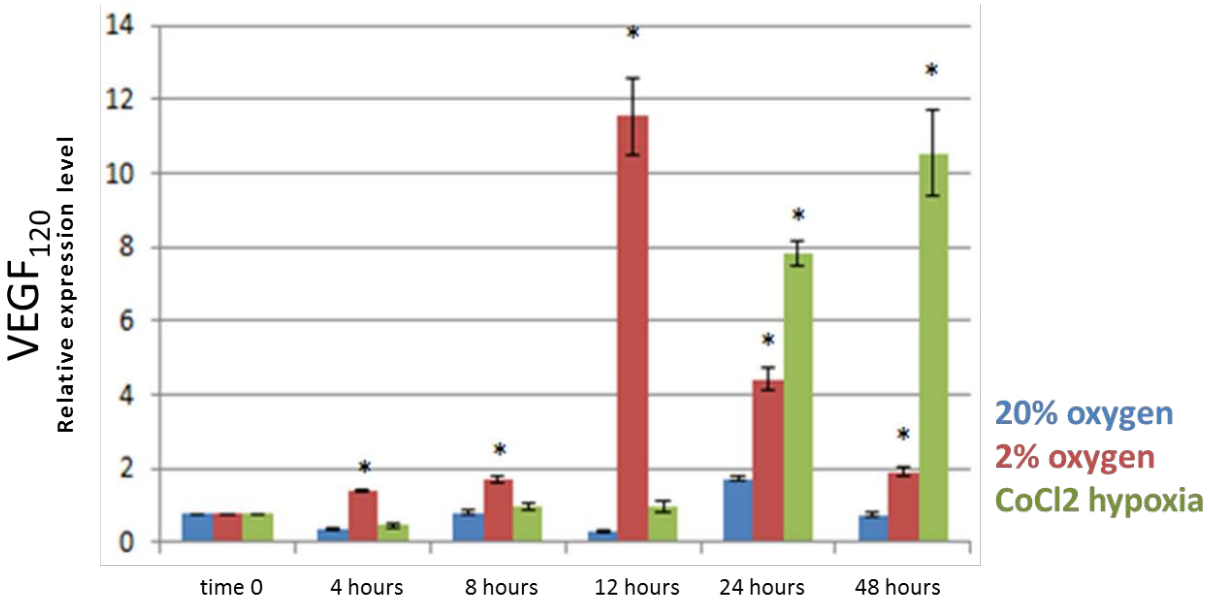

Figure 12. Relative normalized expression levels of $VEGF_{120}$ over time points as measured by q-PCR in canine J3T glioblastoma cells grown according to the Cambridge protocol. Expression is displayed in arbitrary units. Bars denote standard deviation. Asterisks indicate statistically significant difference ($p \leq 0.05$) between hypoxic and normoxic (20% oxygen) samples at each time point.

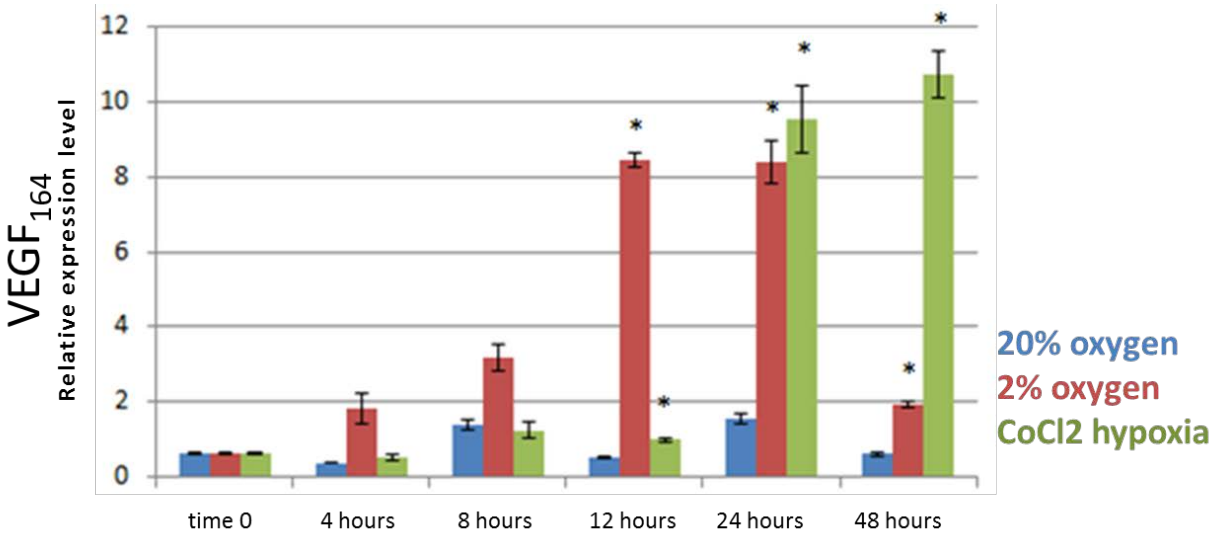

Figure 13. Relative normalized expression levels of $VEGF_{164}$ over time points as measured by q-PCR in canine J3T glioblastoma cells grown according to the Cambridge protocol. Expression is displayed in arbitrary units. Bars denote standard deviation. Asterisks indicate statistically significant difference ($p \leq 0.05$) between hypoxic and normoxic (20% oxygen) samples at each time point.

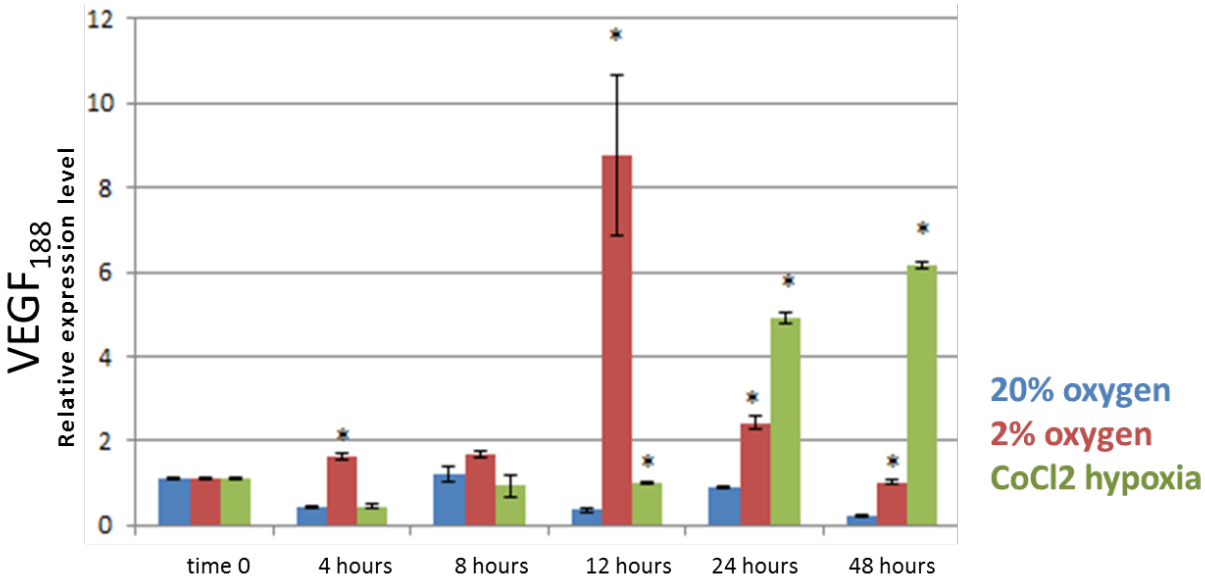

Figure 14. Relative normalized expression levels of $VEGF_{188}$ over time points as measured by q-PCR in canine J3T glioblastoma cells grown according to the Cambridge protocol. Expression is displayed in arbitrary units. Bars denote standard deviation. Asterisks indicate statistically significant difference ($p \leq 0.05$) between hypoxic and normoxic (20% oxygen) samples at each time point.

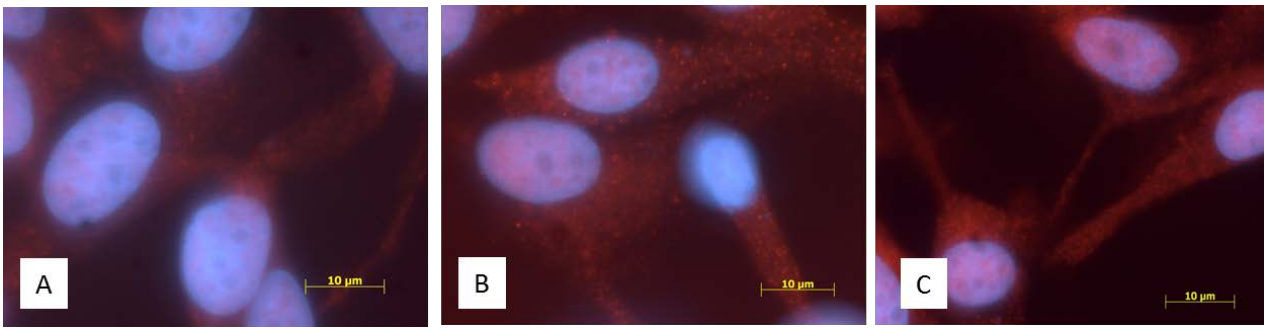

Figure 15. Immunocytochemistry for HIF2α in J3T canine glioblastoma cells after culturing for 24 hours in serum-free medium in 20% oxygen (A), 2% oxygen (B), or 20% oxygen and 100-µM chemical hypoxia mimetic $CoCl_2$. Rabbit polyclonal anti-HIF2α (Novus Biologicals) with secondary goat anti-rabbit Alexafluor 594, DAPI nuclear stain. High-resolution images taken by Dr. Vitaly Vodyanoy's lab using the CytoViva system.

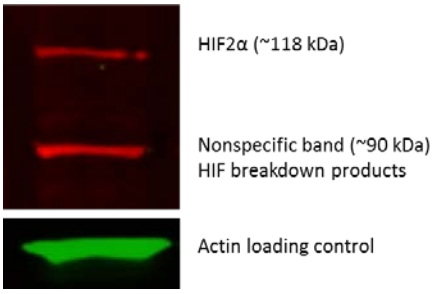

Figure 16. Western blot analysis of J3T canine glioblastoma whole-cell lysates. Rabbit polyclonal anti-HIF2α and mouse monoclonal anti-actin with secondary Odyssey fluorescent-conjugated goat anti-rabbit (red, 680-nm), and goat anti-mouse (green, 800-nm).

Target	Forward sequence (5'-3')	Reverse sequence (5'-3')
$VEGF_{120}$	AGATTATGCGGATCAAACCTCATC	TCGGCTTGTCACATTTTTCTTG
$VEGF_{164}$	AGATTATGCGGATCAAACCTCATC	CCACAGGGATTTTCTTGCCTT
$VEGF_{188}$	AGATTATGCGGATCAAACCTCATC	CTCGAACTGATTTTTTTTCTTGCCTT

Table 3. Primer sequences for isoforms of VEGF, previously published by Dickinson et al. [165].

CHAPTER V.

siRNA-MEDIATED GENE SILENCING OF HIF2α: EFFECTS ON TRANSCRIPTIONAL EXPRESSION OF SELECTED STEM AND ANGIOGENESIS MARKERS AND SUSCEPTIBILITY TO DOXORUBICIN

Introduction

The importance of hypoxia and the HIF pathway in tumor cell growth and progression makes it a promising target for cancer therapy. While HIF1α and HIF2α bind common targets and have some redundant functions, they each also bind unique targets that result in different or even opposing effects. The VHL-deficient renal cell carcinoma lines have offered investigators an opportunity to study the effects of HIFα overexpression, due to the cells' inability to degrade the proteins in an oxygen-dependent fashion. Overexpression of HIF1α and/or HIF2α has been documented in many cancers (reviewed in [147]). Unexpectedly, multiple recent studies also have documented a tumor suppressor role in specific contexts [212-215]. In glioblastoma, HIF2α expression level in tumors, but not HIF1α, is associated with a poor patient prognosis [216], and has been shown by two groups [137, 150] to be a vital component of the acquisition and maintenance of a stem-like/tumorigenic phenotype. Because post-natal expression of HIF2α is more restricted than that of HIF1α, and is not present in normal neural stem cells [137], it has the potential to be a relatively glioblastoma-specific, neural stem cell-sparing therapeutic target. For these reasons, we investigated the effect of transient transfection with small interfering RNAs (siRNA) against HIF2α on mRNA expression of selected CSLC and angiogenesis

markers, and on *in vitro* susceptibility to cell death in the presence of the chemotherapeutic agent doxorubicin.

siRNAs are produced by enzymatic cleavage of a long double-stranded RNA (dsRNA) by the RNase-III class endoribonuclease Dicer into two 21- to 23-nucleotide duplexes that have two-base 3' overhangs [217]. Once formed (or transfected into a cell), siRNAs associate with the RNA Induced Silencing Complex (RISC), the formation of which is also catalyzed by Dicer. One component of the RISC is argonaute, an endonuclease capable of degrading messenger RNA that has a sequence complementary to that of the siRNA guide strand. Dicer-Substrate RNAs are chemically synthesized 27-mer RNA duplexes that are optimized for Dicer processing and show increased potency when compared with 21-mer duplexes that mimic Dicer products and are designed to bypass a cell's Dicer processing machinery [218, 219]. The use of this type of siRNA for targeted gene knockdown also does not activate interferon pathway genes such as protein kinase R that can lead to increased clearance [220]. Because this method of gene knockdown is transient, it has a potential drawback in rapidly dividing cells, namely a dilutional effect produced by both the division of transfected cells with associated partitioning of the cytoplasm and the potential for a survival and proliferation advantage of the small percentage of non-transfected cells.

Materials and methods

Cell culture

J3T canine glioblastoma cells were cultured as previously described per the Cambridge protocol. For 2% oxygen, hypoxic chambers were used as described in Chapter II. For chemical hypoxia, cells were incubated in the presence of 100-µM $CoCl_2$.

q-PCR

RNA extraction, quality control, cDNA synthesis, and q-PCR were performed as previously described, using the BioRad SsoFast evagreen detection agent.

Transfection

siRNAs were purchased from Integrated DNA Technologies (TriFECTa), consisting of 27-mer Dicer-substrate RNA duplexes designed based on a proprietary algorithm to be specific for canine HIF2α. Transfection conditions were optimized using the included fluorescent dye-labeled duplex (Tye 3 DS transfection control), using the cationic lipid transfection agent Lipofectamine 2000 (Life Technologies 11668-019). Optimum conditions (>90% transfection with minimal cell death) were achieved in the J3T canine glioblastoma cell line using a 10-nM concentration of siRNAs and a mid-range concentration of Lipofectamine 2000. Initial experiments were performed to identify which siRNA duplex of the three provided produced the greatest reduction in HIF2α mRNA. Duplex 3 (sense: rGrGrC rGrCrU rGrUrU rGrUrA rGrGrA rUrGrA rGrGrA rCrUrC rCrUrC, antisense: rGrGrA rGrUrC rCrUrC rArUrC rCrUrA rCrArA rCrArG rCrGC C) was chosen for subsequent experiments. Cells were incubated in the presence of Lipofectamine 2000 and siRNAs for four hours, then media was changed prior to any experimental manipulations to minimize toxicity due to the transfection agent.

siRNA-mediated HIF2α gene silencing experiments

Two separate knockdown experiments were conducted for q-PCR evaluation of transcriptional expression of genes of interest. In the first, cells were cultured for 24 hours in either 20% oxygen (normoxia) or 2% oxygen (2% hypoxia). In the second experiment, cells were cultured for 90 hours in either 20% oxygen (normoxia) or 100-μM $CoCl_2$ (chemical

hypoxia). As a control in each experiment, an off-target, "nonsense", siRNA (nsiRNA) with no target specificity in the mammalian genome was used to distinguish the effects of HIF2α gene knockdown from the transfection process alone on the cell.

Doxorubicin assay

To assess the impact of HIF2α knockdown on cell death in the presence of doxorubicin, cells were cultured in normoxia and chemical hypoxia and exposed to 1-μM doxorubicin HCl (MW=579.98 g/mol, sterile, formulated at 2 mg/mL for *in vivo* therapeutic use) for 24 hours both without transfection and after transfection with HIF2α-targeted siRNAs. As in q-PCR experiments, a control consisting of an off-target, nonsense, siRNA (nsiRNA) with no target specificity in the mammalian genome was used to distinguish the effects of gene knockdown from the transfection process alone on the cell. For flow cytometry, cells were dissociated enzymatically (Accutase, Thermo Scientific 21-201-0100V), pelleted by centrifugation for 5 minutes at 300 rcf, washed with PBS, then incubated with a viability dye (eFluor 780, eBioscience 65-0865) for 30 minutes at 4°C protected from light. After this, cells were washed twice in MACS buffer (PBS, 0.5% BSA, 2 mM EDTA, pH=7.2), and finally filtered through a 40-μm mesh cell strainer and kept in the dark at room temperature prior to immediate analysis. The eFluor dye was chosen because the fluorescence spectrum produced by doxorubicin (470-590 nm) overlaps that of the more commonly used live/dead stain propidium iodide (535-617 nm). Cells were analyzed using an Accuri C6 flow cytometer and cFlow Plus software. For q-PCR relative expression data, statistics were performed as previously described in Chapter IV using a two-sample t-test.

Results

In the 24-hour experiment, siRNA-mediated knockdown of HIF2α was confirmed by an approximately 78% decrease in mRNA in normoxia and a 52% decrease in 2% hypoxia as compared to the nsiRNA controls (Figure 16). Comparing the two control (nsiRNA) samples, there was no statistically significant upregulation of HIF2α at 24 hours in 2% hypoxia. For the examined CSLC markers (CD133 and nestin), the only statistically significant decrease in the HIF2α- knockdown group was nestin in normoxia (Figures 17, 18). Comparing the two control (nsiRNA) samples, there was a significant increase in expression of CD133 (~4.5-fold), $VEGF_{120}$ (~1.5-fold), $VEGF_{164}$ (~1.75-fold), and $VEGF_{188}$ (2.5-fold) in 2% hypoxia (Figures 17, 19, 20, 21). In both normoxia and 2% hypoxia, there was no statistically significant difference in expression of any of the VEGF isoforms between HIF2α- knockdown and control groups, though in the normoxia group there was a consistent trend toward a decrease in the knockdown group, with p values in the 0.1 range (Figures 19, 20, 21).

In the 90-hour experiment, siRNA-mediated knockdown of HIF2α was confirmed by an approximately 40% decrease in mRNA in both 20% oxygen (normoxia) and $CoCl_2$-treated (chemical hypoxia) samples as compared to the nsiRNA control (Figure 22). The decreased degree of knockdown in the 90-hour experiment compared to the 24-hour experiment confirmed our expectation of a significant dilutional effect following cell proliferation. In contrast to the 24-hour experiment, when comparing the two control (nsiRNA) samples there was a statistically significant upregulation of HIF2α (~2.5-fold) in the chemical hypoxia control compared to the normoxia control. With the exception of $VEGF_{120}$ in normoxia, none of the examined CSLC or angiogenesis markers showed a statistically significant downregulation due to siRNA-mediated HIF2α gene silencing (Figures 22-27). When comparing the two control (nsiRNA) samples, there was a significant upregulation of nestin (2-fold), $VEGF_{120}$ (~3-fold), $VEGF_{164}$ (~3-fold),

and $VEGF_{188}$ (~5-fold) in chemical hypoxia (Figures 24, 25, 26, 27). Unexpectedly, in the 90-hour experiment CD133 expression was decreased in the chemical hypoxia control sample as compared to the normoxia control sample (Figure 23).

Flow cytometric assessment of live/dead cells using the fluorescence-based eFluor assay following 24 hours of either 1) no treatment, 2) 1-µM doxorubicin, 3) 100-µM $CoCl_2$ (chemical hypoxia), or 4) 1-µM doxorubicin and chemical hypoxia showed cell death rates of 1) 10.7%, 2) 20.4%, 3) 8.0%, and 4) 16.8%, respectively (Figure 28). The rate of cell death in the no-treatment group reflects the fact that for this assay all culture media and PBS washings were collected and included in the assay to ensure uniformity across experimental groups. For knockdown experiments, cell death rates when comparing the doxorubicin-exposed 1) control (nsiRNA) normoxia, 2) HIF2α knockdown normoxia, 3) control (nsiRNA) chemical hypoxia, and 4) HIF2α knockdown chemical hypoxia cells were 1) 17.4%, 2) 16.2%, 3) 15.8%, and 4) 30.9%, respectively, demonstrating a two-fold increase in cell death between the control and knockdown cells in chemical hypoxia (Figure 29). Gates were set to exclude very small forward-scatter events (interpreted as cell fragments), as well as cells that deviated from the 1:1 ratio of vertical and horizontal forward-scatter measurements (interpreted as doublets or groups).

Discussion

The present study demonstrated that while prolonged exposure (90 hours) of canine J3T glioblastoma cells *in vitro* to the chemical hypoxia mimetic $CoCl_2$ led to significant increases in mRNA of nestin, HIF2α, $VEGF_{120}$, $VEGF_{164}$, and $VEGF_{188}$, in our hands transient siRNA-mediated knockdown of the HIF2α gene had minimal effects on abrogating this upregulation. This result could be indicative of several things. Firstly, historical repeated culturing of this cell

line in the presence of fetal calf serum (as discussed in Chapter II) may have caused irreversible differentiation and expression profile alterations, a phenomenon that has been demonstrated in human glioblastoma cells [184] and supported by the observation of erratic and rare formation of spheres in culture. Second, the transient and partial nature of the gene silencing with the use of siRNAs may have allowed enough residual expression to effect downstream changes, and 3) the choice of CSLC genes to examine was based on those linked to poor prognosis and aggressive behavior, rather than those known to be direct downstream targets of HIF2α. The trend toward a decrease in VEGF expression in normoxia after gene silencing, though not statistically significant, suggests that there may be at least some role for HIF2α in this cell line, as HIF2α, but not HIF1α, is known to be expressed for long periods at intermediate (2-7%) hypoxia and normoxia, while HIF1α is only stabilized acutely and in marked (<2%) hypoxia [136]. It is also worth noting that in at least one recent investigation [221], Qiang et al. found that the role of HIF2α in the maintenance of the stem-like fraction of the human glioblastoma cell line U251 had a somewhat different role than that identified for HIF2α in the Rich study. In the Qiang et al. study, HIF1α, not HIF2α, was preferentially expressed in the stem-like fraction (as identified by formation of spheres in serum-free medium for two passages). Exposure to $CoCl_2$ for 24 hours increased the number of nestin-positive cells, but siRNA-mediated gene silencing of HIF2α did not abrogate this effect. The authors suggest that these results may demonstrate some cell-specific variation in the importance of the HIFα isoforms in the maintenance of the stem-like phenotype. Further investigation into the effect of HIF2α gene silencing on known direct targets in the canine J3T cell line and within primary patient-derived specimens at multiple tightly controlled oxygen levels will be needed to more fully elucidate the role of this gene in canine glioblastoma. In our experiments, the finding of a statistically significant decrease in nestin

mRNA in normoxia 24 hours after HIF2α gene silencing is a novel finding that suggests a role for this gene in stem-like expression patterns in canine glioblastoma at higher oxygen levels.

The finding of increased *in vitro* susceptibility (~double) to doxorubicin-induced cell death after siRNA-mediated HIF2α gene silencing is intriguing and bears further investigation. Doxorubicin, particularly when formulated in a way that enhances blood-brain-barrier penetration and allows lower dosages that avoid some of the more problematic side-effects associated with its use, is relatively inexpensive and has a long record of use in dogs. If even transient gene silencing could potentiate its effects, this could be a powerful tool for use in canine patients for whom surgery is not an option.

Overall, our findings indicate that in the canine J3T glioblastoma cell line, there is a role for HIF2α in the transcriptional regulation of both nestin and $VEGF_{120}$ in normoxia, and that siRNA-mediated gene silencing abrogates this effect and increases cell death in the presence of doxorubicin. Additionally, we demonstrate that prolonged chemical hypoxia induces significant upregulation of multiple putative CSLC and angiogenesis-related markers, supporting a role for the hypoxic microenvironment in acquisition of a stem-like phenotype in canine glioblastoma.

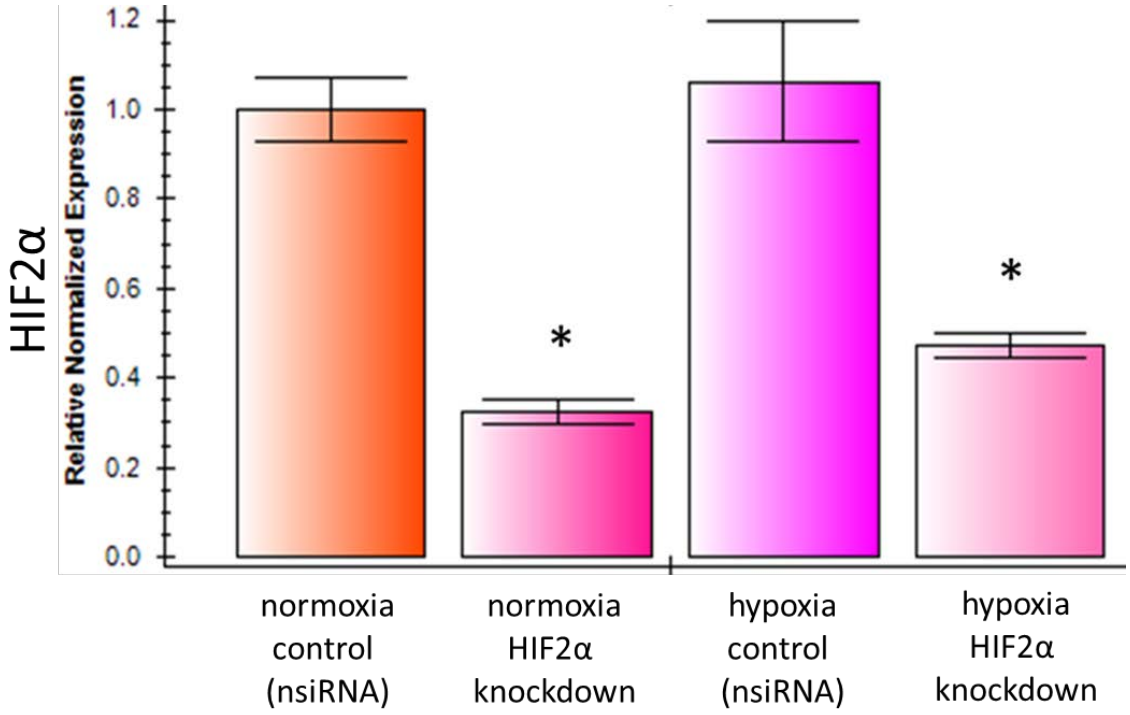

Figure 17. 24-hour HIF2α gene knockdown experiment. Relative normalized expression levels of HIF2α as measured by q-PCR in canine J3T glioblastoma cells grown according to the Cambridge protocol. Expression is displayed in arbitrary units. Bars denote +/- one standard error of the mean. Asterisks indicate statistically significant difference between knockdown and control samples ($p \leq 0.05$) in 20% oxygen (normoxia) and 2% oxygen (hypoxia).

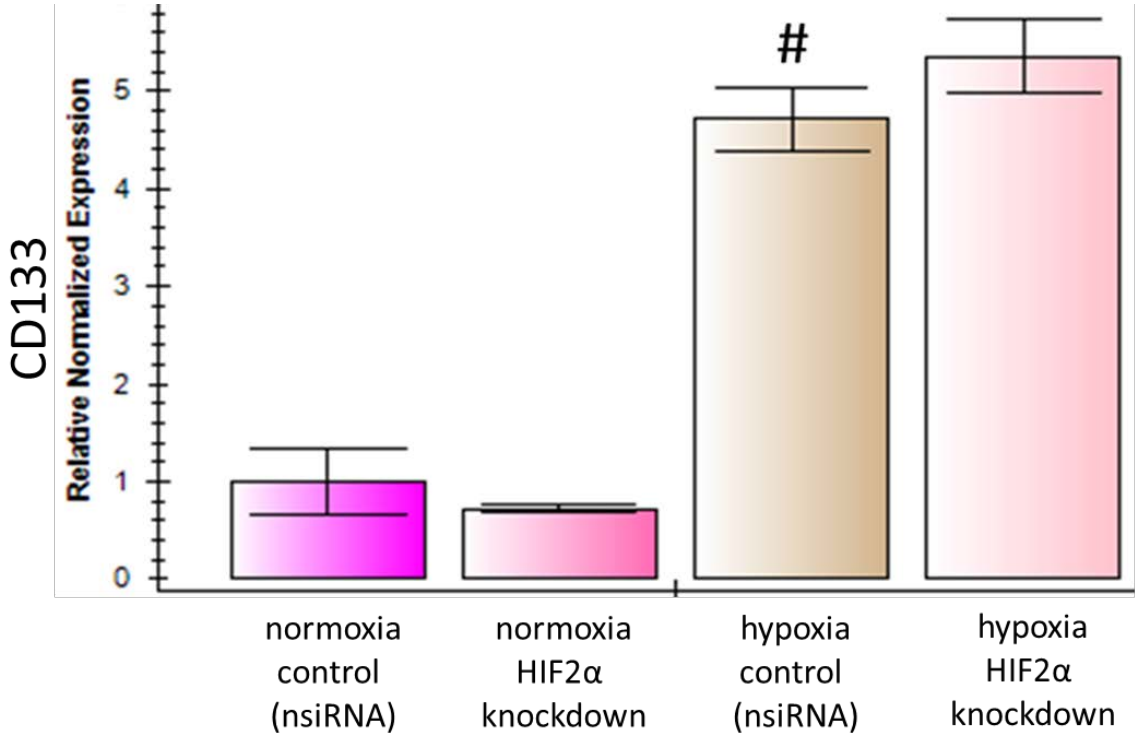

Figure 18. 24-hour HIF2α gene knockdown experiment. Relative normalized expression levels of CD133 as measured by q-PCR in canine J3T glioblastoma cells grown according to the Cambridge protocol. Expression is displayed in arbitrary units. Bars denote +/- one standard error of the mean. Pound sign indicates statistically significant difference between 20% (normoxia) and 2% oxygen (hypoxia) control samples ($p \leq 0.05$).

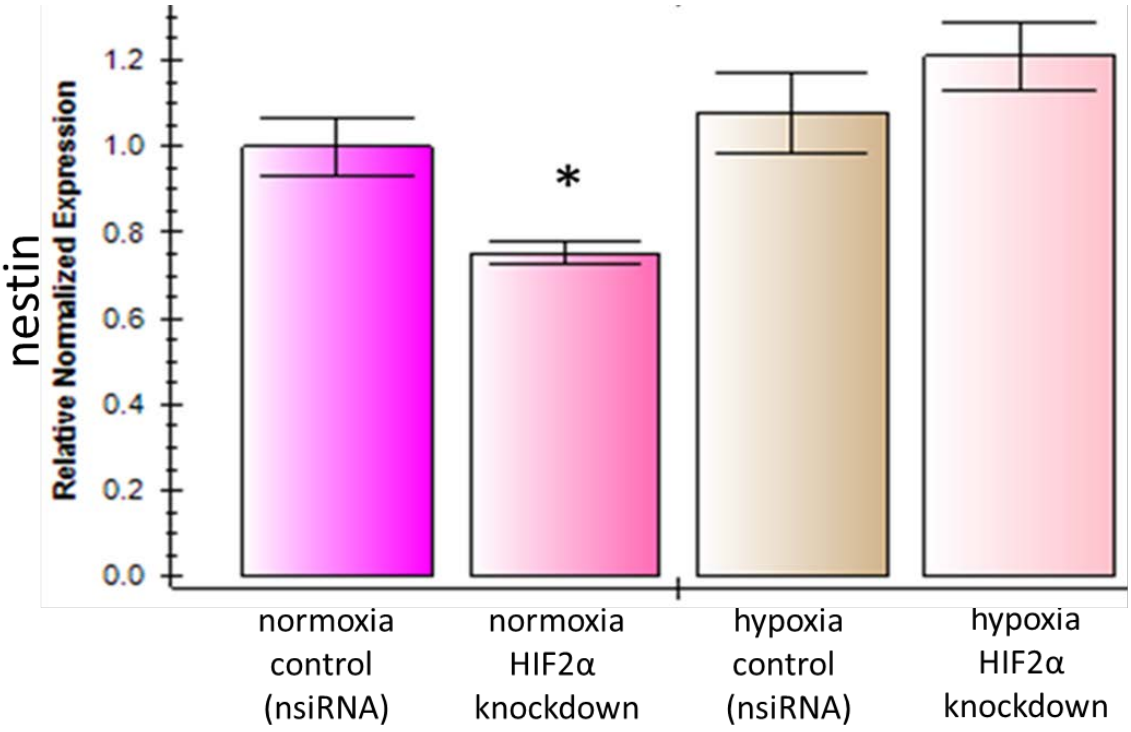

Figure 19. 24-hour HIF2α gene knockdown experiment. Relative normalized expression levels of nestin as measured by q-PCR in canine J3T glioblastoma cells grown according to the Cambridge protocol. Expression is displayed in arbitrary units. Bars denote +/- one standard error of the mean. Asterisk indicates statistically significant difference between knockdown and control samples ($p \leq 0.05$) in 20% oxygen (normoxia) and 2% oxygen (hypoxia).

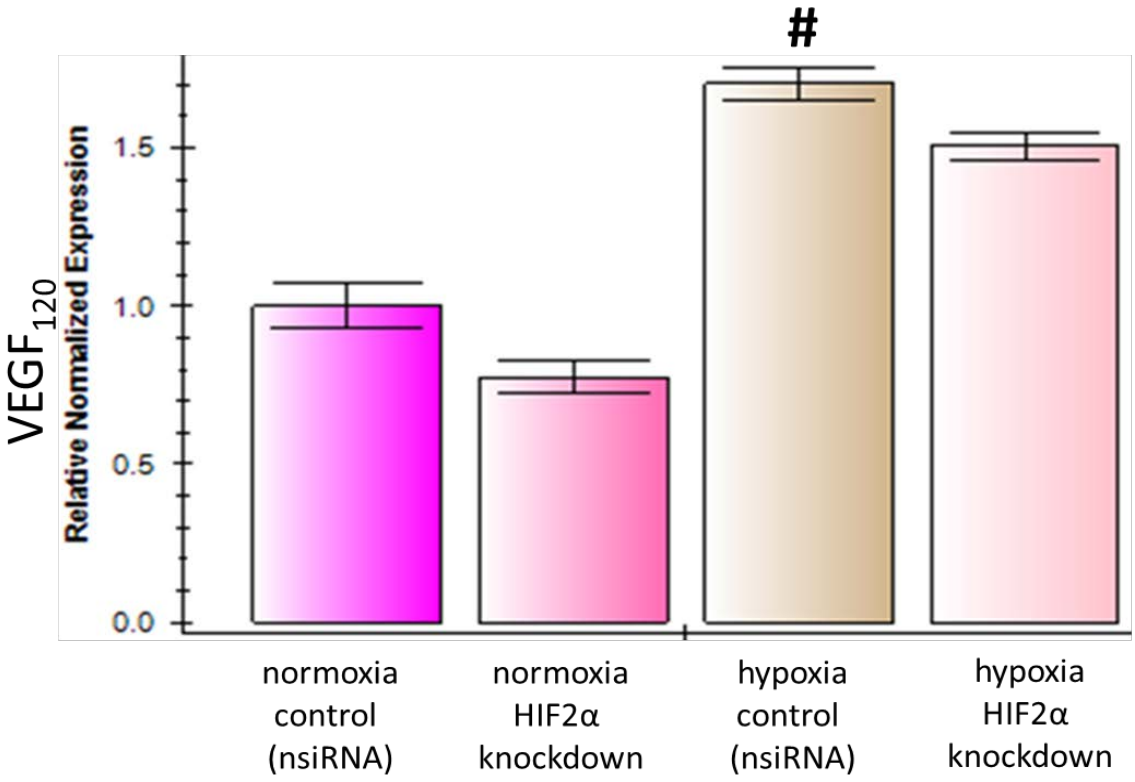

Figure 20. 24-hour HIF2α gene knockdown experiment. Relative normalized expression levels of $VEGF_{120}$ as measured by q-PCR in canine J3T glioblastoma cells grown according to the Cambridge protocol. Expression is displayed in arbitrary units. Bars denote +/- one standard error of the mean. Pound sign indicates statistically significant difference between 20% (normoxia) and 2% oxygen (hypoxia) control samples ($p \leq 0.05$).

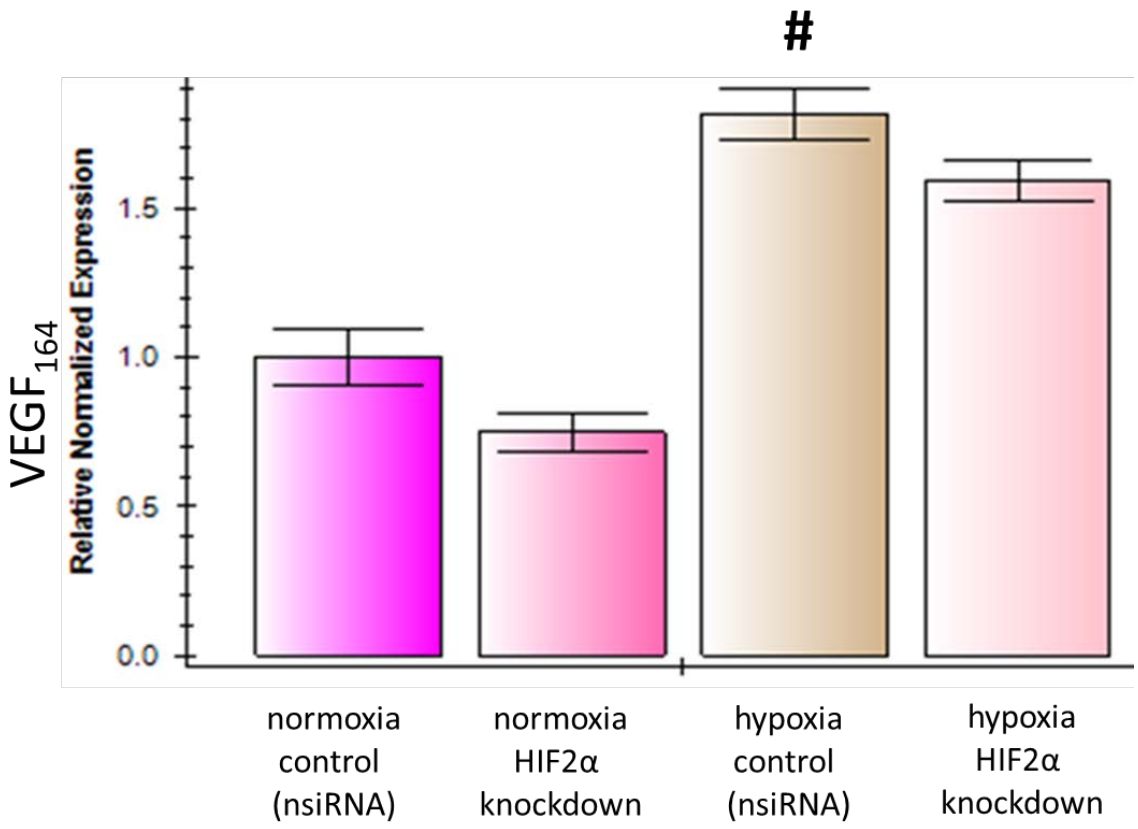

Figure 21. 24-hour HIF2α gene knockdown experiment. Relative normalized expression levels of $VEGF_{164}$ as measured by q-PCR in canine J3T glioblastoma cells grown according to the Cambridge protocol. Expression is displayed in arbitrary units. Bars denote +/- one standard error of the mean. Pound sign indicates statistically significant difference between 20% (normoxia) and 2% oxygen (hypoxia) control samples ($p \leq 0.05$).

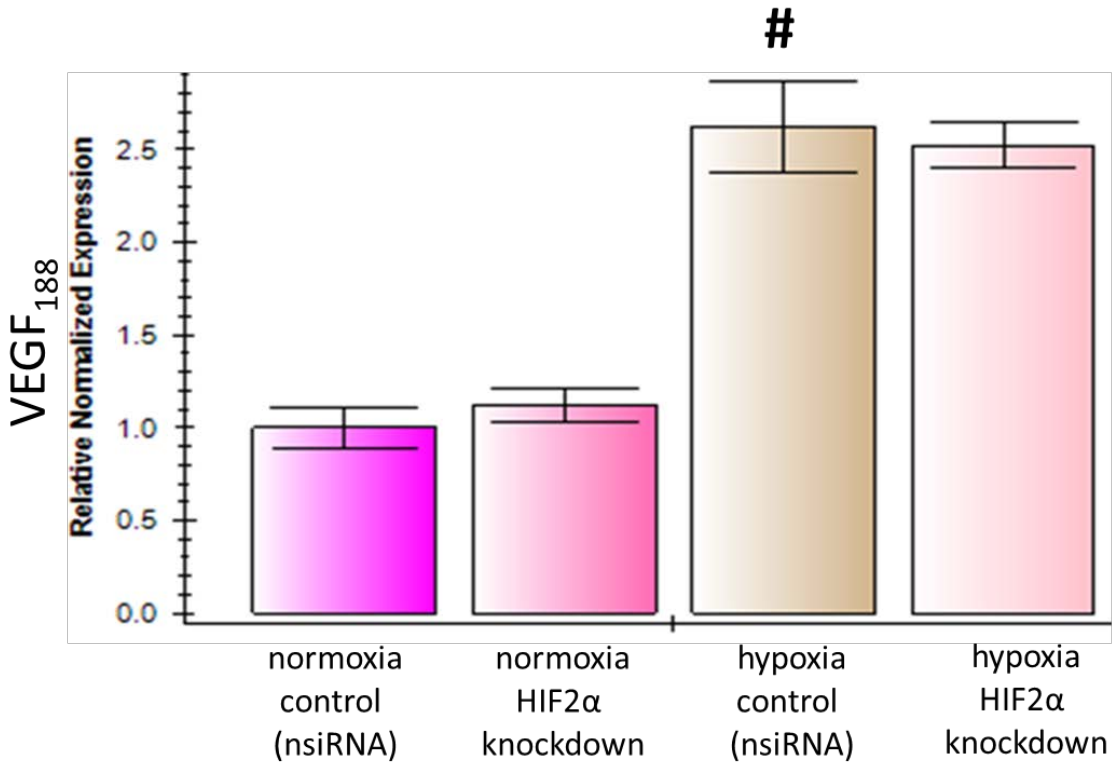

Figure 22. 24-hour HIF2α gene knockdown experiment. Relative normalized expression levels of $VEGF_{188}$ as measured by q-PCR in canine J3T glioblastoma cells grown according to the Cambridge protocol. Expression is displayed in arbitrary units. Bars denote +/- one standard error of the mean. Pound sign indicates statistically significant difference between 20% (normoxia) and 2% oxygen (hypoxia) control samples ($p \leq 0.05$).

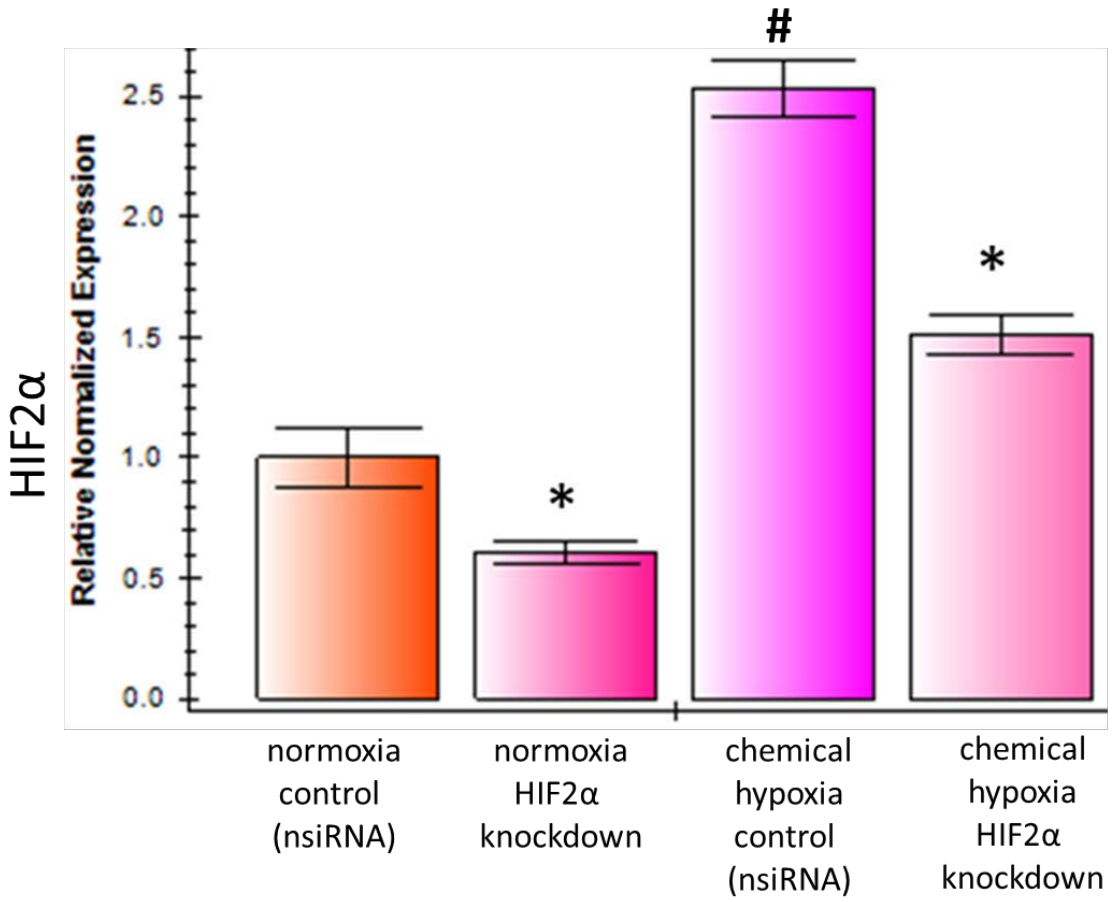

Figure 23. 90-hour HIF2α gene knockdown experiment. Relative normalized expression levels of HIF2α as measured by q-PCR in canine J3T glioblastoma cells grown according to the Cambridge protocol. Expression is displayed in arbitrary units. Bars denote +/- one standard error of the mean. Asterisks indicate statistically significant difference between knockdown and control samples ($p \leq 0.05$) in 20% oxygen (normoxia) and $CoCl_2$ (chemical hypoxia). Pound sign indicates statistically significant difference between 20% oxygen (normoxia) and $CoCl_2$ (chemical hypoxia) control samples ($p \leq 0.05$).

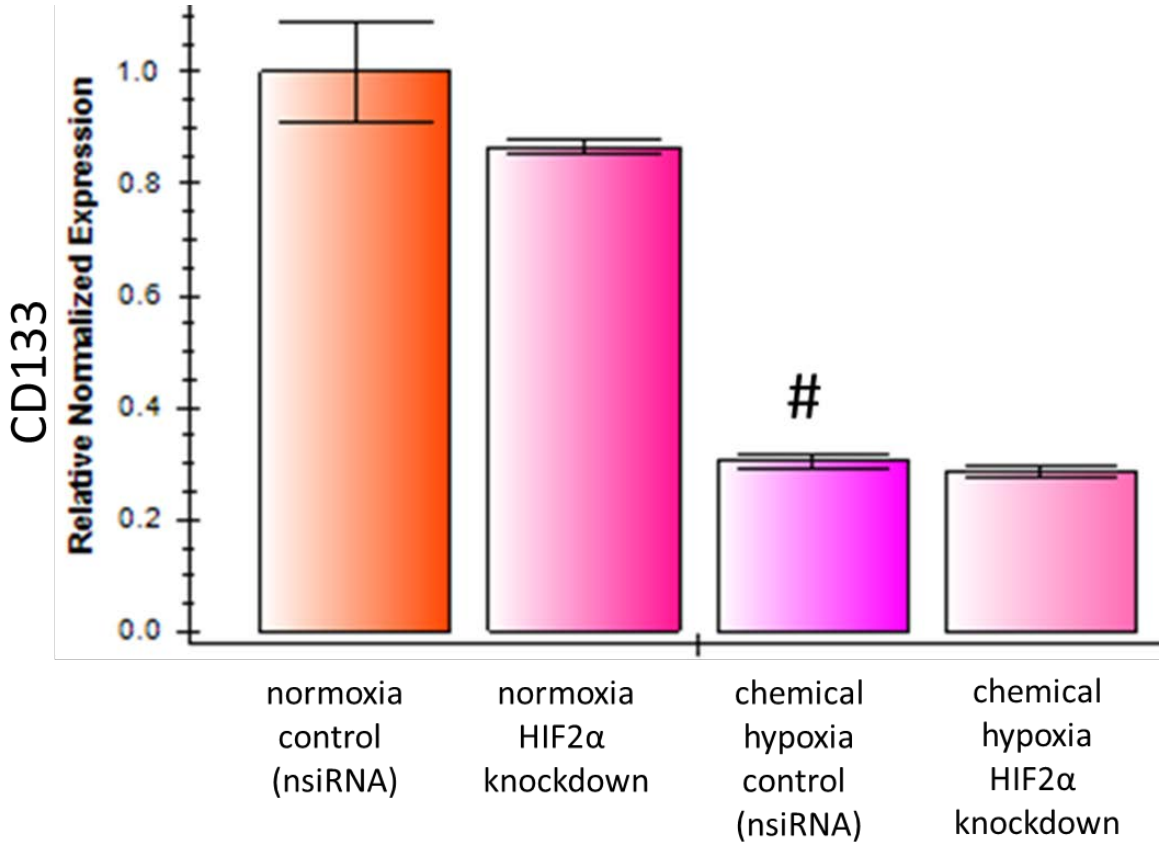

Figure 24. 90-hour HIF2α gene knockdown experiment. Relative normalized expression levels of CD133 as measured by q-PCR in canine J3T glioblastoma cells grown according to the Cambridge protocol. Expression is displayed in arbitrary units. Bars denote +/- one standard error of the mean. Pound sign indicates statistically significant difference between 20% oxygen (normoxia) and $CoCl_2$ (chemical hypoxia) control samples ($p \leq 0.05$).

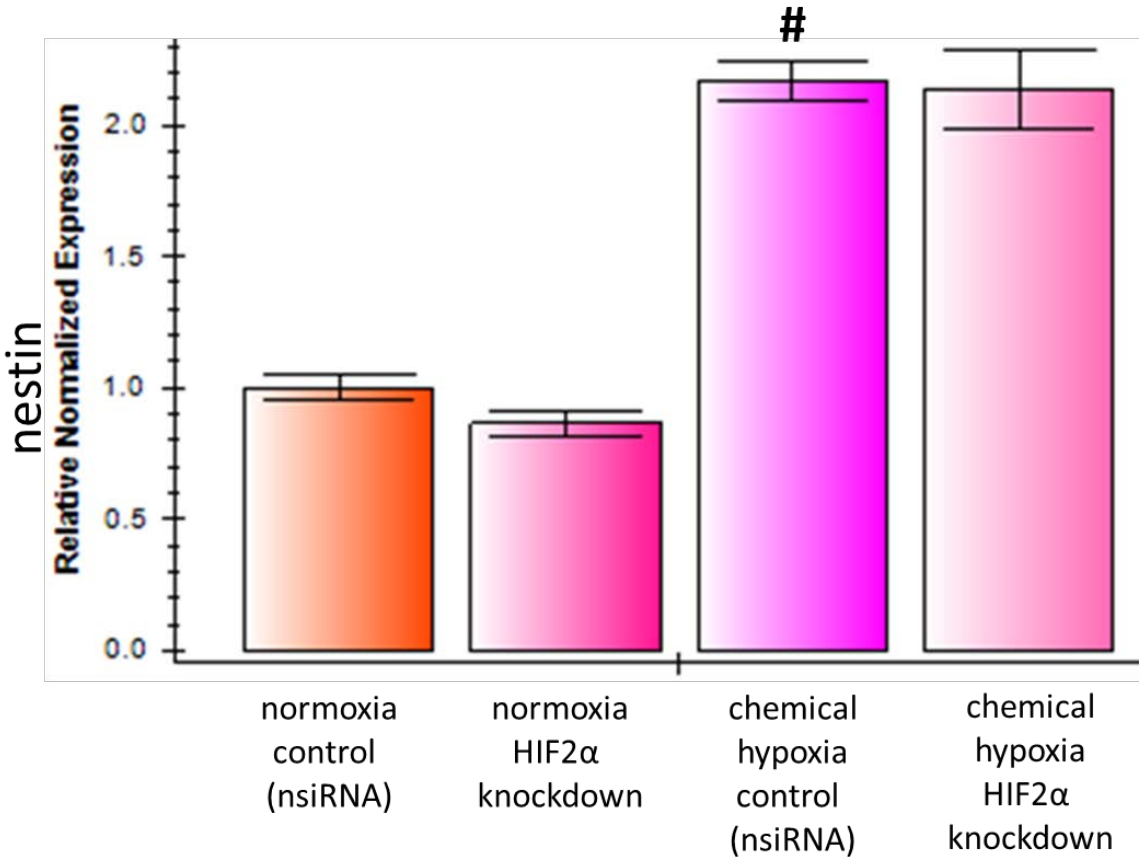

Figure 25. 90-hour HIF2α gene knockdown experiment. Relative normalized expression levels of nestin as measured by q-PCR in canine J3T glioblastoma cells grown according to the Cambridge protocol. Expression is displayed in arbitrary units. Bars denote +/- one standard error of the mean. Pound sign indicates statistically significant difference between 20% oxygen (normoxia) and $CoCl_2$ (chemical hypoxia) control samples ($p \leq 0.05$).

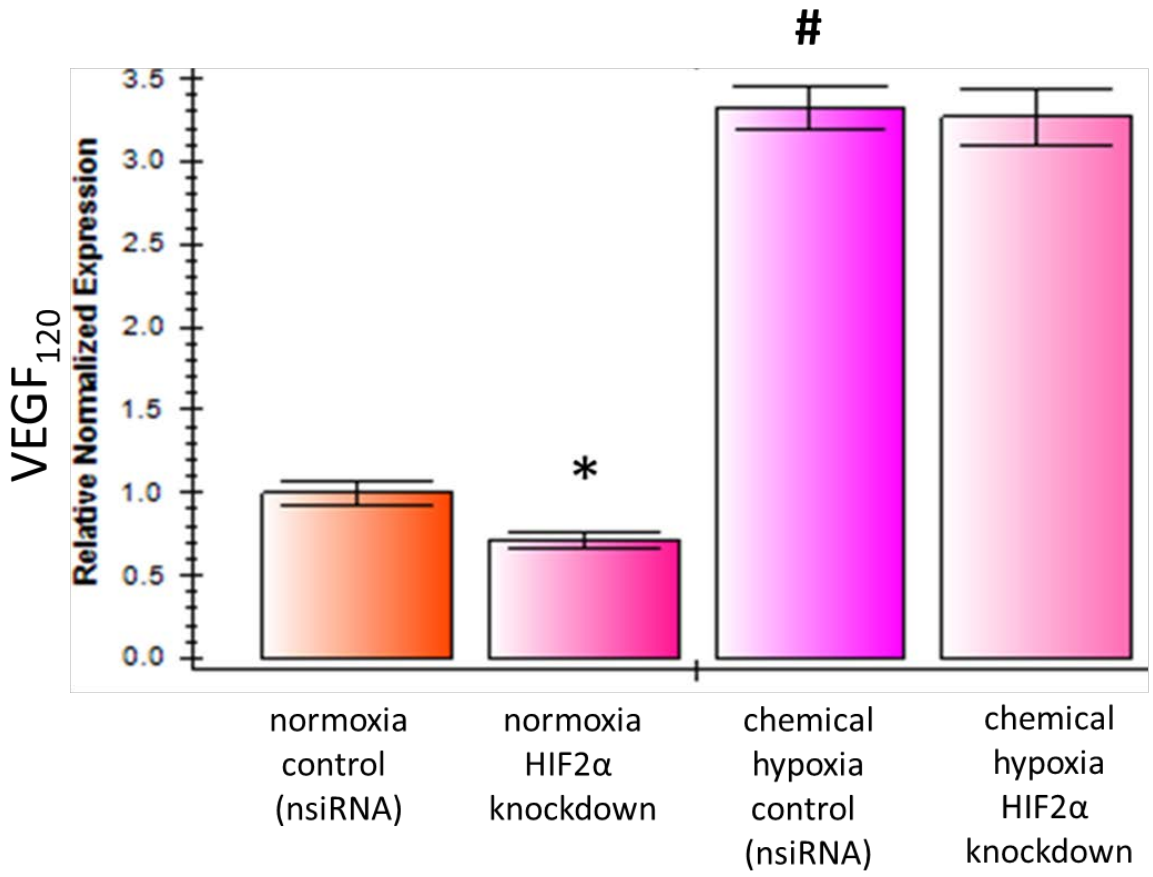

Figure 26. 90-hour HIF2α gene knockdown experiment. Relative normalized expression levels of $VEGF_{120}$ as measured by q-PCR in canine J3T glioblastoma cells grown according to the Cambridge protocol. Expression is displayed in arbitrary units. Bars denote +/- one standard error of the mean. Asterisk indicates statistically significant difference between knockdown and control samples ($p \leq 0.05$) in 20% oxygen (normoxia). Pound sign indicates statistically significant difference between 20% oxygen (normoxia) and $CoCl_2$ (chemical hypoxia) control samples ($p \leq 0.05$).

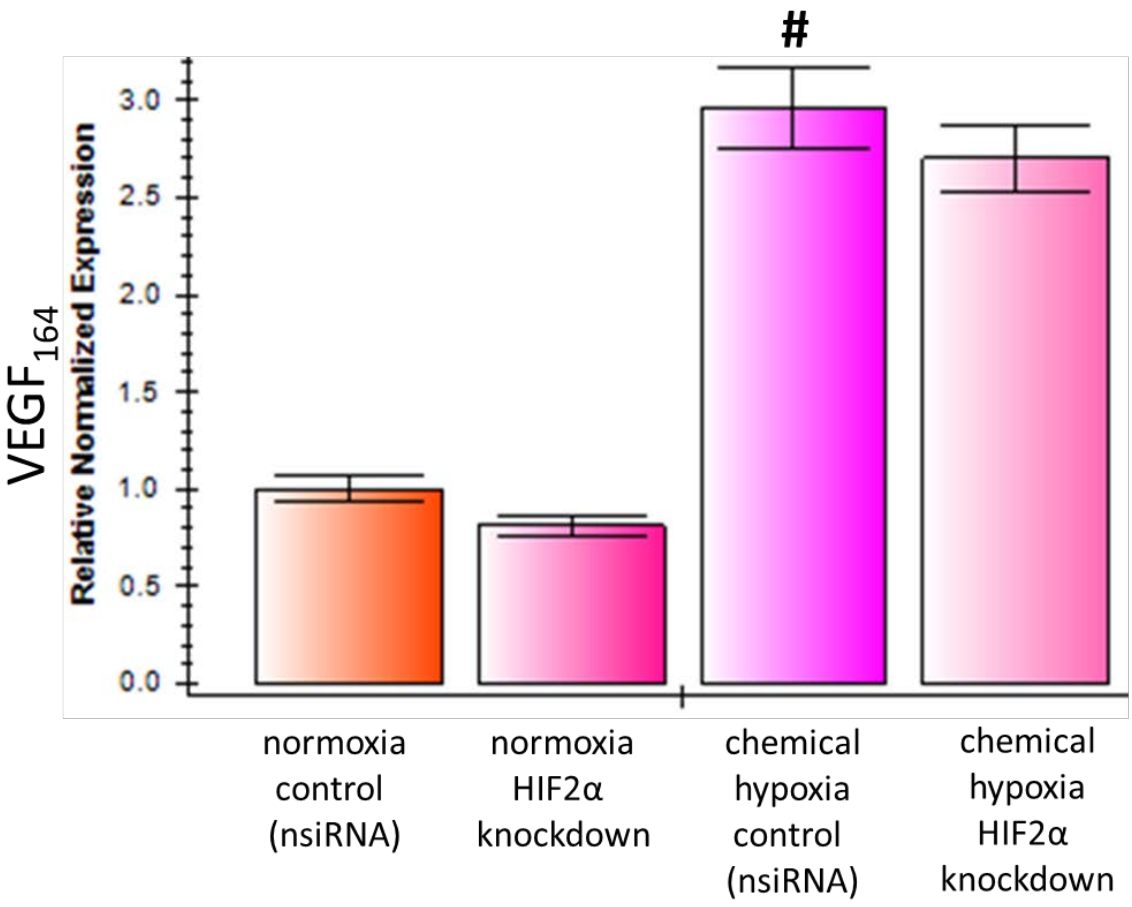

Figure 27. 90-hour HIF2α gene knockdown experiment. Relative normalized expression levels of $VEGF_{164}$ as measured by q-PCR in canine J3T glioblastoma cells grown according to the Cambridge protocol. Expression is displayed in arbitrary units. Bars denote +/- one standard error of the mean. Pound sign indicates statistically significant difference between 20% oxygen (normoxia) and $CoCl_2$ (chemical hypoxia) control samples ($p \leq 0.05$).

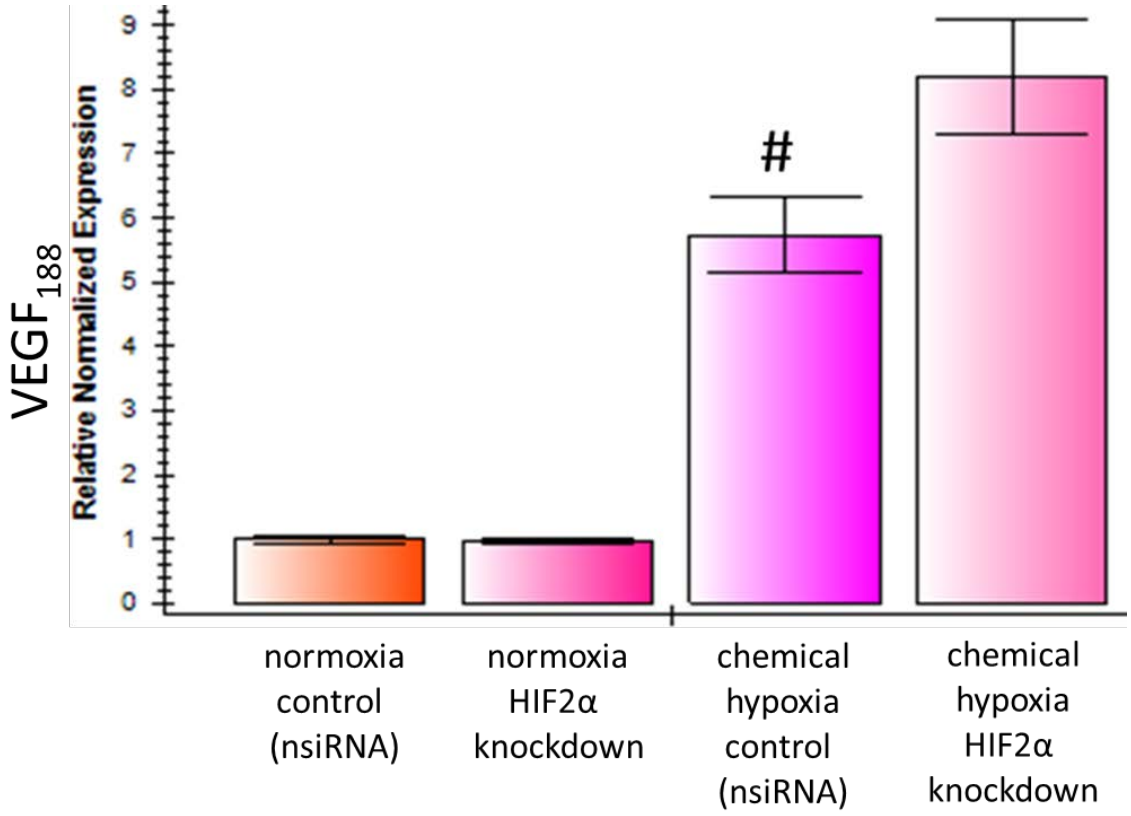

Figure 28. 90-hour HIF2α gene knockdown experiment. Relative normalized expression levels of $VEGF_{188}$ as measured by q-PCR in canine J3T glioblastoma cells grown according to the Cambridge protocol. Expression is displayed in arbitrary units. Bars denote +/- one standard error of the mean. Pound sign indicates statistically significant difference between 20% oxygen (normoxia) and $CoCl_2$ (chemical hypoxia) control samples ($p \leq 0.05$).

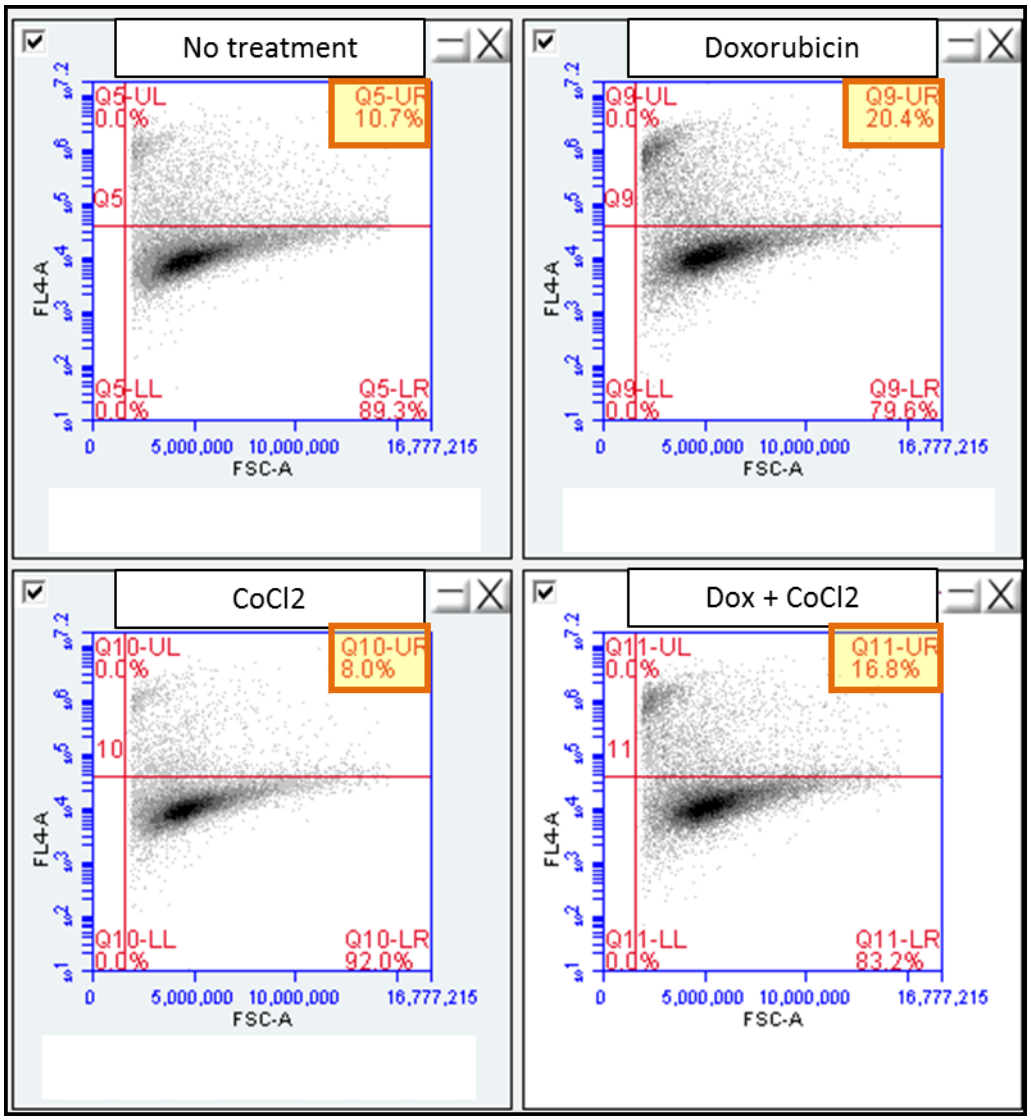

Figure 29. Flow cytometric analysis of live/dead cells using the eFluor assay on J3T cells following 24 hours in culture with either no treatment or in the presence of 1-µM doxorubicin only, $CoCl_2$ only (chemical hypoxia), or both doxorubicin and $CoCl_2$. The percentage of cells in the upper right hand quadrant (orange box) indicates dead cells. Gates were set to exclude very small FSC events interpreted as cell fragments, as well as FSC events with a non-linear relationship between vertical and horizontal FSC measurements interpreted as doublets or multiples. FSC-A =forward scatter, FL4-A =fluorescence.

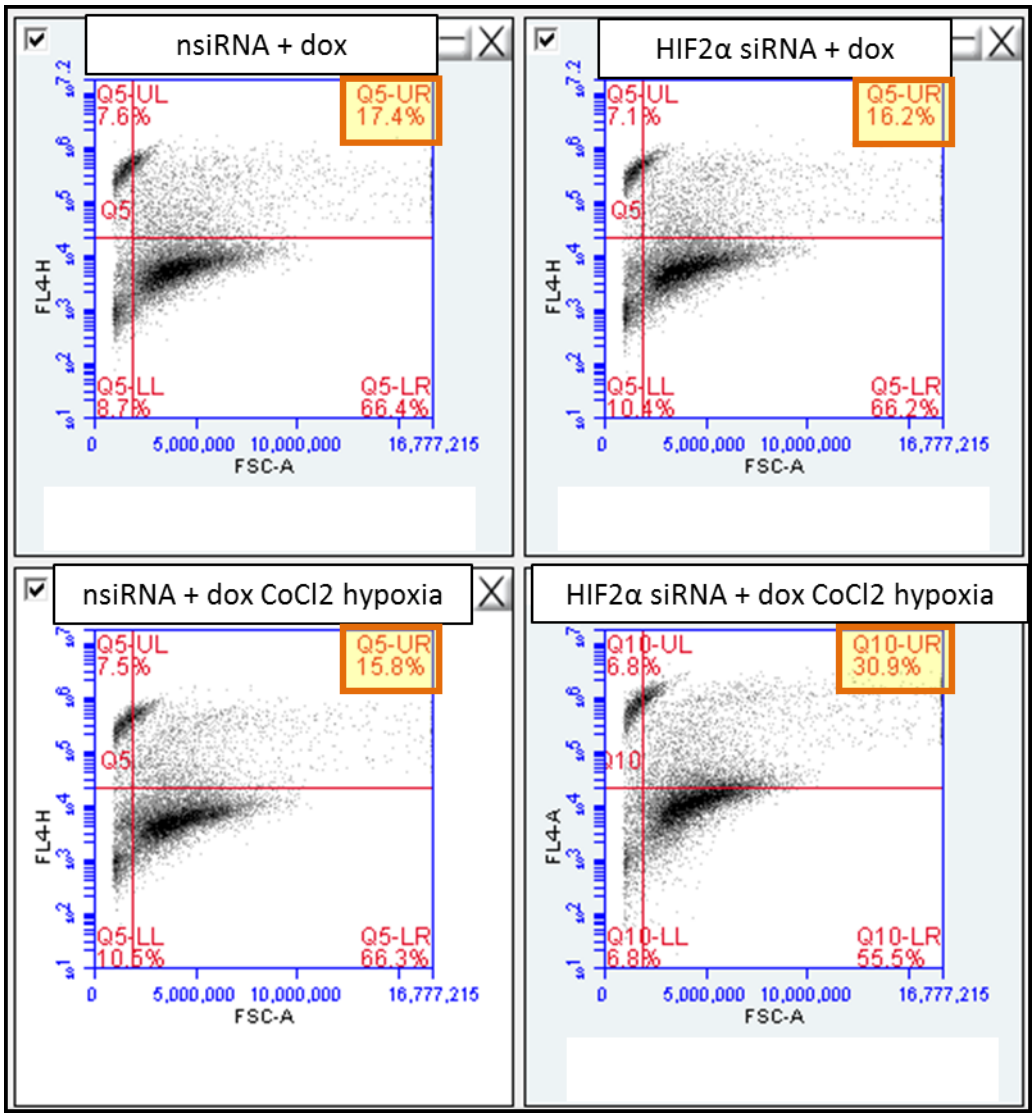

Figure 30. Flow cytometric analysis of live/dead cells using the eFluor assay on J3T cells after HIF2α knockdown (HIF2α siRNA) or control (nsiRNA) and 24-hour exposure to 1-µM doxorubicin in either 20% oxygen (normoxia) or $CoCl_2$ (chemical hypoxia). The percentage of cells in the upper right hand quadrant (orange box) indicates dead cells. Gates were set to exclude very small FSC events interpreted as cell fragments, as well as FSC events with a non-linear relationship between vertical and horizontal FSC measurements interpreted as doublets or multiples. FSC-A =forward scatter, FL4-A =fluorescence.

CHAPTER VI

CONCLUSIONS

Malignant gliomas such as glioblastoma are highly lethal primary brain tumors that occur in both dogs and humans. The use of dogs with naturally-occurring tumors in veterinary clinical trials has the potential to benefit both canine and human patients by serving as a comparative post-translational model for the human disease. For this reason, there is a continuing need to systematically explore the biology of canine malignant gliomas at a molecular and genetic level, both for the sake of the knowledge itself and for the purpose of understanding the comparative biology as it might apply to testing targeted therapies. An area of intense interest in cancer research is the potential role of microenvironmental factors including hypoxia on the acquisition and maintenance of the cancer stem-like phenotype that is purported to drive growth, regrowth, and treatment resistance. At the center of much of the recent investigation of the influence of hypoxia in human glioblastoma is HIF2α, which has been shown to have a pivotal role in mediating the effects of hypoxia on the acquisition and maintenance of the cancer stem-like cell phenotype. Unlike HIF1α, which has been also shown to have an important role in mediating these effects, HIF2α expression is much more restricted and not present in normal neural stem cells. This expression pattern could allow it to be a promising therapeutic target [137] that selectively kills cancer cells while sparing resident normal neural stem cells, a hurdle that potentially plagues CSLC-targeted treatments that use tissue stem cell markers. Further justification for HIF2α's use in targeted therapy is the fact that evaluation of patient samples at

the mRNA level show a negative survival time associated with expression of HIF2α but not HIF1α [137]. This prognostic indicator was further confirmed at mechanistic level in the lab of Jeremy Rich [137, 148], whose group demonstrated that both CSLC and non-stem cell populations (as identified by CD133 expression in primary tumor specimens or xenografts) responded to hypoxia (1% oxygen) with formation of increased number and size of spheres in culture. Additionally, non-stem cells exposed to prolonged hypoxia had transcriptional upregulation of stem cell markers HIF2α, Oct4, Nanog, and C-Myc to levels near or above those present in CSLCs grown in 20% oxygen. Transduction with a non-degradable form of HIF2α into non-stem cells grown in 20% oxygen led to similar increases in the examined stem cell markers, as well as markedly increased tumorigenic capacity in xenograft assays, both of which were abrogated by lentiviral-vectored shRNA-mediated HIF2α gene silencing. Additional findings in that study showed that HIF2α was preferentially involved in the control of VEGF levels in CSLCs, whereas only HIF1α was important in non-stem cells. One finding in their study that corresponds to the lack of CD133 decrease after HIF2α knockdown in our study was the relatively small increase in CD133 mRNA levels produced by transduction of non-degradable HIF2α. This stands in contrast to the *in vivo* immunohistochemical and flow cytometric evidence showing co-expression of these markers in the majority of CSLCs, which could suggest that either CD133 is not directly regulated at the transcriptional level by HIF2α, or that the known pitfalls of CD133 detection (epitope glycosylation, splice variants, tissue-specific isoforms, and cell-cycle dependent expression) impact these investigations.

In human glioblastomas, a variably large subpopulation of cells is identified based on expression of certain markers or demonstration of enzymatic activity or growth patterns in culture, and this subset of CSLCs is postulated to drive the majority of tumor growth, regrowth,

invasiveness, and resistance to chemotherapy and radiation. Unfortunately, currently available methods for identifying these cells for analysis and experimental manipulation are imperfect, and we still lack a complete picture of the plasticity of this state *in vivo* and of the microenvironmental, epigenetic, and internal molecular mechanisms that drive it. The purpose of this body of work was to perform preliminary investigations into the influence of hypoxia on the acquisition and maintenance of a CSLC phenotype in canine glioblastoma in an *in vitro* model. Dogs are being touted increasingly as potential large-animal models of naturally-occurring glioblastoma and could provide a valuable bridge between experimental rodent models and human clinical trials. Although gliomas in dogs are morphologically similar to their counterparts in humans, and although several excellent research groups have contributed to our body of knowledge regarding the biology of the disease in dogs, much work remains to be done to systematically explore the comparative biology of canine and human tumors at the genetic, epigenetic, and molecular level. To that end, we undertook a three-part study to examine some of the effects of a hypoxic environment on the transcriptional expression of a selected panel of putative CSLC and angiogenesis-related markers.

In the first part, we demonstrated that canine J3T glioblastoma cells grown on laminin-coated cultureware in defined serum-free medium for prolonged periods in 2% oxygen had marked upregulation of CD133, nestin, HIF2α, and CD31 as compared to cells grown in serum-supplemented media, or the adherent- or sphere-forming population of cells grown in 20% oxygen. These findings are novel and have never been reported in the dog. Additionally, although not without its drawbacks, we validated the use of a low-cost lab-built hypoxic chamber constructed according to previously published protocols [171]. The use of this low-cost method should be of particular interest to veterinary and comparative researchers who often work with

limited budgets that cannot support the purchase of expensive specialized equipment to produce these experimental conditions. Additionally, we successfully validated the Cambridge protocol for use with the J3T canine glioblastoma cell line. During the attempt to expand the methods detailed in this part to an additional canine glioblastoma cell line, it was discovered that this cell line was misidentified as canine when in fact it was of murine origin. This study, though frustrating, expensive, and time-consuming, reinforces the crucial role of accurate cell line identification in cell culture-based research. Failure to do so can result in spurious and misleading results that potentially damage human and animal health, waste resources, and erode public trust in the scientific community.

In the second part, we examined the transcriptional expression of HIF2α and $VEGF_{120}$, $VEGF_{164}$, and $VEGF_{188}$ over multiple time points in J3T canine glioblastoma cells *in vitro* using two methods of hypoxia induction: the previously utilized hypoxic chamber with 2% oxygen, and the chemical hypoxia mimetic cobalt chloride. When compared to time-point controls in 20% oxygen, both experimental hypoxia methods produced significant upregulation of all VEGF isoforms, but at different peak times, and only the 2% oxygen method induced significant alterations in HIF2α mRNA expression. Nevertheless, immunocytochemistry demonstrated that both methods produce increases in HIF2α protein levels and, importantly, increased localization of the protein to the nucleus.

In the third part, we examined the effect of transient siRNA-mediated silencing of HIF2α on expression of these selected CSLC and angiogenesis markers and susceptibility to doxorubicin in J3T canine glioblastoma cells *in vitro*. siRNA-mediated silencing of HIF2α resulted in a partial knockdown that was less effective in hypoxia and susceptible to dilution effect over time. HIF2α knockdown in normoxia decreased nestin expression, suggesting that

HIF2α is at least partially responsible for nestin expression in these cells. Nestin expression has been documented at the mRNA level in one high-grade canine glioma, and was not present in a low-grade canine glioma [173]. Nestin expression in human gliomas is correlated to both increasing tumor grade [65, 222] and poor survival [223]. Thus, the finding of increased nestin in response to hypoxia, and the partial abrogation of this with HIF2α silencing in the J3T cell line, is significant. Additionally, increasing intratumoral VEGF correlates with increasing tumor grade in dogs, as it does in humans [164, 165], making the finding of significant increases in VEGF in response to experimental hypoxia important from a comparative biology and therapeutic standpoint. Despite the lack of statistical significance in the 24-hour HIF2α knockdown group, there was a distinct trend toward decreased VEGF expression that bears further investigation in other experimental settings. The doubling of cell death after HIF2α knockdown in the presence of doxorubicin is noteworthy because this drug is one that is readily available, inexpensive, has a long track record of use in dogs, and has been the subject of much study in terms of increasing its penetration of the blood-brain-barrier. In veterinary medicine, we are often faced with a wide variety of clients, some of whom are interested and able to pursue expensive and invasive therapeutics, and others who do not wish to do so for either economic or philosophical reasons. Because of this reality, the ability to offer non-invasive therapy with an increased safety and efficacy profile should remain one of our primary goals. This investigation is an early step toward exploring the use of gene silencing in conjunction with chemotherapy for that purpose.

Future directions to augment the findings in these studies and correct any inherent drawbacks in the model would ideally include the use of multiple primary and low-passage canine glioblastoma cell lines, the use of a specialized incubator and work space to produce

consistent oxygen concentration at a variety of levels, and the use of techniques that would allow evaluation of a larger number of candidate genes that could then be evaluated for their utility to serve as diagnostic tools, prognostic indicators, biomarkers, or therapeutic targets.

REFERENCES

1. CBTRUS. *http://www.cbtrus.org/reports/reports.html*. 2010-2011.
2. Altekruse, S.F., et al., *SEER Cancer Statistics Review, 1975-2007*, N.C. Institute, Editor 2009: Bethesda, MD.
3. Louis, D.N., et al., eds. *Tumours: introduction and neuroepithelial tumours*. 8th ed. Greenfield's Neuropathology, ed. L.D. Love S, Ellison DW. Vol. 2. 2008, Edward Arnold, Ltd.: London. p. 1821-2000.
4. Liwnicz, B.H., et al., *Radiation-associated gliomas: a report of four cases and analysis of postradiation tumors of the central nervous system.* Neurosurgery, 1985. **17**(3): p. 436-45.
5. Louis, D.N., et al., eds. *WHO Classification of Tumours of the Central Nervous System* 4th ed. IARC WHO Classification of Tumours. Vol. 1. 2007, IARC Press: Lyon, France.
6. *Prognostic factors for high-grade malignant glioma: development of a prognostic index. A Report of the Medical Research Council Brain Tumour Working Party.* J Neurooncol, 1990. **9**(1): p. 47-55.
7. Phillips, H.S., et al., *Molecular subclasses of high-grade glioma predict prognosis, delineate a pattern of disease progression, and resemble stages in neurogenesis.* Cancer Cell, 2006. **9**(3): p. 157-73.

8. Kriegstein, A. and A. Alvarez-Buylla, *The glial nature of embryonic and adult neural stem cells.* Annu Rev Neurosci, 2009. **32**: p. 149-84.

9. Comm., B., *Embryonic vertebrate central nervous system: revised terminology.* Anat Rec, 1970. **166**: p. 257-261.

10. Aaku-Saraste, E., et al., *Neuroepithelial cells downregulate their plasma membrane polarity prior to neural tube closure and neurogenesis.* Mech Dev, 1997. **69**(1-2): p. 71-81.

11. Stoykova, A., et al., *Pax6-dependent regulation of adhesive patterning, R-cadherin expression and boundary formation in developing forebrain.* Development, 1997. **124**(19): p. 3765-77.

12. Shibata, T., et al., *Glutamate transporter GLAST is expressed in the radial glia-astrocyte lineage of developing mouse spinal cord.* J Neurosci, 1997. **17**(23): p. 9212-9.

13. Feng, L., M.E. Hatten, and N. Heintz, *Brain lipid-binding protein (BLBP): a novel signaling system in the developing mammalian CNS.* Neuron, 1994. **12**(4): p. 895-908.

14. Hartfuss, E., et al., *Characterization of CNS precursor subtypes and radial glia.* Dev Biol, 2001. **229**(1): p. 15-30.

15. Mori, T., A. Buffo, and M. Gotz, *The novel roles of glial cells revisited: the contribution of radial glia and astrocytes to neurogenesis.* Curr Top Dev Biol, 2005. **69**: p. 67-99.

16. Choi, B.H., *Radial glia of developing human fetal spinal cord: Golgi, immunohistochemical and electron microscopic study.* Brain Res, 1981. **227**(2): p. 249-67.

17. Miller, R.H., *Regulation of oligodendrocyte development in the vertebrate CNS.* Prog Neurobiol, 2002. **67**(6): p. 451-67.

18. Richardson, W.D., N. Kessaris, and N. Pringle, *Oligodendrocyte wars.* Nat Rev Neurosci, 2006. **7**(1): p. 11-8.

19. Rowitch, D.H., *Glial specification in the vertebrate neural tube.* Nat Rev Neurosci, 2004. **5**(5): p. 409-19.

20. Bailey, P.C.a.C., H., *A Classification of the Tumors of the Glioma Group on a Histogenetic Basis with a Correlated Study of Prognosis*1926, Philadelphia, PA, USA: Lippincott.

21. Rosenblum, M.L., et al., *Potentials and possible pitfalls of human stem cell analysis.* Cancer Chemother Pharmacol, 1981. **6**(3): p. 227-35.

22. Lapidot, T., et al., *A cell initiating human acute myeloid leukaemia after transplantation into SCID mice.* Nature, 1994. **367**(6464): p. 645-8.

23. Bonnet, D. and J.E. Dick, *Human acute myeloid leukemia is organized as a hierarchy that originates from a primitive hematopoietic cell.* Nat Med, 1997. **3**(7): p. 730-7.

24. Visvader, J.E. and G.J. Lindeman, *Cancer stem cells in solid tumours: accumulating evidence and unresolved questions.* Nat Rev Cancer, 2008. **8**(10): p. 755-68.

25. Liu, G., et al., *Analysis of gene expression and chemoresistance of CD133+ cancer stem cells in glioblastoma.* Mol Cancer, 2006. **5**: p. 67.

26. Bao, S., et al., *Glioma stem cells promote radioresistance by preferential activation of the DNA damage response.* Nature, 2006. **444**(7120): p. 756-60.

27. Lathia, J.D., et al., *Deadly teamwork: neural cancer stem cells and the tumor microenvironment.* Cell Stem Cell, 2011. **8**(5): p. 482-5.

28. Gupta, P.B., et al., *Stochastic state transitions give rise to phenotypic equilibrium in populations of cancer cells.* Cell, 2011. **146**(4): p. 633-44.

29. Reynolds, B.A. and S. Weiss, *Generation of neurons and astrocytes from isolated cells of the adult mammalian central nervous system.* Science, 1992. **255**(5052): p. 1707-10.

30. Ignatova, T.N., et al., *Human cortical glial tumors contain neural stem-like cells expressing astroglial and neuronal markers in vitro.* Glia, 2002. **39**(3): p. 193-206.

31. Bez, A., et al., *Neurosphere and neurosphere-forming cells: morphological and ultrastructural characterization.* Brain Res, 2003. **993**(1-2): p. 18-29.

32. Louis, S.A., et al., *Enumeration of neural stem and progenitor cells in the neural colony-forming cell assay.* Stem Cells, 2008. **26**(4): p. 988-96.

33. Liu, Q., et al., *Molecular properties of CD133+ glioblastoma stem cells derived from treatment-refractory recurrent brain tumors.* J Neurooncol, 2009. **94**(1): p. 1-19.

34. Yuan, X., et al., *Isolation of cancer stem cells from adult glioblastoma multiforme.* Oncogene, 2004. **23**(58): p. 9392-400.

35. Singec, I., et al., *Defining the actual sensitivity and specificity of the neurosphere assay in stem cell biology.* Nat Methods, 2006. **3**(10): p. 801-6.

36. Pollard, S.M., et al., *Glioma stem cell lines expanded in adherent culture have tumor-specific phenotypes and are suitable for chemical and genetic screens.* Cell Stem Cell, 2009. **4**(6): p. 568-80.

37. Fael Al-Mayhani, T.M., et al., *An efficient method for derivation and propagation of glioblastoma cell lines that conserves the molecular profile of their original tumours.* J Neurosci Methods, 2009. **176**(2): p. 192-9.

38. Sun, Y., et al., *Long-term tripotent differentiation capacity of human neural stem (NS) cells in adherent culture.* Mol Cell Neurosci, 2008. **38**(2): p. 245-58.

39. Yin, A.H., et al., *AC133, a novel marker for human hematopoietic stem and progenitor cells.* Blood, 1997. **90**(12): p. 5002-12.

40. Weigmann, A., et al., *Prominin, a novel microvilli-specific polytopic membrane protein of the apical surface of epithelial cells, is targeted to plasmalemmal protrusions of non-epithelial cells.* Proc Natl Acad Sci U S A, 1997. **94**(23): p. 12425-30.

41. Miraglia, S., et al., *A novel five-transmembrane hematopoietic stem cell antigen: isolation, characterization, and molecular cloning.* Blood, 1997. **90**(12): p. 5013-21.

42. Corbeil, D., et al., *Prominin: a story of cholesterol, plasma membrane protrusions and human pathology.* Traffic, 2001. **2**(2): p. 82-91.

43. Fargeas, C.A., et al., *Identification of novel Prominin-1/CD133 splice variants with alternative C-termini and their expression in epididymis and testis.* J Cell Sci, 2004. **117**(Pt 18): p. 4301-11.

44. Mizrak, D., M. Brittan, and M.R. Alison, *CD133: molecule of the moment.* J Pathol, 2008. **214**(1): p. 3-9.

45. Singh, S.K., et al., *Identification of a cancer stem cell in human brain tumors.* Cancer Res, 2003. **63**(18): p. 5821-8.

46. Singh, S.K., et al., *Identification of human brain tumour initiating cells.* Nature, 2004. **432**(7015): p. 396-401.

47. Clement, V., et al., *Limits of CD133 as a marker of glioma self-renewing cells.* Int J Cancer, 2009. **125**(1): p. 244-8.

48. Joo, K.M., et al., *Clinical and biological implications of CD133-positive and CD133-negative cells in glioblastomas.* Lab Invest, 2008. **88**(8): p. 808-15.

49. Shu, Q., et al., *Direct orthotopic transplantation of fresh surgical specimen preserves CD133+ tumor cells in clinically relevant mouse models of medulloblastoma and glioma.* Stem Cells, 2008. **26**(6): p. 1414-24.

50. Wang, J., et al., *CD133 negative glioma cells form tumors in nude rats and give rise to CD133 positive cells.* Int J Cancer, 2008. **122**(4): p. 761-8.

51. Son, M.J., et al., *SSEA-1 is an enrichment marker for tumor-initiating cells in human glioblastoma.* Cell Stem Cell, 2009. **4**(5): p. 440-52.

52. Zeppernick, F., et al., *Stem cell marker CD133 affects clinical outcome in glioma patients.* Clin Cancer Res, 2008. **14**(1): p. 123-9.

53. Beier, D., et al., *CD133 expression and cancer stem cells predict prognosis in high-grade oligodendroglial tumors.* Brain Pathol, 2008. **18**(3): p. 370-7.

54. Blazek, E.R., J.L. Foutch, and G. Maki, *Daoy medulloblastoma cells that express CD133 are radioresistant relative to CD133- cells, and the CD133+ sector is enlarged by hypoxia.* Int J Radiat Oncol Biol Phys, 2007. **67**(1): p. 1-5.

55. Platet, N., et al., *Influence of oxygen tension on CD133 phenotype in human glioma cell cultures.* Cancer Lett, 2007. **258**(2): p. 286-90.

56. Osmond, T.L., K.W. Broadley, and M.J. McConnell, *Glioblastoma cells negative for the anti-CD133 antibody AC133 express a truncated variant of the CD133 protein.* Int J Mol Med, 2010. **25**(6): p. 883-8.

57. Corbeil, D., et al., *The human AC133 hematopoietic stem cell antigen is also expressed in epithelial cells and targeted to plasma membrane protrusions.* J Biol Chem, 2000. **275**(8): p. 5512-20.

58. Florek, M., et al., *Prominin-1/CD133, a neural and hematopoietic stem cell marker, is expressed in adult human differentiated cells and certain types of kidney cancer.* Cell Tissue Res, 2005. **319**(1): p. 15-26.

59. Fargeas, C.A., W.B. Huttner, and D. Corbeil, *Nomenclature of prominin-1 (CD133) splice variants - an update.* Tissue Antigens, 2007. **69**(6): p. 602-6.

60. Shmelkov, S.V., et al., *Alternative promoters regulate transcription of the gene that encodes stem cell surface protein AC133.* Blood, 2004. **103**(6): p. 2055-61.

61. Zimmerman, L., et al., *Independent regulatory elements in the nestin gene direct transgene expression to neural stem cells or muscle precursors.* Neuron, 1994. **12**(1): p. 11-24.

62. Lendahl, U., L.B. Zimmerman, and R.D. McKay, *CNS stem cells express a new class of intermediate filament protein.* Cell, 1990. **60**(4): p. 585-95.

63. Liu, Y., et al., *Oligodendrocyte and astrocyte development in rodents: an in situ and immunohistological analysis during embryonic development.* Glia, 2002. **40**(1): p. 25-43.

64. Messam, C.A., J. Hou, and E.O. Major, *Coexpression of nestin in neural and glial cells in the developing human CNS defined by a human-specific anti-nestin antibody.* Exp Neurol, 2000. **161**(2): p. 585-96.

65. Dahlstrand, J., V.P. Collins, and U. Lendahl, *Expression of the class VI intermediate filament nestin in human central nervous system tumors.* Cancer Res, 1992. **52**(19): p. 5334-41.

66. Almqvist, P.M., et al., *Immunohistochemical detection of nestin in pediatric brain tumors.* J Histochem Cytochem, 2002. **50**(2): p. 147-58.

67. Ehrmann, J., Z. Kolar, and J. Mokry, *Nestin as a diagnostic and prognostic marker: immunohistochemical analysis of its expression in different tumours.* J Clin Pathol, 2005. **58**(2): p. 222-3.

68. Tohyama, T., et al., *Nestin expression in embryonic human neuroepithelium and in human neuroepithelial tumor cells.* Lab Invest, 1992. **66**(3): p. 303-13.

69. Shih, A.H. and E.C. Holland, *Notch signaling enhances nestin expression in gliomas.* Neoplasia, 2006. **8**(12): p. 1072-82.

70. Sahlgren, C., et al., *Notch signaling mediates hypoxia-induced tumor cell migration and invasion.* Proc Natl Acad Sci U S A, 2008. **105**(17): p. 6392-7.

71. Capela, A. and S. Temple, *LeX/ssea-1 is expressed by adult mouse CNS stem cells, identifying them as nonependymal.* Neuron, 2002. **35**(5): p. 865-75.

72. Capela, A. and S. Temple, *LeX is expressed by principle progenitor cells in the embryonic nervous system, is secreted into their environment and binds Wnt-1.* Dev Biol, 2006. **291**(2): p. 300-13.

73. Lalande, M.E. and R.G. Miller, *Fluorescence flow analysis of lymphocyte activation using Hoechst 33342 dye.* J Histochem Cytochem, 1979. **27**(1): p. 394-7.

74. Challen, G.A. and M.H. Little, *A side order of stem cells: the SP phenotype.* Stem Cells, 2006. **24**(1): p. 3-12.

75. Wan, F., et al., *The utility and limitations of neurosphere assay, CD133 immunophenotyping and side population assay in glioma stem cell research.* Brain Pathol, 2010. **20**(5): p. 877-89.

76. Bleau, A.M., et al., *PTEN/PI3K/Akt pathway regulates the side population phenotype and ABCG2 activity in glioma tumor stem-like cells.* Cell Stem Cell, 2009. **4**(3): p. 226-35.

77. Chiba, T., et al., *Side population purified from hepatocellular carcinoma cells harbors cancer stem cell-like properties.* Hepatology, 2006. **44**(1): p. 240-51.

78. Haraguchi, N., et al., *Characterization of a side population of cancer cells from human gastrointestinal system.* Stem Cells, 2006. **24**(3): p. 506-13.

79. Patrawala, L., et al., *Side population is enriched in tumorigenic, stem-like cancer cells, whereas ABCG2+ and ABCG2- cancer cells are similarly tumorigenic.* Cancer Res, 2005. **65**(14): p. 6207-19.

80. Chua, C., et al., *Characterization of a side population of astrocytoma cells in response to temozolomide.* J Neurosurg, 2008. **109**(5): p. 856-66.

81. Wu, C. and B.A. Alman, *Side population cells in human cancers.* Cancer Lett, 2008. **268**(1): p. 1-9.

82. Wu, C., et al., *Side population cells isolated from mesenchymal neoplasms have tumor initiating potential.* Cancer Res, 2007. **67**(17): p. 8216-22.

83. Harris, M.A., et al., *Cancer stem cells are enriched in the side population cells in a mouse model of glioma.* Cancer Res, 2008. **68**(24): p. 10051-9.

84. Borst, P. and R.O. Elferink, *Mammalian ABC transporters in health and disease.* Annu Rev Biochem, 2002. **71**: p. 537-92.

85. Scharenberg, C.W., M.A. Harkey, and B. Torok-Storb, *The ABCG2 transporter is an efficient Hoechst 33342 efflux pump and is preferentially expressed by immature human hematopoietic progenitors.* Blood, 2002. **99**(2): p. 507-12.

86. Wu, C.P., C.H. Hsieh, and Y.S. Wu, *The emergence of drug transporter-mediated multidrug resistance to cancer chemotherapy.* Mol Pharm, 2011. **8**(6): p. 1996-2011.

87. Zhou, S., et al., *Bcrp1 gene expression is required for normal numbers of side population stem cells in mice, and confers relative protection to mitoxantrone in hematopoietic cells in vivo.* Proc Natl Acad Sci U S A, 2002. **99**(19): p. 12339-44.

88. Kondo, T., T. Setoguchi, and T. Taga, *Persistence of a small subpopulation of cancer stem-like cells in the C6 glioma cell line.* Proc Natl Acad Sci U S A, 2004. **101**(3): p. 781-6.

89. Tirino, V., et al., *Detection and characterization of CD133+ cancer stem cells in human solid tumours.* PLoS One, 2008. **3**(10): p. e3469.

90. Adamski, D., et al., *Effects of Hoechst 33342 on C2C12 and PC12 cell differentiation.* FEBS Lett, 2007. **581**(16): p. 3076-80.

91. Srivastava, V.K. and J. Nalbantoglu, *Flow cytometric characterization of the DAOY medulloblastoma cell line for the cancer stem-like phenotype.* Cytometry A, 2008. **73**(10): p. 940-8.

92. Steuer, B., B. Breuer, and A. Alonso, *Differentiation of EC cells in vitro by the fluorescent dye Hoechst 33342.* Exp Cell Res, 1990. **186**(1): p. 149-57.

93. Zheng, X., et al., *Most C6 cells are cancer stem cells: evidence from clonal and population analyses.* Cancer Res, 2007. **67**(8): p. 3691-7.

94. Perozich, J., et al., *Relationships within the aldehyde dehydrogenase extended family.* Protein Sci, 1999. **8**(1): p. 137-46.

95. Ma, I. and A.L. Allan, *The role of human aldehyde dehydrogenase in normal and cancer stem cells.* Stem Cell Rev, 2011. **7**(2): p. 292-306.

96. Rasper, M., et al., *Aldehyde dehydrogenase 1 positive glioblastoma cells show brain tumor stem cell capacity.* Neuro Oncol, 2010. **12**(10): p. 1024-33.

97. Yang, Z.J. and R.J. Wechsler-Reya, *Hit 'em where they live: targeting the cancer stem cell niche.* Cancer Cell, 2007. **11**(1): p. 3-5.

98. Gilbertson, R.J. and J.N. Rich, *Making a tumour's bed: glioblastoma stem cells and the vascular niche.* Nat Rev Cancer, 2007. **7**(10): p. 733-6.

99. Hjelmeland, A.B., et al., *Twisted tango: brain tumor neurovascular interactions.* Nat Neurosci, 2011. **14**(11): p. 1375-81.

100. Majmundar, A.J., W.J. Wong, and M.C. Simon, *Hypoxia-inducible factors and the response to hypoxic stress.* Mol Cell, 2010. **40**(2): p. 294-309.

101. Gu, Y.Z., et al., *Molecular characterization and chromosomal localization of a third alpha-class hypoxia inducible factor subunit, HIF3alpha.* Gene Expr, 1998. **7**(3): p. 205-13.

102. Huang, L.E., et al., *Activation of hypoxia-inducible transcription factor depends primarily upon redox-sensitive stabilization of its alpha subunit.* J Biol Chem, 1996. **271**(50): p. 32253-9.

103. Yu, A.Y., et al., *Temporal, spatial, and oxygen-regulated expression of hypoxia-inducible factor-1 in the lung.* Am J Physiol, 1998. **275**(4 Pt 1): p. L818-26.

104. Kaelin, W.G., Jr., *The von Hippel-Lindau tumour suppressor protein: O2 sensing and cancer.* Nat Rev Cancer, 2008. **8**(11): p. 865-73.

105. Maxwell, P.H., et al., *The tumour suppressor protein VHL targets hypoxia-inducible factors for oxygen-dependent proteolysis.* Nature, 1999. **399**(6733): p. 271-5.

106. Kaelin, W.G., Jr. and P.J. Ratcliffe, *Oxygen sensing by metazoans: the central role of the HIF hydroxylase pathway.* Mol Cell, 2008. **30**(4): p. 393-402.

107. Kimura, H., et al., *Identification of hypoxia-inducible factor 1 ancillary sequence and its function in vascular endothelial growth factor gene induction by hypoxia and nitric oxide.* J Biol Chem, 2001. **276**(3): p. 2292-8.

108. Elvidge, G.P., et al., *Concordant regulation of gene expression by hypoxia and 2-oxoglutarate-dependent dioxygenase inhibition: the role of HIF-1alpha, HIF-2alpha, and other pathways.* J Biol Chem, 2006. **281**(22): p. 15215-26.

109. Lisy, K. and D.J. Peet, *Turn me on: regulating HIF transcriptional activity.* Cell Death Differ, 2008. **15**(4): p. 642-9.

110. Arany, Z., et al., *An essential role for p300/CBP in the cellular response to hypoxia.* Proc Natl Acad Sci U S A, 1996. **93**(23): p. 12969-73.

111. Ema, M., et al., *Molecular mechanisms of transcription activation by HLF and HIF1alpha in response to hypoxia: their stabilization and redox signal-induced interaction with CBP/p300.* EMBO J, 1999. **18**(7): p. 1905-14.

112. Carrero, P., et al., *Redox-regulated recruitment of the transcriptional coactivators CREB-binding protein and SRC-1 to hypoxia-inducible factor 1alpha.* Mol Cell Biol, 2000. **20**(1): p. 402-15.

113. Lando, D., et al., *Asparagine hydroxylation of the HIF transactivation domain a hypoxic switch.* Science, 2002. **295**(5556): p. 858-61.

114. Bruning, U., et al., *MicroRNA-155 promotes resolution of hypoxia-inducible factor 1alpha activity during prolonged hypoxia.* Mol Cell Biol, 2011. **31**(19): p. 4087-96.

115. Taguchi, A., et al., *Identification of hypoxia-inducible factor-1 alpha as a novel target for miR-17-92 microRNA cluster.* Cancer Res, 2008. **68**(14): p. 5540-5.

116. Chamboredon, S., et al., *Hypoxia-inducible factor-1alpha mRNA: a new target for destabilization by tristetraprolin in endothelial cells.* Mol Biol Cell, 2011. **22**(18): p. 3366-78.

117. Dioum, E.M., et al., *Regulation of hypoxia-inducible factor 2alpha signaling by the stress-responsive deacetylase sirtuin 1.* Science, 2009. **324**(5932): p. 1289-93.

118. Lim, J.H., et al., *Sirtuin 1 modulates cellular responses to hypoxia by deacetylating hypoxia-inducible factor 1alpha.* Mol Cell, 2010. **38**(6): p. 864-78.

119. Xenaki, G., et al., *PCAF is an HIF-1alpha cofactor that regulates p53 transcriptional activity in hypoxia.* Oncogene, 2008. **27**(44): p. 5785-96.

120. Carbia-Nagashima, A., et al., *RSUME, a small RWD-containing protein, enhances SUMO conjugation and stabilizes HIF-1alpha during hypoxia.* Cell, 2007. **131**(2): p. 309-23.

121. Cheng, J., et al., *SUMO-specific protease 1 is essential for stabilization of HIF1alpha during hypoxia.* Cell, 2007. **131**(3): p. 584-95.

122. Greer, S.N., et al., *The updated biology of hypoxia-inducible factor.* EMBO J, 2012. **31**(11): p. 2448-60.

123. Pan, Y., et al., *Multiple factors affecting cellular redox status and energy metabolism modulate hypoxia-inducible factor prolyl hydroxylase activity in vivo and in vitro.* Mol Cell Biol, 2007. **27**(3): p. 912-25.

124. Masson, N., et al., *The FIH hydroxylase is a cellular peroxide sensor that modulates HIF transcriptional activity.* EMBO Rep, 2012. **13**(3): p. 251-7.

125. Hoffman, D.L., J.D. Salter, and P.S. Brookes, *Response of mitochondrial reactive oxygen species generation to steady-state oxygen tension: implications for hypoxic cell signaling.* Am J Physiol Heart Circ Physiol, 2007. **292**(1): p. H101-8.

126. Kim, H.S., et al., *SIRT3 is a mitochondria-localized tumor suppressor required for maintenance of mitochondrial integrity and metabolism during stress.* Cancer Cell, 2010. **17**(1): p. 41-52.

127. Finley, L.W., et al., *SIRT3 opposes reprogramming of cancer cell metabolism through HIF1alpha destabilization.* Cancer Cell, 2011. **19**(3): p. 416-28.

128. Mandal, S., et al., *Mitochondrial function controls proliferation and early differentiation potential of embryonic stem cells.* Stem Cells, 2011. **29**(3): p. 486-95.

129. Zhang, J., et al., *UCP2 regulates energy metabolism and differentiation potential of human pluripotent stem cells.* EMBO J, 2011. **30**(24): p. 4860-73.

130. Tian, H., S.L. McKnight, and D.W. Russell, *Endothelial PAS domain protein 1 (EPAS1), a transcription factor selectively expressed in endothelial cells.* Genes Dev, 1997. **11**(1): p. 72-82.

131. Peng, J., et al., *The transcription factor EPAS-1/hypoxia-inducible factor 2alpha plays an important role in vascular remodeling.* Proc Natl Acad Sci U S A, 2000. **97**(15): p. 8386-91.

132. Compernolle, V., et al., *Loss of HIF-2alpha and inhibition of VEGF impair fetal lung maturation, whereas treatment with VEGF prevents fatal respiratory distress in premature mice.* Nat Med, 2002. **8**(7): p. 702-10.

133. Scortegagna, M., et al., *The HIF family member EPAS1/HIF-2alpha is required for normal hematopoiesis in mice.* Blood, 2003. **102**(5): p. 1634-40.

134. Bertout, J.A., S.A. Patel, and M.C. Simon, *The impact of O2 availability on human cancer.* Nat Rev Cancer, 2008. **8**(12): p. 967-75.

135. Nilsson, H., et al., *HIF-2alpha expression in human fetal paraganglia and neuroblastoma: relation to sympathetic differentiation, glucose deficiency, and hypoxia.* Exp Cell Res, 2005. **303**(2): p. 447-56.

136. Holmquist-Mengelbier, L., et al., *Recruitment of HIF-1alpha and HIF-2alpha to common target genes is differentially regulated in neuroblastoma: HIF-2alpha promotes an aggressive phenotype.* Cancer Cell, 2006. **10**(5): p. 413-23.

137. Li, Z., et al., *Hypoxia-inducible factors regulate tumorigenic capacity of glioma stem cells.* Cancer Cell, 2009. **15**(6): p. 501-13.

138. Guyton, A.C., Hall, J.E., *Textbook of medical physiology*2006, Philadelphia: Elsevier.

139. Evans, S.M., et al., *Hypoxia is important in the biology and aggression of human glial brain tumors.* Clin Cancer Res, 2004. **10**(24): p. 8177-84.

140. Dings, J., et al., *Clinical experience with 118 brain tissue oxygen partial pressure catheter probes.* Neurosurgery, 1998. **43**(5): p. 1082-95.

141. Evans, S.M., et al., *Comparative measurements of hypoxia in human brain tumors using needle electrodes and EF5 binding.* Cancer Res, 2004. **64**(5): p. 1886-92.

142. Uchida, T., et al., *Prolonged hypoxia differentially regulates hypoxia-inducible factor (HIF)-1alpha and HIF-2alpha expression in lung epithelial cells: implication of natural antisense HIF-1alpha.* J Biol Chem, 2004. **279**(15): p. 14871-8.

143. Koh, M.Y., et al., *The hypoxia-associated factor switches cells from HIF-1alpha- to HIF-2alpha-dependent signaling promoting stem cell characteristics, aggressive tumor growth and invasion.* Cancer Res, 2011. **71**(11): p. 4015-27.

144. Kim, W.Y., et al., *HIF2alpha cooperates with RAS to promote lung tumorigenesis in mice.* J Clin Invest, 2009. **119**(8): p. 2160-70.

145. Imaizumi, T., et al., *Expression of the tumor-rejection antigen SART1 in brain tumors.* Int J Cancer, 1999. **83**(6): p. 760-4.

146. Kawamoto, M., et al., *Expression of the SART-1 tumor rejection antigen in breast cancer.* Int J Cancer, 1999. **80**(1): p. 64-7.

147. Keith, B., R.S. Johnson, and M.C. Simon, *HIF1alpha and HIF2alpha: sibling rivalry in hypoxic tumour growth and progression.* Nat Rev Cancer, 2012. **12**(1): p. 9-22.

148. Heddleston, J.M., et al., *The hypoxic microenvironment maintains glioblastoma stem cells and promotes reprogramming towards a cancer stem cell phenotype.* Cell Cycle, 2009. **8**(20): p. 3274-84.

149. Yan, Q., et al., *The hypoxia-inducible factor 2alpha N-terminal and C-terminal transactivation domains cooperate to promote renal tumorigenesis in vivo.* Mol Cell Biol, 2007. **27**(6): p. 2092-102.

150. Seidel, S., et al., *A hypoxic niche regulates glioblastoma stem cells through hypoxia inducible factor 2 alpha.* Brain, 2010. **133**(Pt 4): p. 983-95.

151. Mole, D.R., et al., *Genome-wide association of hypoxia-inducible factor (HIF)-1alpha and HIF-2alpha DNA binding with expression profiling of hypoxia-inducible transcripts.* J Biol Chem, 2009. **284**(25): p. 16767-75.

152. Parker, H.G., et al., *Genetic structure of the purebred domestic dog.* Science, 2004. **304**(5674): p. 1160-4.

153. Dobson, J.M., et al., *Canine neoplasia in the UK: estimates of incidence rates from a population of insured dogs.* J Small Anim Pract, 2002. **43**(6): p. 240-6.

154. McGrath, J.T., *Intracranial pathology of the dog.* Acta Neuropathol, 1962. **1(supp)**: p. 3-4.

155. Hayes, H.M., Priester, W.A Jr., Pendergrass, T.W., *Occurrence of nervous-tissue tumors in cattle, horses, cats and dogs.* Int J Cancer, 1975. **15**: p. 39-47.

156. Wong, A.J., et al., *Increased expression of the epidermal growth factor receptor gene in malignant gliomas is invariably associated with gene amplification.* Proc Natl Acad Sci U S A, 1987. **84**(19): p. 6899-903.

157. Lal, A., et al., *Mutant epidermal growth factor receptor up-regulates molecular effectors of tumor invasion.* Cancer Res, 2002. **62**(12): p. 3335-9.

158. Stoica, G., et al., *Morphology, immunohistochemistry, and genetic alterations in dog astrocytomas.* Vet Pathol, 2004. **41**(1): p. 10-9.

159. Higgins, R.J., et al., *Spontaneous canine gliomas: overexpression of EGFR, PDGFRalpha and IGFBP2 demonstrated by tissue microarray immunophenotyping.* J Neurooncol, 2010. **98**(1): p. 49-55.

160. Ferrara, N., H.P. Gerber, and J. LeCouter, *The biology of VEGF and its receptors.* Nat Med, 2003. **9**(6): p. 669-76.

161. Siemeister, G., et al., *Reversion of deregulated expression of vascular endothelial growth factor in human renal carcinoma cells by von Hippel-Lindau tumor suppressor protein.* Cancer Res, 1996. **56**(10): p. 2299-301.

162. Machein, M.R. and K.H. Plate, *VEGF in brain tumors.* J Neurooncol, 2000. **50**(1-2): p. 109-20.

163. Dickinson, P.J., et al., *Expression of receptor tyrosine kinases VEGFR-1 (FLT-1), VEGFR-2 (KDR), EGFR-1, PDGFRalpha and c-Met in canine primary brain tumours.* Vet Comp Oncol, 2006. **4**(3): p. 132-40.

164. Rossmeisl, J.H., et al., *Expression of vascular endothelial growth factor in tumors and plasma from dogs with primary intracranial neoplasms.* Am J Vet Res, 2007. **68**(11): p. 1239-45.

165. Dickinson, P.J., et al., *Vascular endothelial growth factor mRNA expression and peritumoral edema in canine primary central nervous system tumors.* Vet Pathol, 2008. **45**(2): p. 131-9.

166. Louis, D.N., *The p53 gene and protein in human brain tumors.* J Neuropathol Exp Neurol, 1994. **53**(1): p. 11-21.

167. York, D., et al., *TP53 Mutations in Canine Brain Tumors.* Vet Pathol, 2012.

168. Petitjean, A., et al., *Impact of mutant p53 functional properties on TP53 mutation patterns and tumor phenotype: lessons from recent developments in the IARC TP53 database.* Hum Mutat, 2007. **28**(6): p. 622-9.

169. Soda, Y., et al., *Transdifferentiation of glioblastoma cells into vascular endothelial cells.* Proc Natl Acad Sci U S A, 2011. **108**(11): p. 4274-80.

170. Ricci-Vitiani, L., et al., *Tumour vascularization via endothelial differentiation of glioblastoma stem-like cells.* Nature, 2010. **468**(7325): p. 824-8.

171. Wright, W.E. and J.W. Shay, *Inexpensive low-oxygen incubators.* Nat Protoc, 2006. **1**(4): p. 2088-90.

172. Chomczynski, P. and N. Sacchi, *Single-step method of RNA isolation by acid guanidinium thiocyanate-phenol-chloroform extraction.* Anal Biochem, 1987. **162**(1): p. 156-9.

173. Stoica, G., et al., *Identification of cancer stem cells in dog glioblastoma.* Vet Pathol, 2009. **46**(3): p. 391-406.

174. Livak, K.J. and T.D. Schmittgen, *Analysis of relative gene expression data using real-time quantitative PCR and the 2(-Delta Delta C(T)) Method.* Methods, 2001. **25**(4): p. 402-8.

175. Xue, Z., *Using SAS to Analyze the Summary Data*, in *Northeast SAS Users Group (NESUG)*2006: Philadelphia, PA.

176. Hlobilkova, A., et al., *Analysis of VEGF, Flt-1, Flk-1, nestin and MMP-9 in relation to astrocytoma pathogenesis and progression.* Neoplasma, 2009. **56**(4): p. 284-90.

177. Schiffer, D., A. Manazza, and I. Tamagno, *Nestin expression in neuroepithelial tumors.* Neurosci Lett, 2006. **400**(1-2): p. 80-5.

178. McCord, A.M., et al., *Physiologic oxygen concentration enhances the stem-like properties of CD133+ human glioblastoma cells in vitro.* Mol Cancer Res, 2009. **7**(4): p. 489-97.

179. Soeda, A., et al., *Hypoxia promotes expansion of the CD133-positive glioma stem cells through activation of HIF-1alpha.* Oncogene, 2009. **28**(45): p. 3949-59.

180. Berens, M.E., et al., *Allogeneic astrocytoma in immune competent dogs.* Neoplasia, 1999. **1**(2): p. 107-12.

181. Berens, M.E., et al., *Tumorigenic, invasive, karyotypic, and immunocytochemical characteristics of clonal cell lines derived from a spontaneous canine anaplastic astrocytoma.* In Vitro Cell Dev Biol Anim, 1993. **29A**(4): p. 310-8.

182. Inoue, S., et al., *Novel Animal Glioma Models that Separately Exhibit Two Different Invasive and Angiogenic Phenotypes of Human Glioblastomas.* World Neurosurg, 2011.

183. Onishi, M., et al., *Bimodal anti-glioma mechanisms of cilengitide demonstrated by novel invasive glioma models.* Neuropathology, 2012.

184. Lee, J., et al., *Tumor stem cells derived from glioblastomas cultured in bFGF and EGF more closely mirror the phenotype and genotype of primary tumors than do serum-cultured cell lines.* Cancer Cell, 2006. **9**(5): p. 391-403.

185. Cooper, J.K., et al., *Species identification in cell culture: a two-pronged molecular approach.* In Vitro Cell Dev Biol Anim, 2007. **43**(10): p. 344-51.

186. Parodi, B., et al., *Species identification and confirmation of human and animal cell lines: a PCR-based method.* Biotechniques, 2002. **32**(2): p. 432-4, 436, 438-40.

187. *Cell line misidentification: the beginning of the end.* Nat Rev Cancer, 2010. **10**(6): p. 441-8.

188. Gartler, S.M., *Genetic markers as tracers in cell culture.* Natl Cancer Inst Monogr, 1967. **26**: p. 167-95.

189. Buehring, G.C., E.A. Eby, and M.J. Eby, *Cell line cross-contamination: how aware are Mammalian cell culturists of the problem and how to monitor it?* In Vitro Cell Dev Biol Anim, 2004. **40**(7): p. 211-5.

190. Chatterjee, R., *Cell biology. Cases of mistaken identity.* Science, 2007. **315**(5814): p. 928-31.

191. Liscovitch, M. and D. Ravid, *A case study in misidentification of cancer cell lines: MCF-7/AdrR cells (re-designated NCI/ADR-RES) are derived from OVCAR-8 human ovarian carcinoma cells.* Cancer Lett, 2007. **245**(1-2): p. 350-2.

192. Boonstra, J.J., et al., *Verification and unmasking of widely used human esophageal adenocarcinoma cell lines.* J Natl Cancer Inst, 2010. **102**(4): p. 271-4.

193. Nardone, M. *An Open Letter Regarding the Misidentification and Cross-Contamination of Cell Lines: Significance and*

Recommendations for Correction. 2007; Available from: http://www.hpacultures.org.uk/media/A0D/E3/Open_Letter_Final_7-11-07.pdf.

194. Capes-Davis, A., et al., *Check your cultures! A list of cross-contaminated or misidentified cell lines.* Int J Cancer, 2010. **127**(1): p. 1-8.

195. Piret, J.P., et al., *CoCl2, a chemical inducer of hypoxia-inducible factor-1, and hypoxia reduce apoptotic cell death in hepatoma cell line HepG2.* Ann N Y Acad Sci, 2002. **973**: p. 443-7.

196. Ferrara, N. and T. Davis-Smyth, *The biology of vascular endothelial growth factor.* Endocr Rev, 1997. **18**(1): p. 4-25.

197. Robinson, C.J. and S.E. Stringer, *The splice variants of vascular endothelial growth factor (VEGF) and their receptors.* J Cell Sci, 2001. **114**(Pt 5): p. 853-65.

198. Hatva, E., et al., *Expression of endothelial cell-specific receptor tyrosine kinases and growth factors in human brain tumors.* Am J Pathol, 1995. **146**(2): p. 368-78.

199. Huang, H., et al., *Expression of VEGF and its receptors in different brain tumors.* Neurol Res, 2005. **27**(4): p. 371-7.

200. Maia, A.C., Jr., et al., *MR cerebral blood volume maps correlated with vascular endothelial growth factor expression and tumor grade in nonenhancing gliomas.* AJNR Am J Neuroradiol, 2005. **26**(4): p. 777-83.

201. Nam, D.H., et al., *Expression of VEGF and brain specific angiogenesis inhibitor-1 in glioblastoma: prognostic significance.* Oncol Rep, 2004. **11**(4): p. 863-9.

202. Plate, K.H., et al., *Vascular endothelial growth factor is a potential tumour angiogenesis factor in human gliomas in vivo.* Nature, 1992. **359**(6398): p. 845-8.

203. Plate, K.H., et al., *Vascular endothelial growth factor and glioma angiogenesis: coordinate induction of VEGF receptors, distribution of VEGF protein and possible in vivo regulatory mechanisms.* Int J Cancer, 1994. **59**(4): p. 520-9.

204. Takano, S., et al., *Concentration of vascular endothelial growth factor in the serum and tumor tissue of brain tumor patients.* Cancer Res, 1996. **56**(9): p. 2185-90.

205. Zhou, Y.H., et al., *The expression of PAX6, PTEN, vascular endothelial growth factor, and epidermal growth factor receptor in gliomas: relationship to tumor grade and survival.* Clin Cancer Res, 2003. **9**(9): p. 3369-75.

206. Hamerlik, P., et al., *Autocrine VEGF-VEGFR2-Neuropilin-1 signaling promotes glioma stem-like cell viability and tumor growth.* J Exp Med, 2012. **209**(3): p. 507-20.

207. Mackenzie, F. and C. Ruhrberg, *Diverse roles for VEGF-A in the nervous system.* Development, 2012. **139**(8): p. 1371-80.

208. Jingjing, L., et al., *Vascular endothelial growth factor is increased following coronary artery occlusion in the dog heart.* Mol Cell Biochem, 2000. **214**(1-2): p. 23-30.

209. Scheidegger, P., et al., *Vascular endothelial growth factor (VEGF) and its receptors in tumor-bearing dogs.* Biol Chem, 1999. **380**(12): p. 1449-54.

210. Kouadjo, K.E., et al., *Housekeeping and tissue-specific genes in mouse tissues.* BMC Genomics, 2007. **8**.

211. Vainrub, A., O. Pustovyy, and V. Vodyanoy, *Resolution of 90 nm (lambda/5) in an optical transmission microscope with an annular condenser.* Opt Lett, 2006. **31**(19): p. 2855-7.

212. Maranchie, J.K., et al., *The contribution of VHL substrate binding and HIF1-alpha to the phenotype of VHL loss in renal cell carcinoma.* Cancer Cell, 2002. **1**(3): p. 247-55.

213. Kondo, K., et al., *Inhibition of HIF is necessary for tumor suppression by the von Hippel-Lindau protein.* Cancer Cell, 2002. **1**(3): p. 237-46.

214. Acker, T., et al., *Genetic evidence for a tumor suppressor role of HIF-2alpha.* Cancer Cell, 2005. **8**(2): p. 131-41.

215. Mazumdar, J., et al., *HIF-2alpha deletion promotes Kras-driven lung tumor development.* Proc Natl Acad Sci U S A, 2010. **107**(32): p. 14182-7.

216. Scrideli, C.A., et al., *Prognostic significance of co-overexpression of the EGFR/IGFBP-2/HIF-2A genes in astrocytomas.* J Neurooncol, 2007. **83**(3): p. 233-9.

217. Mello, C.C. and D. Conte, Jr., *Revealing the world of RNA interference.* Nature, 2004. **431**(7006): p. 338-42.

218. Kim, D.H., et al., *Synthetic dsRNA Dicer substrates enhance RNAi potency and efficacy.* Nat Biotechnol, 2005. **23**(2): p. 222-6.

219. Rose, S.D., et al., *Functional polarity is introduced by Dicer processing of short substrate RNAs.* Nucleic Acids Res, 2005. **33**(13): p. 4140-56.

220. Manche, L., et al., *Interactions between double-stranded RNA regulators and the protein kinase DAI.* Mol Cell Biol, 1992. **12**(11): p. 5238-48.

221. Qiang, L., et al., *HIF-1alpha is critical for hypoxia-mediated maintenance of glioblastoma stem cells by activating Notch signaling pathway.* Cell Death Differ, 2012. **19**(2): p. 284-94.

222. Strojnik, T., et al., *Neural stem cell markers, nestin and musashi proteins, in the progression of human glioma: correlation of nestin with prognosis of patient survival.* Surg Neurol, 2007. **68**(2): p. 133-43; discussion 143-4.

223. Wan, F., et al., *Association of stem cell-related markers and survival in astrocytic gliomas.* Biomarkers, 2011. **16**(2): p. 136-43.